AD-A128 678 APPLICATION OF AN INTEGRAL EQUATION METHOD TO SCATTERING BY DIELECTRIC CY..(U) OHIO STATE UNIV COLUMBUS ELECTROSCIENCE LAB R E VAN DOEREN 24 FEB 69

UNCLASSIFIED ESL-TR-2604-1 N00019-68-C-0267 F/G 12/1 NL

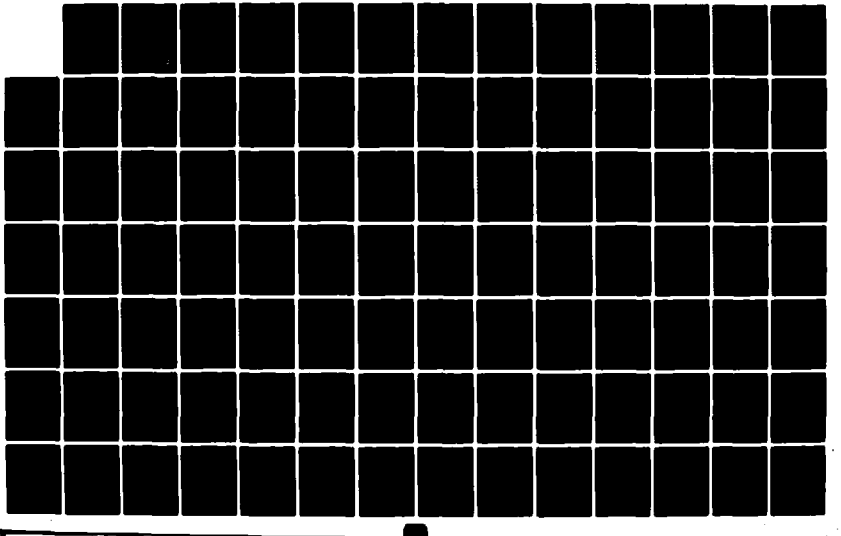

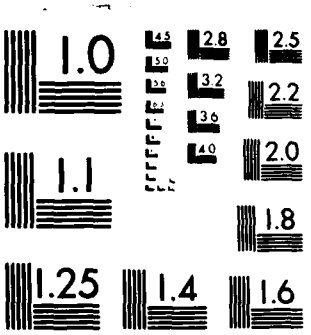

MICROCOPY RESOLUTION TEST CHART
NATIONAL BUREAU OF STANDARDS-1963-A

(1)

APPLICATION OF AN INTEGRAL EQUATION METHOD TO SCATTERING BY DIELECTRIC CYLINDRICAL SHELLS HAVING FINITE LENGTH

R. E. Van Doeren

The Ohio State University

ElectroScience Laboratory

(formerly Antenna Laboratory)

Department of Electrical Engineering

Columbus, Ohio 43212

TECHNICAL REPORT 2604-1

24 February 1969

Department of the Navy
Naval Air Systems Command
Washington, D.C. 20360

APPLICATION OF AN INTEGRAL EQUATION METHOD TO SCATTERING BY DIELECTRIC CYLINDRICAL SHELLS HAVING FINITE LENGTH

R. E. Van Doeren

TECHNICAL REPORT 2604-1
24 February 1969

Department of the Navy
Naval Air Systems Command
Washington, D.C. 20360

ACKNOWLEDGMENTS

This work was supported in part by Contract N00019-68-C-0267 between the Naval Air Systems Command, Washington, D.C., and the Ohio State University Research Foundation. The material contained in this report is also used as a Dissertation submitted to the Department of Electrical Engineering, The Ohio State University as partial fulfillment for the degree Doctor of Philosophy.

The author would like to thank the Ohio State University Computer Center for the computer time donated for performance of some of the computations included here.

The suggestions and encouragement of Prof. J. H. Richmond of the Ohio State University were of great value in carrying out the research reported in this Dissertation. The review and suggestions made by Prof. C.H. Walter, Prof. W. H. Peake and Prof. C. E. Nielsen are also very much appreciated. Mr. S. A. Redick carefully performed measurements of importance in the outcome of this research.

ABSTRACT

An integral equation for the electromagnetic field within a dielectric body is given. The equation is set up for numerical solution for the case of thin-wall cylindrical dielectric shells having finite length.

The solution of the integral equation utilizes a truncated double Fourier expansion of the field in the shell. The integral equation is then enforced at enough points within the shell wall to obtain a sufficient system of linear equations in the unknown expansion coefficients of the field. Numerical integration over the shell volume is used to obtain the coefficients in the system of linear equations. The system of equations is solved numerically for the expansion coefficients of the field in the shell. Calculation of the backscattered fields and the backscattering cross section are then performed.

A comparison of the calculated and measured backscattering cross section is made for rings with arbitrary plane wave incidence and for tubes with axial plane wave incidence. The agreement is excellent in all cases considered.

The numerical methods, experimental arrangement, computer programs and suitable extension of this work are discussed.

CONTENTS

CONTENTS (continued)

CHAPTER I

INTRODUCTION

It is a relatively difficult task to accurately calculate the scattering characteristics of dielectric bodies when they are placed in an arbitrary electromagnetic field. Knowledge of dielectric scattering is important when a protective dielectric shell is placed over an antenna and when radar mapping is used for geophysical or military purposes. The research discussed in this paper was motivated primarily by interest in the scattering from protective dielectric shells (radomes) when placed over an antenna.

By comparison with the effort expended on electromagnetic scattering from perfectly conducting bodies, the amount of research on scattering from dielectric bodies is small. Some of the earliest work on dielectric scattering was done by Lord Rayleigh. Stratton [1] points out that Rayleigh applied the electromagnetic theory of light to scattering by dielectric bodies which are small in comparison with a wavelength. Lord Rayleigh used his results to describe scattering by colloidal particles and to explain the blue cast of the sky.

Rigorous solutions for plane wave scattering from dielectric bodies have been found for the sphere,[2] the infinite circular cylinder,[3,4] the infinite elliptic cylinder,[5] the infinite parabolic cylinder[6] and the infinite plane dielectric slab.[7] Tice and Adney[8] formulated a rigorous solution for a dipole within a spherical shell and

Andreasen[9] developed an asymptotic solution for a dipole within a thin spherical shell.

The homogeneous vector Helmholtz equation must be satisfied in a source-free homogeneous medium by the vector potential functions for the electromagnetic field. Morse and Feshbach[10] have observed that this equation is separable in only six coordinate systems (rectangular, circular cylindrical, elliptic cylindrical, parabolic cylindrical, spherical and conical). They also point out that, although rigorous series solution can be obtained for the remaining five coordinate systems in which the scalar Helmholtz equation is separable,[11] "the fitting of boundary conditions is well-nigh impossible of attainment." The number of problems for which a rigorous series solution is practical is therefore severely restricted.

Various approximate methods have been used to study the scattering from finite dielectric bodies. Cohen[12] developed approximate scattering formulas based on the reaction concept and applied these formulas to the infinite dielectric cylinder. Montroll and Hart[13] derived formulas for the scattering of finite cylinders by approximating the fields in the finite cylinder by those in the infinite cylinder. Lind[14] also used the infinite cylinder field to approximate that in a finite cylinder but added a "normal mode" correction to this solution. Oguchi[15] derived formulas for the scattering by dielectric spheroids of small eccentricity by considering the spheroids to be perturbations of a sphere. Phillipson[16] calculated the scattering from dielectric rings using an iteration method. Geometrical optics was applied by

Peters and Thomas[17] to scattering from thin-wall spherical shells and by Kouyoumjian, et.al.[18] and Peters, et.al.[19] to more general dielectric bodies.

For the Scattering from an arbitrary dielectric body, rigorous series methods are impractical and the accuracy of the approximate techniques is unknown. For these reasons, another approach, the integral equation method, has been applied in recent years to some dielectric scattering problems. The integral equation method is fundamentally a rigorous numerical technique for finding the fields within a dielectric volume.

The power of the integral equation method was recognized in an early report by Rhodes.[20] A recent book by Harrington[21] devotes a considerable amount of discussion to the solution of integral equations for field problems by means of the method of moments. Richmond has used the integral equation method successfully to solve a varied group of dielectric scattering problems: calculation of radome diffraction patterns,[22] diffraction by metallic or dielectric toroids with a coaxial magnetic line source,[23] scattering from finite dielectric cylinders[24] and scattering from infinite dielectric cylinders of arbitrary cross section.[25,26] Waterman[27] has recently applied an "extended" integral equation method to scattering by dielectric bodies; he utilizes spherical mode expansions and satisfies the integral equation over the body's interior region.

The solution of an integral equation for the field within a body is usually accomplished by approximating the equation by a system of linear equations. The unknowns in the system are either the field it-

self at a number of points within the body or a set of expansion coefficients for the field in the body. Solution of large systems of equations and repeated computation of complicated volume integrals require large, high speed computers. It is for this reason that the integral equation method was not applied extensively prior to the advent of the modern generations of digital computers.

In general, a radome can be an arbitrary three-dimensional shape, may be inhomogeneous and is placed in the relatively complex near field of a radar antenna. Solution of such a difficult scattering problem must proceed in a sequence of smaller, yet significant, steps. Thus, as the first step in this paper, the integral equation method is applied to the problem of calculating the scattering by thin-wall dielectric circular cylindrical tubes of finite length. In Chapter II the equivalent source currents for the scattered field and the basic integral equation are discussed. The expansion of the field in the shell, the derivation of the system of linear equations and the Fourier expansion of an incident plane wave are described in Chapter III. The techniques of numerical integration, the special manner of integrating through the singularity and the far field calculation are discussed in Chapter IV. In Chapter V a comparison is made of the calculated and measured plane-wave backscattering from dielectric rings and cylindrical shells. Conclusions are presented in Chapter VI. A discussion of the experimental method and a description of the computer programs used are presented in the Appendices.

CHAPTER II

FORMULATION OF THE INTEGRAL EQUATION

A. The Equivalent Currents

The following equivalence principle and its derivation were developed by Rhodes.[20] The derivation below is the same as that given by Richmond.[28]

The time dependence $e^{+j\omega t}$ is understood and linear, non-magnetic ($\mu=\mu_0$), isotropic dielectric media are assumed. The medium may be inhomogeneous and lossy, i.e., it may have a complex permittivity.

Let a current source $\underline{J}(x,y,z)$ in a medium $(\mu_i(x,y,z),\ \epsilon_i(x,y,z)$ generate a field $(\underline{E}_i(x,y,z),\ \underline{H}_i(x,y,z)$. This field will satisfy Maxwell's curl equations:

$$(1) \qquad \begin{cases} \nabla \times \underline{H}_i = \underline{J} + j\,\omega\epsilon_i\,\underline{E}_i \\ \nabla \times \underline{E}_i = -j\,\omega\,\mu_i\,\underline{H}_i \end{cases}$$

Let the same current source $\underline{J}(x,y,z)$ in a new medium $(\mu\ (x,y,z),\ \epsilon(x,y,z))$ generate a different field $(\underline{E}(x,y,z),\ \underline{H}(x,y,z))$. This new field must also satisfy Maxwell's curl equation:

$$(2) \qquad \begin{cases} \nabla \times \underline{H} = \underline{J} + j\,\omega\,\epsilon\,\underline{E} \\ \nabla \times \underline{E} = -j\,\omega\,\mu\,\underline{H} \end{cases}$$

The difference between these fields is called the scattered field:

$$(3) \qquad \begin{cases} \underline{E}_s = \underline{E} - \underline{E}_i \\ \underline{H}_s = \underline{H} - \underline{H}_i \end{cases}$$

If Maxwell's equations for the two sets of fields are subtracted, we obtain the curl equations for the scattered field:

$$(4) \qquad \begin{cases} \nabla \times \underline{H}_s = j\,\omega(\varepsilon - \varepsilon_i)\ \underline{E} + j\,\omega\,\varepsilon_i\,\underline{E}_s \\ \nabla \times \underline{E}_s = -j\,\omega(\mu - \mu_i)\ \underline{H} - j\,\omega\,\mu_i\,\underline{H}_s \end{cases}$$

The term $j\,\omega(\varepsilon - \varepsilon_i)\,\underline{E}$ (which is nonzero only where $\varepsilon \neq \varepsilon_i$) may be interpreted as an equivalent electric current density radiating in the original medium, $(\mu_i\ \varepsilon_i)$. Similarly, the term $-j\,\omega(\mu - \mu_i)\underline{H}_2$ can be interpreted as an equivalent magnetic current density radiating in the original medium (μ_i, ε_i). These current densities are the sole sources of the scattered field.

In this investigation, the original medium is chosen to be free space so $\varepsilon_i = \varepsilon_o$. Furthermore, all media are assumed nonmagnetic so that $\mu_i = \mu = \mu_o$ and the equivalent magnetic current density vanishes. The electric current density, $j\,\omega(\varepsilon - \varepsilon_o)\,\underline{E}$, then becomes the sole source of the scattered field and radiates in unbounded free space.

As noted earlier, the equivalent current concept can be applied to inhomogeneous, lossy dielectric media.

B. The Integral Equation

The fields radiated by a source current density $\underline{J}$ in free space can be calculated using an integral form such as

$$(5) \qquad E^p = \iiint_V \underline{J} \cdot \underline{G}_p (\underline{r},\underline{r}') \, dv' \quad ,$$

where E^p is the p-th component of the radiated field, $\underline{J}$ is the source current density, V' is the source volume and $\underline{G}_p$ represents the free space vector Green's function for the p-th component. The equations given by Richmond[28] and given in Eq. (9) can readily be put into the above form. Substituting the equivalent current density of Eq. (4) into Eq. (5) and using this result in Eq. (3), we obtain our integral equation for the field in the dielectric body and the exterior free-space region:

$$(6) \qquad E^p = E_i^p + \iiint_V j \omega(\varepsilon - \varepsilon_o) \underline{E} \cdot \underline{G}_p (\underline{r},\underline{r}') \, dv'$$

To determine the field, it is sufficient to enforce Eq. (6) in the interior region.

Equation (6) must be satisfied for each of the three components of the field such as E^x, E^y, and E^z in rectangular coordinates or E^ρ, E^ϕ and E^z in the cylindrical system.

Solution of Eq. (6) yields a solution for the total field within the body. Then the field at any exterior point can be calculated from Eq. (6). For the scattering by cylindrical dielectric shells, a tech-

nique for solving the integral equation is outlined below. Up to this point the analysis covers lossy and lossless, homogeneous and inhomogeneous dielectric bodies with arbitrary size and shape. Now to illustrate the techniques we hereafter restrict our attention to a specific case: thin-wall, homogeneous, dielectric circular cylindrical shells.

The shell is assumed homogeneous and sufficiently thin that any radial variation of the fields is negligible within the shell. The shell and its coordinate system are illustrated in Fig. 1. At any point, z, along the shell, the field components can be expanded in a Fourier series in ϕ. The expansion coefficients in this series are functions of z and are likewise expanded in a Fourier series (in z). Both series are truncated to finite sums as a practical matter. The degree of truncation depends on the particular shell and the incident field.

The expansion coefficients are determined by enforcing Eq. (6) at many points in the shell to obtain a set of simultaneous linear equations in the expansion coefficients. The system is solved for the expansion coefficients, or equivalently, for the field within the shell. Finally, when the total field within the shell is known, the asymptotic form of Eq. (6) is employed to calculate the distant field.

CHAPTER III

SOLUTION OF THE INTEGRAL EQUATION

A. Field Expansion and the System of Linear Equations

The coordinate system and a cylindrical shell are shown in Fig. 1. The circumflex indicates a unit vector.

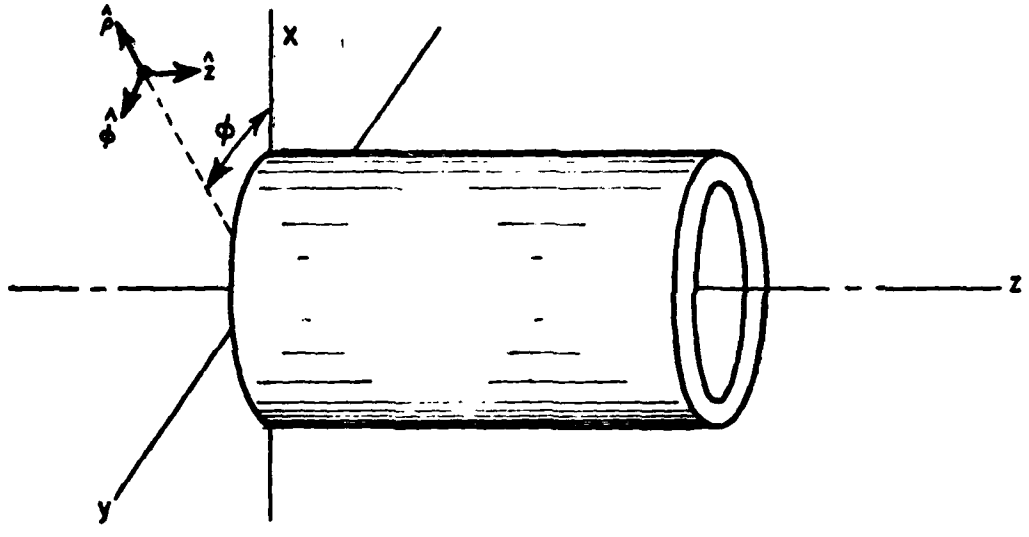

Fig. 1--Cylindrical coordinate system and cylindrical shell.

The shell is assumed to be sufficiently thin that field variations with ρ can be neglected within the shell. In the dielectric region, the fields can be expanded in a Fourier Series as follows:

$$(7)\qquad \begin{cases} E^{\rho}(z) = \sum_{n=0}^{\infty} [A_n^{\rho}(z)\cos(n\phi) + B_n^{\rho}(z)\sin n\phi] \\ E^{\phi}(z) = \sum_{n=0}^{\infty} [A_n^{\phi}(z)\cos(n\phi) + B_n^{\phi}(z)\sin n\phi] \\ E^{z}(z) = \sum_{n=0}^{\infty} [A_n{}^{z}(z)\cos n\phi + B_n^{\phi}(z)\sin n\phi] \end{cases}$$

In Eq. (7), as noted, the A_n's and B_n's are functions of position along the shell and can be represented by a Fourier series in z. The period of the expansion is p where p is greater than or equal to the shell length. The expansions of the A_n's and B_n's follows:

$$(8)\qquad \begin{cases} A_n^{\rho}(z) = \sum_{m=0}^{\infty} [a_{mn}^{\rho}\cos(\frac{2m\pi}{p}z) + as_{mn}^{\rho}\sin(\frac{2m\pi}{p}z)] \\ B_n^{\rho}(z) = \sum_{m=0}^{\infty} [b_{mn}^{\rho}\cos(\frac{2m\pi}{p}z) + bs_{mn}^{\rho}\sin(\frac{2m\pi}{p}z)] \\ A_n^{\phi}(z) = \sum_{m=0}^{\infty} [a_{mn}^{\phi}\cos(\frac{2m\pi}{p}z) + as_{mn}^{\phi}\sin(\frac{2m\pi}{p}z)] \\ B_n^{\phi}(z) = \sum_{m=0}^{\infty} [b_{mn}^{\phi}\cos(\frac{2m\pi}{p}z) + bs_{mn}^{\phi}\sin(\frac{2m\pi}{p}z)] \\ A_n{}^{z}(z) = \sum_{m=0}^{\infty} [a_{mn}^{z}\cos(\frac{2m\pi}{p}z) + as_{mn}^{z}\sin(\frac{2m\pi}{p}z)] \\ B_n^{z}(z) = \sum_{m=0}^{\infty} [b_{mn}^{z}\cos(\frac{2m\pi}{p}z) + bs_{mn}^{z}\sin(\frac{2m\pi}{p}z)] \end{cases}$$

In the circular cylindrical system, there will be no coupling between modes of different index n in the ϕ-expansion. For this reason it is possible to solve the integral equation for one value of n at a

time, to obtain the solution for all necessary n and then to superimpose the results to determine the total field within the shell. This allows a considerable saving in computer storage compared with solving the entire system in one fell swoop. The z-expansion must be considered in its (truncated) entirety for each value of n, however.

Eq. (6) is to be enforced at a number of points in the shell. For numerical purposes, the shell is divided into equal-length elemental rings, each ring being short compared with the wavelength. The numerical integrations over the tube (shell) are performed on a ring-by-ring basis and the total integral is found by summing the contributions of all of the rings. Fig. 2 illustrates the subdivision of the cylindrical shell.

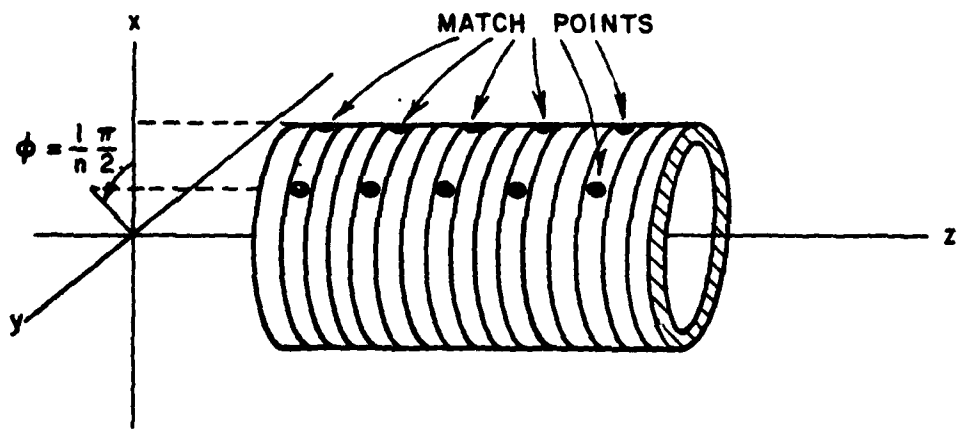

Fig. 2-- Division of shell into elemental rings.

The match points (points of enforcement of the integral equation) are at the center of the wall cross section of the matching rings (two per ring) and are located at $\phi=0$ and $\phi=\frac{1}{n}\frac{\pi}{2}$. The matching rings are evenly spaced along the tube. If M is the maximum index of the z-expansion, (2M + 1) matching rings are required to obtain a complete system of equations in the field expansion coefficients.

The next step is to evaluate the integrals for the scattered field at points in the shell. In the following work, attention is confined to the n-th mode in ϕ; it is understood that in general many such modes may be needed to obtain an accurate solution for the total field in the shell.

The following equations are given by Richmond[28] for the cartesian components of the field generated in free space by a source current density with components J^x, J^y, and J^z:

$$(9)\quad \begin{cases} E^x = \dfrac{\sqrt{\mu_o/\epsilon_o}}{4\pi jk} \iiint_{v'} e^{-jkr}\{P(r)\,J^x + (x-x')Q(r)[(x-x')J^x \\ \qquad + (y-y')J^y + (z-z')\,J^z]\}\,dv' \\ E^y = \dfrac{\sqrt{\mu_o/\epsilon_o}}{4\pi jk} \iiint_{v'} e^{-jkr}\{P(r)\,J^y + (y-y')Q(r)[(x-x')J^x \\ \qquad + (y-y')J^y + (z-z')J^z]\}\,dv' \\ E^z = \dfrac{\sqrt{\mu_o/\epsilon_o}}{4\,jk} \iiint_{v'} e^{-jkr}\{P(r)\,J^z + (z-z')Q(r)[(x-x')J^x \\ \qquad + (y-y')J^y + (z-z')J^z]\}\,dv' \end{cases}$$

In Eq. (9),

$$(10)\qquad \begin{cases} P(r) = \dfrac{-1 - j\,kr + k^2 r^2}{r^3} \\[2ex] Q(r) = \dfrac{3 + 3j\,kr - k^2 r^2}{r^5} \end{cases}$$

In Eqs. (9) and (10), $k = \omega\sqrt{\mu_o \varepsilon_o} = 2\pi/\lambda$ and

$$r = \sqrt{\rho^2 + \rho'^2 - 2\rho\rho'\cos(\phi-\phi') + (z-z')^2}$$

is the distance from the source to the observation point. The equivalent current density, $j\omega(\varepsilon-\varepsilon_0)\underline{E}$, is substituted into Eq. (9) to obtain an expression for the scattered field in terms of the total field. The field components are then converted to circular cylindrical components and the field expansion of Eq. (7) and (8) used to get the following result for the n-th mode scattered field where $c_m = \cos(\frac{2m\pi}{p} z)$, $s_m = \sin(\frac{2m\pi}{p}z)$ and $\varepsilon_r = \varepsilon/\varepsilon_0$.

$$(11)\qquad E^x_{sn} = \frac{\varepsilon_r - 1}{4\pi} \sum_{m=0}^{\infty} \iiint_{v'} e^{-jkr} \cdot$$

$$\left\{ P(r) \left[\begin{array}{l} \{(a^{\rho}_{mn} c_m + as^{\rho}_{mn} s_m)\cos n\phi' + (b^{\rho}_{mn} c_m + bs^{\rho}_{mn} s_m)\sin n\phi'\}\cos\phi' \\ -\{(a^{\phi}_{mn} c_m + as^{\phi}_{mn} s_m)\cos n\phi' + (b^{\phi}_{mn} c_m + bs^{\phi}_{mn} s_m)\sin n\phi'\}\sin\phi' \end{array} \right] \right.$$

$$+Q(r)(x-x')^2 \left[\begin{array}{l} \{(a^{\rho}_{mn} c_m + as^{\rho}_{mn} s_m)\cos n\phi' + (b^{\rho}_{mn} c_m + bs^{\rho}_{mn} s_m)\sin n\phi'\}\cos\phi' \\ -\{(a^{\phi}_{mn} c_m + as^{\phi}_{mn} s_m)\cos n\phi' + (b^{\phi}_{mn} c_m + bs^{\phi}_{mn} s_m)\sin n\phi'\}\sin\phi' \end{array} \right]$$

$$+ Q(r)(x-x')(y-y')\left[\begin{array}{l}\{(a^{\rho}_{mn}c_m + as^{\rho}_{mn}s_m)\cos n\phi' + (b^{\rho}_{mn}c_{mn} + bs^{\rho}_{mn}s_m)\\ \qquad \sin n\phi'\}\sin\phi' \\ +\{(a^{\phi}_{mn}c_m + as^{\phi}_{mn}s_m)\cos n\phi' + (b^{\phi}_{mn}c_m + bs^{\phi}_{mn}s_m)\\ \qquad \sin n\phi'\}\cos\phi'\end{array}\right]$$

(11) (cont.)

$$+ Q(r)(x-x')(z-z')\left[(a^{z}_{mn}c_m + as^{z}_{mn}s_m)\cos n\phi' + (b^{z}_{mn}c_m + bs^{z}_{mn}s_m)\sin n\phi'\right]\Bigg\}\, dv'$$

$$(12)\qquad E^{y}_{sn} = \frac{\epsilon_r - 1}{4\pi}\sum_{m=0}^{\infty}\iiint_{v'} e^{-jkr}\cdot$$

$$\Bigg\{+ P(r)\left[\begin{array}{l}\{(a^{\rho}_{mn}c_m + as^{\rho}_{mn}s_m)\cos n\phi' + (b^{\rho}_{mn}c_m + bs^{\rho}_{mn}s_m)\sin n\phi'\}\sin\phi' \\ +\{(a^{\phi}_{mn}c_m + as^{\phi}_{mn}s_m)\cos n\phi' + (b^{\phi}_{mn}c_m + bs^{\phi}_{mn}s_m)\sin n\phi'\}\cos\phi'\end{array}\right]$$

$$+ Q(r)(y-y')(x-x')\left[\begin{array}{l}\{(a^{\rho}_{mn}c_m + as^{\rho}_{mn}s_m)\cos n\phi' + (b^{\rho}_{mn}c_m + bs^{\rho}_{mn}s_m)\\ \qquad \sin n\phi'\}\cos\phi' \\ -\{(a^{\phi}_{mn}c_m + as^{\phi}_{mn}s_m)\cos n\phi' + (b^{\phi}_{mn}c_m + bs^{\phi}_{mn}s_m)\\ \qquad \sin n\phi'\}\sin\phi'\end{array}\right]$$

$$+ Q(r)\,(y-y')^2\left[\begin{array}{l}\{(a^{\rho}_{mn}c_m + as^{\rho}_{mn}s_m)\cos n\phi' + (b^{\rho}_{mn}c_m + bs^{\rho}_{mn}s_m)\\ \qquad \sin n\phi'\}\sin\phi' \\ +\{(a^{\phi}_{mn}c_m + as^{\phi}_{mn}s_m)\cos n\phi' + (b^{\phi}_{mn}c_m + bs^{\phi}_{mn}s_m)\\ \qquad \sin n\phi'\}\cos\phi'\end{array}\right]$$

$$+ Q\,(r)(y-y')(z-z')\left[(a^{z}_{mn}c_m + as^{z}_{mn}s_m)\cos n\phi' + (b^{z}_{mn}c_m + bs^{z}_{mn}s_m)\sin n\phi'\right]\Bigg\}\, dv'$$

$$(13)\qquad E_{sn}^{z} = \frac{\varepsilon_r - 1}{4\pi} \sum_{m=0}^{\infty} \iiint_{v'} e^{-jkr}$$

$$\Bigg\{ P(r)\left[(a_{mn}^{z}c_m + as_{mn}^{z}s_m)\cos n\phi' + (b_{mn}^{z}c_m + bs_{mn}^{z}s_m)\sin n\phi'\right],$$

$$+ Q(r)(z-z')(x-x')\Bigg[\begin{array}{l}\{(a_{mn}^{\rho}c_m + as_{mn}^{\rho}s_m)\cos n\phi' + (b_{mn}^{\rho}c_m + bs_{mn}^{\rho}s_m) \\ \qquad \sin n\phi'\}\cos\phi' \\ -\{(a_{mn}^{\phi}c_m + as_{mn}^{\phi}s_m)\cos n\phi' + (b_{mn}^{\phi}c_m + bs_{mn}^{\phi}s_m) \\ \qquad \sin n\phi'\}\sin\phi'\end{array}\Bigg]$$

$$+ Q(r)(z-z')(y-y')\Bigg[\begin{array}{l}\{(a_{mn}^{\rho}c_m + as_{mn}^{\rho}s_m)\cos n\phi' + (b_{mn}^{\rho}c_m + bs_{mn}^{\rho}s_m) \\ \qquad \sin n\phi'\}\sin\phi' \\ +\{(a_{mn}^{\phi}c_m + as_{mn}^{\phi}s_m)\cos n\phi' + (b_{mn}^{\phi}c_m + bs_{mn}^{\phi}s_m) \\ \qquad \sin n\phi'\}\cos\phi'\end{array}\Bigg]$$

$$+ Q(r)(z-z')^2\left[(a_{mn}^{z}c_m + as_{mn}^{z}s_m)\cos n\phi' + (b_{mn}^{z}c_m + bs_{mn}^{z}s_m)\sin n\phi'\right]\Bigg\} dv'$$

The symmetries of the integrands for the scattered fields about $\phi = 0$ and $\phi = \frac{1}{n}\frac{\pi}{2}$ permit a convenient correspondence between the integrations for a match point at $\phi = 0$ and one at $\phi = \frac{1}{n}\frac{\pi}{2}$. Only the integration for $\phi = 0$ need be calculated and the ones for $\phi = \frac{1}{n}\frac{\pi}{2}$ can be obtained from them. Also, the odd symmetry of some of the integrand terms results in those terms integrating to zero for a match point at $\phi = 0$ or $\phi = \frac{1}{n}\frac{\pi}{2}$. After making use of the odd symmetry of certain terms and of the relationship between the $\phi = 0$ and $\phi = \frac{1}{n}\frac{\pi}{2}$ calculations, the cylindrical components of the scattered field for a given matching ring can be written:

$$
(14)\begin{cases}
E^{\rho}_{sn}(0,z) = (\varepsilon_r-1)\sum\limits_{m=0}^{\infty}\left\{\begin{matrix} a^{\rho}_{mn}\,A1_{mn}(z) + a^{z}_{mn}\,A2_{mn}(z) + b^{\phi}_{mn}\,A3_{mn}(z) \\ + as^{\rho}_{mn}\,B1_{mn}(z) + as^{z}_{mn}\,B2_{mn}(z) + bs^{\phi}_{mn}\,B3_{mn}(z)\end{matrix}\right\} \\
E^{\phi}_{sn}(o,z) = (\varepsilon_r-1)\sum\limits_{m=0}^{\infty}\left\{\begin{matrix} b^{\rho}_{mn}\,A4_{mn}(z) + b^{z}_{mn}\,A5_{mn}(z) + a^{\phi}_{mn}\,A6_{mn}(z) \\ + bs^{\rho}_{mn}\,B4_{mn}(z) + bs^{z}_{mn}\,B5_{mn}(z) + as^{\phi}_{mn}\,B6_{mn}(z)\end{matrix}\right\} \\
E^{z}_{sn}(0,z) = (\varepsilon_r-1)\sum\limits_{m=0}^{\infty}\left\{\begin{matrix} a_{mn}\,A7_{mn}(z) + a^{z}_{mn}\,A8_{mn}(z) + b^{\phi}_{mn}\,A9_{mn}(z) \\ + as^{\rho}_{mn}\,B7_{mn}(z) + as^{z}_{mn}\,B8_{mn}(z) + bs^{\phi}_{mn}\,B9_{mn}(z)\end{matrix}\right\}
\end{cases}
$$

$$
(15)\begin{cases}
E^{\rho}_{sn}\left(\frac{1}{n}\frac{\pi}{2},z\right) = (\varepsilon_r-1)\sum\limits_{m=0}^{\infty}\left\{\begin{matrix} b^{\rho}_{mn}\,A1_{mn}(z) + b^{z}_{mn}\,A2_{mn}(z) - a^{\phi}_{mn}\,A3_{mn}(z) \\ + bs^{\rho}_{mn}\,B1_{mn}(z) + bs^{z}_{mn}\,B2_{mn}(z) - as^{\phi}_{mn}\,B3_{mn}(z)\end{matrix}\right\} \\
E^{\phi}_{sn}\left(\frac{1}{n}\frac{\pi}{2},z\right) = (\varepsilon_r-1)\sum\limits_{m=0}^{\infty}\left\{\begin{matrix} -a^{\rho}_{mn}\,A4_{mn}(z) - a^{z}_{mn}\,A5_{mn}(z) + b^{\phi}_{mn}\,A6_{mn}(z) \\ -as^{\rho}_{mn}\,B4_{mn}(z) - as^{z}_{mn}\,B5_{mn}(z) + bs^{\phi}_{mn}\,B6_{mn}(z)\end{matrix}\right\} \\
E^{z}_{sn}\left(\frac{1}{n}\frac{\pi}{2},z\right) = (\varepsilon_r-1)\sum\limits_{m=0}^{\infty}\left\{\begin{matrix} b^{\rho}_{mn}\,A7_{mn}(z) + b^{z}_{mn}\,A8_{mn}(z) - a^{\phi}_{mn}\,A9_{mn}(z) \\ + bs^{\rho}_{mn}\,B7_{mn}(z) + bs^{z}_{mn}\,B8_{mn}(z) - as^{\phi}_{mn}\,B9_{mn}(z)\end{matrix}\right\}
\end{cases}.
$$

$A1_{mn}(z)$ through $A9_{mn}(z)$ and $B1_{mn}(z)$ through $B9_{mn}(z)$ are defined below. The integrals are to be calculated for an observation point at the center of the shell wall cross section for $\phi = 0$ and z equal to the z-coordinate of the match point in question.

$$
\begin{aligned}
A1_{mn}^{(z)} &= \frac{1}{4\pi} \iiint_{v'} e^{-jkr} \{P(r)\cos\phi' + Q(r)(x-x')^2 \cos\phi' \\
&\quad + Q(r)(x-x')(y-y')\} \cos\left(\frac{2m\pi}{p} z'\right) \cos n\phi' \, dv' \\
A2_{mn}^{(z)} &= \frac{1}{4\pi} \iiint_{v'} e^{-jkr} \{Q(r)(x-x')(z-z')\} \cos\left(\frac{2m\pi}{p} z'\right) \cos n\phi' dv' \\
A3_{mn}^{(z)} &= \frac{1}{4\pi} \iiint_{v'} e^{-jkr} \{-P(r)\sin\phi' - Q(r)(x-x')^2 \sin\phi' \\
&\quad + Q(r)(x-x')(y-y')\cos\phi'\} \cos\left(\frac{2m\pi}{p} z'\right) \sin n\phi' \, dv' \\
A4_{mn}^{(z)} &= \frac{1}{4\pi} \iiint_{v'} e^{-jkr} \{P(r)\sin\phi' + Q(r)(x-x')(y-y')\cos\phi' \\
&\quad + Q(r)(y-y')^2 \sin\phi'\} \cos\left(\frac{2m\pi}{p} z'\right) \sin n\phi' \, dv' \\
A5_{mn}^{(z)} &= \frac{1}{4\pi} \iiint_{v'} e^{-jkr} \{Q(r)(y-y')(z-z')\} \cos\left(\frac{2m\pi}{p} z'\right) \sin n\phi' dv' \\
A6_{mn}^{(z)} &= \frac{1}{4\pi} \iiint_{v'} e^{-jkr} \{P(r)\cos\phi' - Q(r)(x-x')(y-y')\sin\phi' \\
&\quad + Q(r)(y-y')^2 \cos\phi'\} \cos\left(\frac{2m\pi}{p} z'\right) \cos n\phi\phi \, dv' \\
A7_{mn}^{(z)} &= \frac{1}{4\pi} \iiint_{v'} e^{-jkr} \{Q(r)(z-z')(x-x')\cos\phi' \\
&\quad + Q(r)(z-z')(y-y')\sin\phi'\} \cos\left(\frac{2m\pi}{p} z'\right) \cos n\phi' \, dv' \\
A8_{mn}^{(z)} &= \frac{1}{4\pi} \iiint_{v'} e^{-jkr} \{P(r) + Q(r)(z-z')^2\} \cos\left(\frac{2m\pi}{p} z'\right) \cos n\phi' \, dv' \\
A9_{mn}^{(z)} &= \frac{1}{4\pi} \iiint_{v'} e^{-jkr} \{-Q(r)(z-z')(x-x')\sin\phi' \\
&\quad + Q(r)(z-z')(y-y')\cos\phi'\} \cos\left(\frac{2m\pi}{p} z'\right) \sin n\phi' \, dv'
\end{aligned}
\tag{16}
$$

$B1_{mn}^{(z)}$ through $B9_{mn}^{(z)}$ are found directly by replacing $\cos(\frac{2m\pi}{p}z')$ by $\sin(\frac{2m\pi}{p}z')$ in the corresponding equations for $A1_{mn}^{(z)}$ through $A9_{mn}^{(z)}$. The integrations for the $B_{mn}^{(z)}$'s are also evaluated at $\phi = 0$.

The field expansion of Eq. (8) and the results given in Eqs. (14) and (15) are used in Eq. (3) to obtain the set of linear equations corresponding to one point along the shell, i.e., for one matching ring. The summation over m has been truncated to a maximum index value of $m = M$. For this case a total of $(2M + 1)$ sets of the following equations will be necessary to have a sufficient system. In Eq. (17), the dependence of $A1_{mn}$, etc. upon z has not been shown explicitly; it is understood that these coefficients are functions of the z-coordinates of the matching rings.

(17)

$$\left\{\sum_{m=0}^{M}\left[a_{mn}^{\rho}\cos\left(\frac{2m\pi}{p}z\right)+as_{mn}^{\rho}\sin\left(\frac{2m\pi}{p}z\right)\right]\right\}=a_{in}^{\rho}(z)+(\varepsilon_r-1)\sum_{m=0}^{M}\left\{\begin{array}{l}a_{mn}^{\rho}A1_{mn}+as_{mn}B1_{mn}^{\rho}+a_{mn}^{z}A2_{mn}\\+as_{mn}^{z}B2_{mn}+b_{mn}^{\phi}A3_{mn}+bs_{mn}^{\phi}B3_{mn}\end{array}\right\}$$

$$\left\{\sum_{m=0}^{M}\left[a_{mn}^{\phi}\cos\left(\frac{2m\pi}{p}z\right)+as_{mn}^{\phi}\sin\left(\frac{2m\pi}{p}z\right)\right]\right\}=a_{in}^{\phi}(z)+(\varepsilon_r-1)\sum_{m=0}^{M}\left\{\begin{array}{l}b_{mn}^{\rho}A4_{mn}+bs_{mn}^{\rho}B4_{mn}+b_{mn}^{z}A5_{mn}\\+bs_{mn}^{z}B5_{mn}+a_{mn}^{\phi}A6_{mn}+as_{mn}^{\phi}B6_{mn}\end{array}\right\}$$

$$\left\{\sum_{m=0}^{M}\left[a_{mn}^{z}\cos\left(\frac{2m\pi}{p}z\right)+as_{mn}^{z}\sin\left(\frac{2m\pi}{p}z\right)\right]\right\}=a_{in}^{z}(z)+(\varepsilon_r-1)\sum_{m=0}^{M}\left\{\begin{array}{l}a_{mn}^{\rho}A7_{mn}+as_{mn}^{\rho}B7_{mn}+a_{mn}^{z}A8_{mn}\\+as_{mn}^{z}B8_{mn}+b_{mn}^{\phi}A9_{mn}+bs_{mn}^{\phi}B9_{mn}\end{array}\right\}$$

$$\left\{\sum_{m=0}^{M}\left[b_{mn}^{\rho}\cos\left(\frac{2m\pi}{p}z\right)+bs_{mn}^{\rho}\cos\left(\frac{2m\pi}{p}z\right)\right]\right\}=b_{in}^{\rho}(z)+(\varepsilon_r-1)\sum_{m=0}^{M}\left\{\begin{array}{l}b_{mn}^{\rho}A1_{mn}+bs_{mn}^{\rho}B1_{mn}+b_{mn}^{z}A2_{mn}\\+bs_{mn}^{z}B2_{mn}-a_{mn}^{\phi}A3_{mn}-as_{mn}^{\phi}B3_{mn}\end{array}\right\}$$

$$
\text{(17) cont.}\begin{cases}
\sum_{m=0}^{M} \begin{Bmatrix} b^{\phi}_{mn}\cos(\frac{2m\pi}{P}z) \\ +bs^{\phi}_{mn}\sin(\frac{2m\pi}{P}z) \end{Bmatrix} = b^{\phi}_{in}(z) + (\varepsilon_r - 1)\sum_{m=0}^{M} \begin{Bmatrix} -a^{\rho}_{mn}A4_{mn} - as^{\rho}_{mn}B4_{mn} - a^{z}_{mn}A5_{mn} \\ -as^{z}_{mn}B5_{mn} + b^{\phi}_{mn}A6_{mn} + bs^{\phi}_{mn}B6_{mn} \end{Bmatrix} \\
\sum_{m=0}^{M} \begin{Bmatrix} b^{z}_{mn}\cos(\frac{2m\pi}{P}z) \\ +bs^{z}_{mn}\sin(\frac{2m\pi}{P}z) \end{Bmatrix} = b^{z}_{in}(z) + (\varepsilon_r - 1)\sum_{m=0}^{M} \begin{Bmatrix} b^{\phi}_{mn}A7_{mn} + bs^{\rho}_{mn}B7_{mn} + b^{z}_{mn}A8_{mn} \\ +bs^{z}_{mn}B8_{mn} - a^{\phi}_{mn}A9_{mn} - as^{\phi}_{mn}B9_{mn} \end{Bmatrix}
\end{cases}
$$

The $a^{\rho}_{in}(z)$, $a^{\phi}_{in}(z)$, etc. are the n-th mode expansion coefficients in the Fourier expansion (in ϕ) of the incident field at the particular matching ring in question.

B. Incident Field Expansion

In general, the incident field may be very complex, e.g., the near field of an antenna. To illustrate the technique, however, we shall consider the case for which the incident field is a linearly polarized plane wave with arbitrary propagation angle θ. For this case a formula for the Fourier expansion of the incident field can be found quite readily.

The Fourier expansion of the incident plane wave over a ring of radius a can be found from the general form of the plane wave at any point in space. Fig. 3 illustrates the geometry.

The phase of the incident wave is relative to the origin and the rectangular field components have been converted to circular cylindrical components in the equations below.

For the TE case, the incident electric field is given by:

$$
\text{(18)} \qquad \underline{E}^{TE}_{i}(\rho,\phi,z) = (\hat{\rho}\cos\phi - \hat{\phi}\sin\phi)\, e^{+jk\rho\sin\phi\sin\theta}\, e^{+jkz\cos\theta}
$$

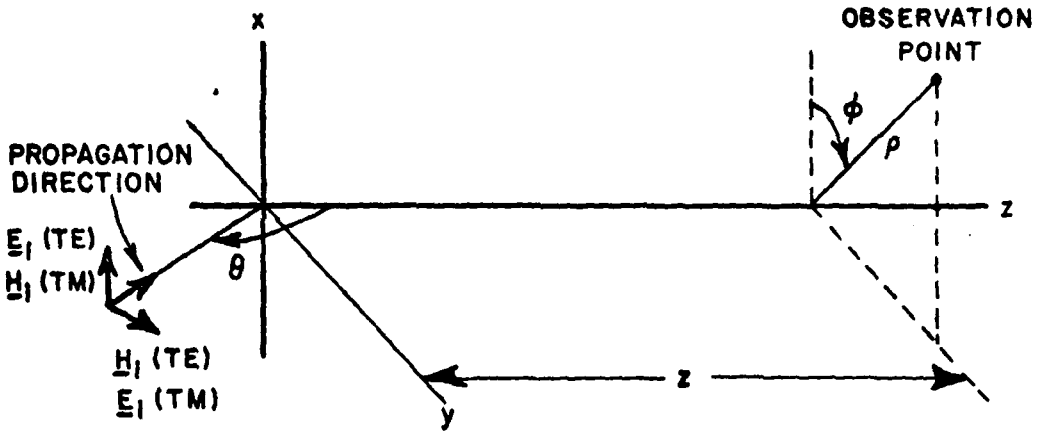

Fig. 3--Linearly polarized incident plane wave.

The Fourier-Bessel expansion is needed:

$$(19) \qquad e^{ju\rho\sin\phi} = e^{ju\rho\cos(\phi-\frac{\pi}{2})} = \sum_{n=0}^{\infty} N_n j^n J_n(u\rho)\cos n(\phi-\tfrac{\pi}{2})$$

In Eq. (19), $u = k\sin\theta$

$$N_n = \begin{cases} 1 & n = 0 \\ 2 & n \geq 1 \end{cases}$$

J_n is the n-th order Bessel function of the first kind.

Equation (19) is used in Eq. (18) and after simplification, the TE incident field can be expressed by the following Fourier expansion:

$$(20)\quad \underline{E}_i^{TE}(\rho,\phi,z) = \hat{\rho}\left\{\sum_{n=1,3,5\ldots}[J_{n-1}(u\rho)+J_{n+1}(u\rho)]\cos n\phi + \sum_{n=2,4,6\ldots} j\,[J_{n-1}(u\rho)+J_{n+1}(u\rho)]\sin n\phi\right\}e^{jkz\cos\theta}$$

$$+\hat{\phi}\left\{-j\,J_1(u\rho) + \sum_{n=1,3,5\ldots} -[J_{n-1}(u\rho)-J_{n+1}(u\rho)]\sin n\phi + \sum_{n=2,4,6\ldots} j\,[J_{n-1}(u\rho)-J_{n+1}(u\rho)]\cos n\phi\right\}e^{jkz\cos\theta}$$

For the TM case, the incident electric field is given by:

$$(21)\quad \underline{E}_i^{TM} = (\hat{\rho}\cos\theta\sin\phi + \hat{\phi}\cos\theta\cos\phi - \hat{z}\sin\theta)\,e^{ju\rho\sin\phi}e^{jkz\cos\theta}$$

Comparison with Eq. (18) shows that with the exception of the z-component, the TM expansion can be obtained directly by using the results of the TE expansion. The final result is:

$$(22)\quad \underline{E}_i^{TM}(\rho,\phi,z) = \hat{\rho}\cos\left\{j\,J_1(u\rho) + \sum_{n=1,3,5\ldots}[J_{n-1}(u\rho)-J_{n+1}(u\rho)]\sin n\phi + \sum_{n=2,4,6\ldots} -j\,[J_{n-1}(u\rho)-J_{n+1}(u\rho)]\cos n\phi\right\}e^{jkz\cos\theta}$$

$$+\hat{\phi}\cos\theta\left\{\sum_{n=1,3,5\ldots}[J_{n-1}(u\rho)+J_{n+1}(u\rho)]\cos n\phi + \sum_{n=2,4,6\ldots} j\,[J_{n-1}(u\rho)+J_{n+1}(u\rho)]\sin n\phi\right\}e^{jkz\cos\theta}$$

(22) cont.

$$- \hat{z} \sin\theta \left\{ J_0(ua) + \sum_{n=2,4,6\ldots} 2J_n(u\rho) \cos n\phi + \sum_{n=1,3,5\ldots} j2\, J_n(u\rho) \sin n\phi \right\} e^{jkz\cos\theta}$$

The Fourier expansions over a ring of radius a can be found by substituting a for ρ in Eqs. (20) and (22).

CHAPTER IV

INTEGRATION PROCEDURES

This Chapter discusses the techniques of numerical integration used in the solution of the cylindrical shell scattering problem. The general method of calculating the scattered field in the shell, the formula for handling integration through the singular points and the formulas for calculation of the far scattered fields are discussed.

A., General

The coefficients defined in Eq. (16) must be evaluated at $\phi = 0$ for each value of the ϕ mode index n and the z-mode index m at each of the matching rings. The general procedure for the numerical integration is to divide the shell into elemental rings as shown in Fig. 2. The integrals are then calculated over each ring for each of the match points at $\phi = 0$ and the total integration is obtained by adding the contribution of all the rings.

Integration over a given elemental ring is accomplished by dividing the ring into a number of subcells as shown in Fig. 4. The maximum arc-length of any subcell is much less than a free space wavelength and the angle subtended by the subcell at the ring center is small compared with the smallest period needed in the ϕ-expansion.

For the case of a match point far from a given ring, the trapezoidal rule of numerical integration is applied over the entire ring with the center of each subcell providing one data point. For the case of a match point close to the ring, finer subdivision of the cells closest

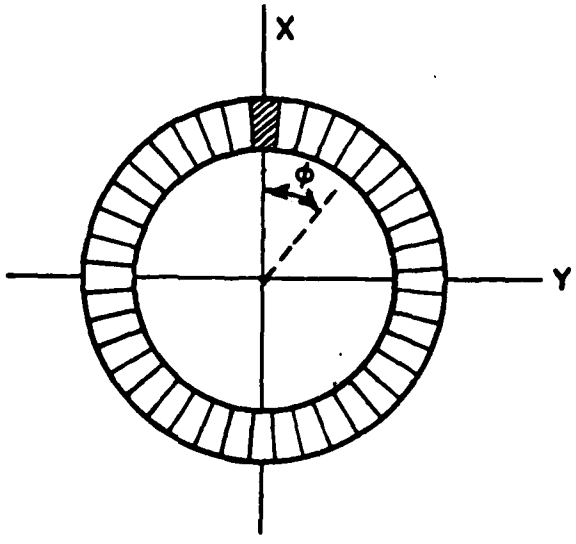

Fig. 4--Ring subdivision for numerical integration.

to the match point is required to obtain accurate results.

The case in which the match point is within the ring being integrated over is a rather special one. Examination of P(r) and Q(r) in Eq. (10) reveals that one can expect severe numerical computation problems as r approaches zero. In this case, the usual numerical integration procedure (including finer subdivision for cells near the match point) is used to calculate the contribution of all the parts of the ring except for that of the cross-hatched cell in Fig. 4; this cell is the so-called singular cell.

The contribution of the singular cell at its center is then calculated from analytical formulas. These formulas are derived in the next section.

B. The Field at the Center of the Singular Cell

Three basic assumptions are used to obtain the singular cell contribution at its own center. First, it is assumed that the cell can be closely approximated by a rectangular parallelopiped. Second, the cell is assumed sufficiently small that any field variations within its volume can be neglected. Finally, the linear dimensions of the singular cell are assumed to be much smaller than the wavelength.

The rectangular parallelopiped is a suitable approximation to the shape of the singular cell in an elemental ring of a thin cylindrical shell.

The second assumption is also valid since the odd symmetry of the sin $n\phi$ mode about the center plane of the singular cell can be shown to result in zero field at the cell center due to sin $n\phi$ current densities. This leaves only the cos $n\phi$ variation with ϕ and this term has a zero slope at the center plane of the cell. The period of the z-expansion is assumed large enough that variations with z along the singular cell can be safely neglected.

The singular cell problem is therefore reduced to finding the electric field at the center of a rectangular box of uniform current density flowing in an arbitrary direction. Consider the box of current density to be aligned with a local cartesian coordinate system with the origin at the center of the box as shown in Fig. 5.

Examination of the symmetry of Eq. (9) for this case shows that only J^x will contribute to E^x, J^y to E^y and J^z to E^z. Thus, the solution needs to be developed for only one component of current and a

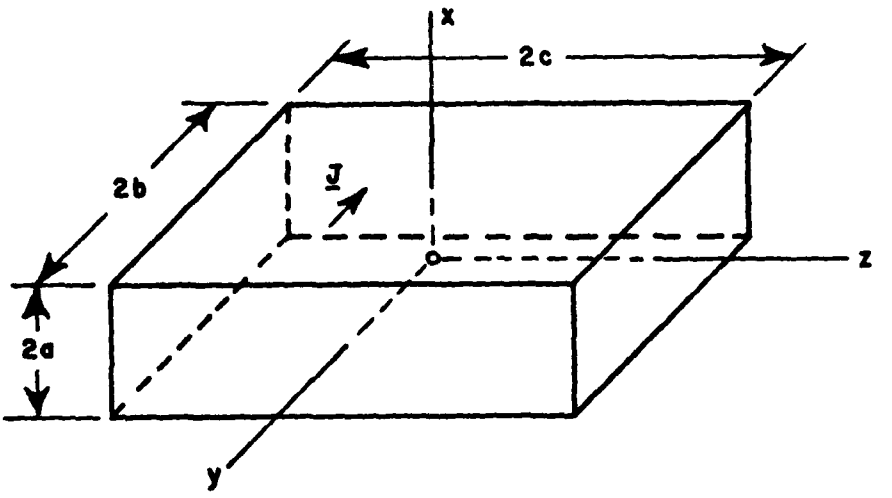

Fig. 5--Rectangular parallelopiped of current density $\underline{J}$.

cyclic rotation of the coordinates will give the solutions for the other components. The solution will be found for $\underline{J} = \hat{x}\, J^x$.

Consider Maxwell's curl equation relating the electric field to the curl of the magnetic field:

$$\underline{E} = \frac{1}{j\omega\epsilon_0} [\nabla \times \underline{H} - \underline{J}] \tag{23}$$

$\underline{J}$ is assumed known and uniform in the small box. In order to evaluate the field of this source at the center of the box, then, $\nabla \times \underline{H}$ must be found at the center.

By symmetry, for this particular problem, there will be no magnetic field at the center of the box, nor will there be any magnetic field

whatever at any point on the x-axis (for an x-directed current density). Thus, for this case, $H^x(x,o,o) = 0$ and $\frac{\partial H^y}{\partial X} = \frac{\partial H^z}{\partial X} = 0$. The curl operation on $\underline{H}$ can therefore be written as follows:

$$(24) \qquad \nabla \times \underline{H}\Big|_{(o,o,o)} = \begin{vmatrix} \hat{x} & \hat{y} & \hat{z} \\ 0 & \frac{\partial}{\partial y} & \frac{\partial}{\partial z} \\ 0 & H^y & H^z \end{vmatrix}_{(o,o,o)} = \hat{x}\left[\frac{\partial H^z}{\partial y} - \frac{\partial H^y}{\partial z}\right]_{(o,o,o)}$$

The partial derivatives of H^z and H^y will be found by evaluating the magnetic field at the center of the box (known by symmetry to be zero) and at a small distances Δy and Δz along the y-and z-axes. The partial derivatives are then found from the definition:

$$(25) \qquad \begin{cases} \frac{\partial H^y}{\partial z} = \lim_{\Delta z \to 0} \frac{\Delta H^y}{\Delta z} = \lim_{\Delta z \to 0} \frac{H^y(o,o,\Delta z) - H^y(o,o,o)}{\Delta z} \\ \\ \frac{\partial H^z}{\partial y} = \lim_{\Delta y \to 0} \frac{\Delta H^y}{\Delta z} = \lim_{\Delta y \to 0} \frac{H^z(o,\Delta y,o) - H^z(o,o,o)}{\Delta y} \end{cases}$$

Fig. 6 shows a view looking down the x-axis at the box of current. From symmetry considerations, it can be seen that Region I will not contribute to the magnetic field at $(o,\Delta y,o)$, the magnetic field at that point will be strictly due to Region II. Fig. 7 shows the geometry which is now considered. For the special case when the distance and dimensions are small compared to the wavelength, the x-component of the magnetic field at a point a distance $y = b$ from the center of the slab of current can be shown to be:

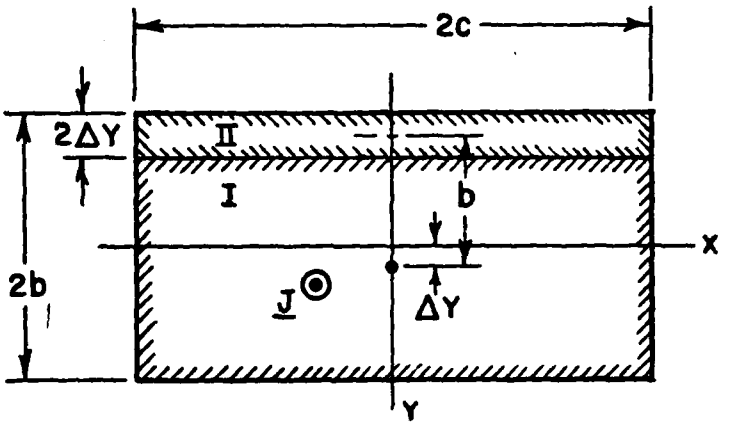

Fig. 6--View of the box of current from the positive x-axis.

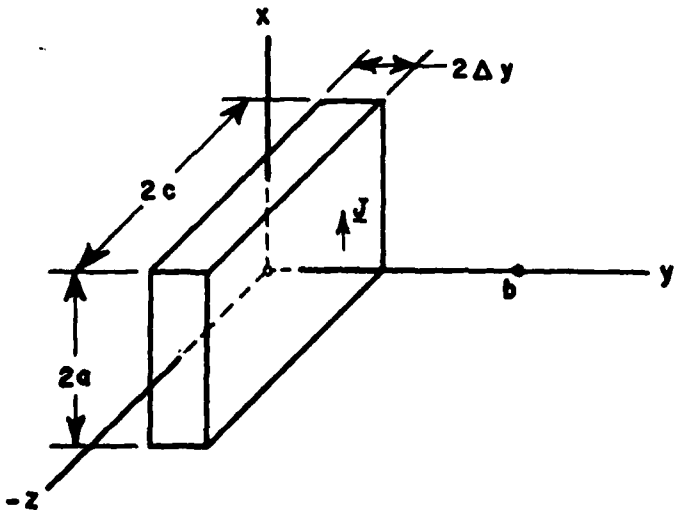

Fig. 7--Geometry for calculation of magnetic field.

$$(26) \qquad H^z = \frac{2J^x \Delta y}{\pi} \tan^{-1}\left(\frac{ac}{b\sqrt{a^2+b^2+c^2}}\right)$$

Similarly, the y-component of the field a distance z=c along the z-axis can be shown to be:

$$(27) \qquad H^y = -\frac{2J^x \Delta z}{\pi} \tan^{-1}\left(\frac{ab}{c\sqrt{a^2+b^2+c^2}}\right)$$

Reference to Fig. 6 reveals that the incremental fields sought are those fields just calculated. Namely,

$$(28) \qquad \begin{cases} H^z(0,\Delta y,0) = \dfrac{2J^x y}{\pi} \tan^{-1}\left(\dfrac{ac}{b\sqrt{a^2+b^2+c^2}}\right) \\ H^y(0,0,z) = -\dfrac{2J^x \Delta z}{\pi} \tan^{-1}\left(\dfrac{ab}{c\sqrt{a^2+b^2+c^2}}\right) \end{cases}$$

These are used in Eq. (25) to find:

$$(29) \qquad \begin{cases} \dfrac{\partial H^y}{\partial z} = -\dfrac{2J^x}{\pi} \tan^{-1}\left(\dfrac{ab}{c\sqrt{a^2+b^2+c^2}}\right) \\ \dfrac{\partial H^z}{\partial y} = \dfrac{2J^x}{\pi} \tan^{-1}\left(\dfrac{ac}{b\sqrt{a^2+b^2+c^2}}\right) \end{cases}$$

Use of Eq. (29) in Eq.(23) gives the final result for the electric field at the center of a box of x-directed current density J^x:

$$(30)\qquad E^x = \frac{1}{j\omega\varepsilon_0}\left\{\frac{2J^x}{\pi}\left[\tan^{-1}\left(\frac{ac}{b\sqrt{a^2+b^2+c^2}}\right)+\tan^{-1}\left(\frac{ab}{c\sqrt{a^2+b^2+c^2}}\right)\right]-J^x\right\}$$

Similarly, for E^y and E^z,

$$(31)\qquad E^y = \frac{1}{j\omega\varepsilon_0}\left\{\frac{2J^y}{\pi}\left[\tan^{-1}\left(\frac{ba}{c\sqrt{a^2+b^2+c^2}}\right)+\tan^{-1}\left(\frac{bc}{a\sqrt{a^2+b^2+c^2}}\right)\right]-J^y\right\}$$

$$(32)\qquad E^z = \frac{1}{j\omega\varepsilon_0}\left\{\frac{2J^z}{\pi}\left[\tan^{-1}\left(\frac{cb}{a\sqrt{a^2+b^2+c^2}}\right)+\tan^{-1}\left(\frac{ca}{b\sqrt{a^2+b^2+c^2}}\right)\right]-J^z\right\}$$

If J^x, J^y and J^z are replaced by the equivalent currents of Eq. (4), we have directly the scattered fields at the center of the singular cell contributed by the current in that cell:

$$(33)\qquad \begin{cases} E_s^x = (\varepsilon_r-1)\,E^x\left\{\frac{2}{\pi}\left[\tan^{-1}\left(\frac{ac}{b\sqrt{a^2+b^2+c^2}}\right)+\tan^{-1}\left(\frac{ab}{c\sqrt{a^2+b^2+c^2}}\right)\right]-1\right\} \\ E_s^y = (\varepsilon_r-1)\,E^y\left\{\frac{2}{\pi}\left[\tan^{-1}\left(\frac{ba}{c\sqrt{a^2+b^2+c^2}}\right)+\tan^{-1}\left(\frac{bc}{a\sqrt{a^2+b^2+c^2}}\right)\right]-1\right\} \\ E_s^z = (\varepsilon_r-1)\,E^y\left\{\frac{2}{\pi}\left[\tan^{-1}\left(\frac{cb}{a\sqrt{a^2+b^2+c^2}}\right)+\tan^{-1}\left(\frac{ca}{b\sqrt{a^2+b^2+c^2}}\right)\right]-1\right\} \end{cases}$$

It was pointed out earlier that within the singular cell, only the equivalent current component in the direction of one of the local coordinates will contribute to that component of the scattered field. The above formulas will therefore be applied only in calculating the values of coefficients in Eqs.(14) and (15) which represent self-coupling terms. For example, there will be singular cell contributions necessary in the

calculation of $Al_{mn}(z)$ and $Bl_{mn}(z)$ in Eq. (14) since these represent the "self-coupling" of E^{ρ} to E_s^{ρ}.

C. The Far Scattered Fields

This section gives the derivation of the formulas for the far scattered fields of a ring of current having ρ, ϕ and z components of current density. The far fields of a cylindrical shell of current are then obtained by superposition of the fields of the elemental rings making up the shell.

The far field of a source in terms of cylindrical source components as given by Richmond[28] is given in Eq.(34). The primed coordinates are the source coordinates and Fig. 8 defines the geometry for the far field calculation.

$$(34)\quad \begin{cases} E^{\theta} = \dfrac{j\omega\mu}{4\pi}\dfrac{e^{-jkr_o}}{r_o} \iiint_{V'} [-J^{\rho'}\cos(\phi-\phi')\cos\theta - J^{\phi'}\sin(\phi-\phi')\cos\theta \\ \qquad + J^{z'}\sin\theta]\, e^{jk[\rho'\cos(\phi-\phi')\sin\theta + z'\cos\theta]} \cdot \rho'\, d\rho'\, dz'\, d\phi' \\ E^{\phi} = \dfrac{j\omega\mu}{4\pi}\dfrac{e^{-jkr_o}}{r_o} \iiint_{V'} [J^{\rho'}\sin(\phi-\phi') - J^{\phi'}\cos(\phi-\phi')] \cdot \\ \qquad e^{jk[\rho'\cos(\phi-\phi')\sin\theta + z'\cos\theta]} \cdot \rho'\, d\rho'\, dz'\, d\phi' \end{cases}$$

For the case of a very short, thin ring, of length ℓ, thickness t and mean radius a, the integrations over ρ' and z' can be replaced by a multiplication by $(t\cdot\ell)$. In addition, if we replace J^{ρ}, J^{ϕ} and J^{z} by

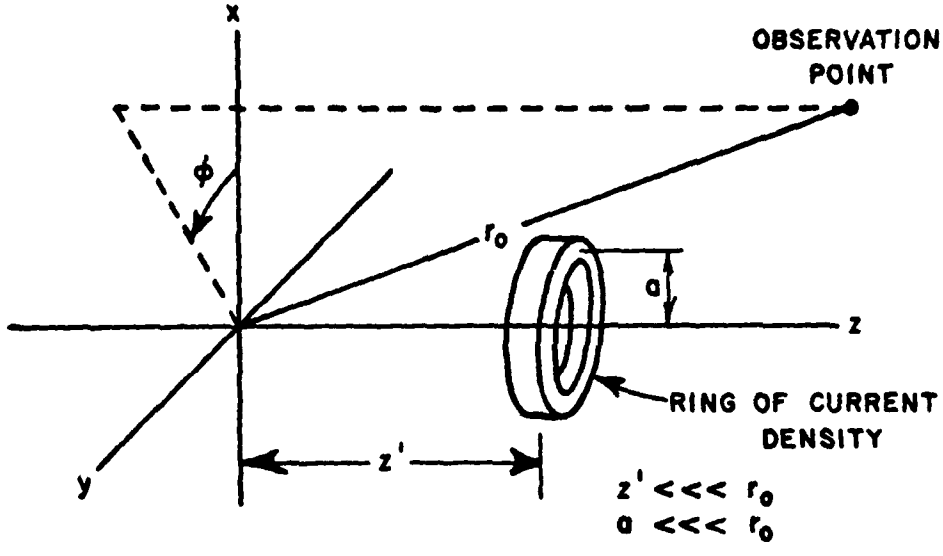

Fig. 8--Geometry for the far field calculation.

the equivalent current of Eqs. (4), we find, for the scattered fields,

$$
(35)\quad
\begin{cases}
E_s = \dfrac{k^2-k_\epsilon^2}{4\pi}\ \dfrac{e^{-jkr_o}}{r_o}\ e^{+jk\,z'\cos\theta}\ (\,t\cdot\ell\cdot a)\cdot \\
\qquad \displaystyle\int_0^{2\pi} [E^{\rho'}\cos\theta\cos(\phi-\phi') - E^{\phi'}\sin(\phi-\phi')\cos\theta \\
\qquad\qquad + E^{z'}\sin\theta]\ e^{jka\sin\theta\ \cos(\phi-\phi')}\ d\phi' \\
E_s^{\phi} = \dfrac{k^2-k_\epsilon^2}{4\pi}\ \dfrac{e^{-jkr_o}}{r_o}\ e^{jkz'\cos\theta}(t\cdot\ell\cdot a)\cdot \\
\qquad \displaystyle\int_0^{2\pi} [E^{\rho'}\sin(\phi-\phi') - E^{\phi'}\cos(\phi-\phi')]\ e^{jka\sin\theta\ \cos(\phi-\phi')}\ d\phi',
\end{cases}
$$

where $k^2 - k_\varepsilon^2 = \omega^2\mu_0(\varepsilon_0-\varepsilon)$.

The field expansion of Eqs. (7) and (8) is used in Eq. (35) and, in addition we let $c_m = \cos(\frac{2m\pi}{p}z)$, $s_m = \sin(\frac{2m\pi}{p}z)$ and

$$\underline{K} = (t\cdot\ell\cdot a)\,\frac{k^2-k_\varepsilon^2}{4\pi}\,\frac{e^{-jkr_o}}{r_o}\,e^{jkz'\cos\theta}$$

in order to find (for the n-th mode in ϕ):

$$
\begin{cases}
E^{\theta}_{sn} = \underline{K}\sum_{m=0}^{M}\Big\{ c_m \int_0^{2\pi} \big[-(a^{\rho}_{mn}\cos n\phi' + b^{\rho}_{mn}\sin n\phi')\cos\theta\ \cos(\phi-\phi') \\
\quad -(a^{\phi}_{mn}\cos n\phi' + b^{\phi}_{mn}\sin n\phi')\cos\theta\ \sin(\phi-\phi') \\
\quad +(a^{z}_{mn}\cos n\phi' + b^{z}_{mn}\sin n\phi')\sin\theta\big]\ e^{jka\sin\theta\ \cos(\phi-\phi')}d\phi' \\
\quad + s_m \int_0^{2\pi} \big[-(as^{\rho}_{mn}\cos\phi' + bs^{\rho}_{mn}\sin n\phi')\cos\theta\ \cos(\phi-\phi') \\
\quad -(as^{\phi}_{mn}\cos n\phi' + bs^{\phi}_{mn}\sin n\phi')\cos\theta\ \sin(\phi-\phi') \\
\quad +(as_{mn}\cos n\phi' + bs^{z}_{mn}\sin n\phi')\sin\theta\big]\ e^{jka\sin\theta\ \cos(\phi-\phi')}d\phi'\Big\} \\
E^{\phi}_{sn} = \underline{K}\sum_{m=0}^{M}\Big\{ c_m \int_0^{2\pi} \big[(a^{\rho}_{mn}\cos n\phi' + b^{\rho}_{mn}\sin n\phi')\sin(\phi-\phi') \\
\quad -(a^{\phi}_{mn}\cos n\phi' + b^{\phi}_{mn}\sin n\phi')\cos(\phi-\phi')\big]\ e^{jka\sin\theta\ \cos(\phi-\phi')}d\phi' \\
\quad + s_m \int_0^{2\pi} \big[(as^{\rho}_{mn}\cos n\phi' + bs^{\rho}_{mn}\sin n\phi')\sin(\phi-\phi') \\
\quad -(as^{\phi}_{mn}\cos n\phi' + bs^{\phi}_{mn}\sin n\phi')\cos(\phi-\phi')\big]\ e^{jka\sin\theta\ \cos(\phi-\phi')}d\phi\Big\}
\end{cases}
\tag{36}
$$

For the cases considered in this paper the incident field is a plane wave at $\phi = \frac{\pi}{2}$. If this value of ϕ and the Fourier-Bessel series (Eq. (19)) are used in Eq. (36), the final result for the far scattered fields of a ring of "equivalent current density" can be shown to be:

$$
\left.
\begin{aligned}
E^{\theta}_{sn} = \pi \underline{K} \sum_{m=0}^{M} \Bigg\{ & \begin{bmatrix} c_m(b^{\rho}_{mn} - a^{\phi}_{mn}) \\ +s_m(bs^{\rho}_{mn} - as^{\phi}_{mn}) \end{bmatrix} \cos\theta \;\; \cos(n+1)\tfrac{\pi}{2} \cdot j^{n+1} \cdot J_{n+1}(ua) \\
& \begin{bmatrix} c_m(-b^{\rho}_{mn} - a^{\phi}_{mn}) \\ +s_m(-bs^{\rho}_{mn} - as^{\phi}_{mn}) \end{bmatrix} \cos\theta \;\; \cos(n-1)\tfrac{\pi}{2} \cdot j^{|n-1|} J_{|n-1|}(ua) \\
& + \begin{bmatrix} c_m(-a^{\rho}_{mn} - b^{\phi}_{mn}) \\ +s_m(-as^{\rho}_{mn} - bs^{\phi}_{mn}) \end{bmatrix} \cos\theta \;\; \sin(n+1)\tfrac{\pi}{2} \cdot j^{n+1} \cdot J_{n+1}(ua) \\
& + \begin{bmatrix} c_m(a^{\rho}_{mn} - b^{\phi}_{mn}) \\ +s_m(as^{\rho}_{mn} - bs^{\phi}_{mn}) \end{bmatrix} \cos\phi \;\; \sin(n-1)\tfrac{\pi}{2} \cdot j^{|n-1|} \cdot J_{|n-1|}(ua) \\
& + 2 \begin{bmatrix} (c_m a^{z}_{mn} + s_m as^{z}_{mn}) \cos n\tfrac{\pi}{2} \\ +(c_m b^{z}_{mn} + s_m bs^{z}_{mn}) \sin n\tfrac{\pi}{2} \end{bmatrix} \sin\theta \cdot j^{n} J_n(ua) \Bigg\} \\
E^{\phi}_{sn} = \pi \underline{K} \sum_{m=0}^{M} \Bigg\{ & \begin{bmatrix} c_m(a^{\rho}_{mn} + b^{\phi}_{mn}) \\ +s_m(as^{\rho}_{mn} + bs^{\phi}_{mn}) \end{bmatrix} \cos(n+1)\tfrac{\pi}{2} \cdot j^{n+1} \cdot J_{n+1}(ua) \\
& + \begin{bmatrix} c_m(a^{\rho}_{mn} - b^{\phi}_{mn}) \\ +s_m(as^{\rho}_{mn} - bs^{\phi}_{mn}) \end{bmatrix} \cos(n-1)\tfrac{\pi}{2} \cdot j^{|n-1|} \cdot J_{|n-1|}(ua) \\
& + \begin{bmatrix} c_m(b^{\rho}_{mn} - a^{\phi}_{mn}) \\ +s_m(bs^{\rho}_{mn} - as^{\phi}_{mn}) \end{bmatrix} \sin(n+1)\tfrac{\pi}{2} \cdot j^{n+1} \cdot J_{n+1}(ua) \\
& + \begin{bmatrix} c_m(b^{\rho}_{mn} + a^{\phi}_{mn}) \\ +s_m(bs^{\rho}_{mn} + as^{\phi}_{mn}) \end{bmatrix} \sin(n-1)\tfrac{\pi}{2} \cdot j^{|n-1|} \cdot J_{|n-1|}(ua) \Bigg\}
\end{aligned}
\right\} \quad (37)
$$

The scattering cross section of a scattering body is defined as follows:

$$\sigma(\theta,\phi) = \lim_{r \to \infty} 4\pi r^2 \frac{|E_s(\theta,\phi)|^2}{|E_i|^2} \tag{38}$$

In order to calculate the scattering cross section, then it is simply a matter of calculating the far scattered field and then applying Eq. (38). It should be noted that $\underline{\overline{K}}$ in Eq. (37) involves a factor $1/r$ which eliminates the r^2 in Eq. (38). E_i, of course, is the field incident upon the body and in this case is taken to be of unit magnitude so that $|E_i|^2 = 1$.

CHAPTER V

COMPARISON OF CALCULATED AND MEASURED RESULTS

The cases considered are all for the backscattering of a linearly polarized plane wave incident on a homogeneous cylindrical shell and parallel to the plane $\phi = \frac{\pi}{2}$. The wave is polarized TE (transverse electric) or TM (transverse magnetic) to the shell axis and has a propagation angle θ with respect to the shell axis.

A. Dielectric Ring Backscattering

The first case considered is for the plane wave incident along the ring axis. This is followed by a calculation for both TE and TM plane waves with arbitrary incidence angles. For arbitrary incidence, many modes in ϕ are needed to obtain the field in the ring. Figure 9 illustrates the geometry.

The ring is sufficiently short that only the zero order mode of the z-expansion is needed. Because of the symmetries in this case, many of the integrals in Eq. (16) are equal to zero and considerable simplification of Eq. (17) results. The set of simultaneous equations for the n-th mode in ϕ is as follows:

$$
(39)\quad \begin{cases}
a^{\rho}_{on} = a^{\rho}_{in} + (\varepsilon_r - 1)\,\{a^{\rho}_{on}\, A1_{on} + b^{\phi}_{on} A3_{on}\} \\
b^{\phi}_{on} = b^{\phi}_{in} + (\varepsilon_r - 1)\,\{-a^{\rho}_{on}\, A4_{on} + b^{\phi}_{on} A6_{on}\} \\
a^{\phi}_{on} = a^{\phi}_{in} + (\varepsilon_r - 1)\,\{b^{\rho}_{on}\, A4_{on} + a^{\phi}_{on}\, A6_{on}\} \\
b^{\rho}_{on} = b^{\rho}_{in} + (\varepsilon_r - 1)\,\{b^{\rho}_{on}\, A1_{on} - a^{\phi}_{on}\, A3_{on}\}
\end{cases}
$$

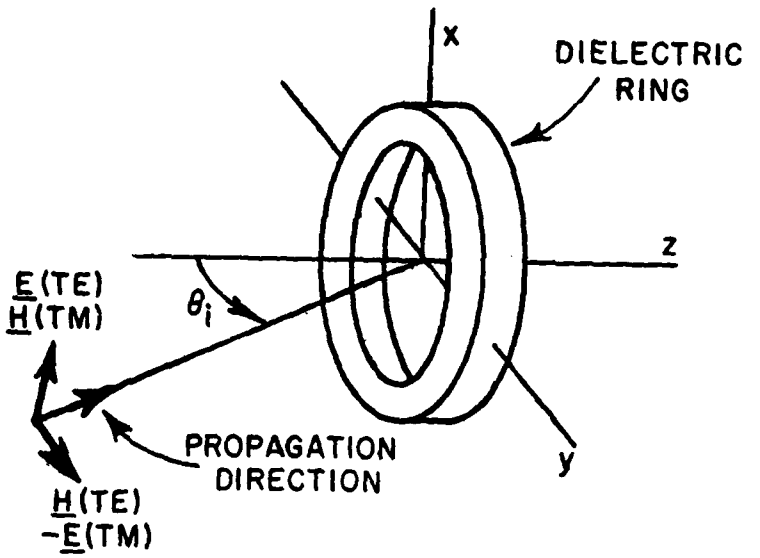

Fig. 9--Geometry of dielectric ring problem

(39) cont.

$$\begin{cases} a^z_{on} = a^z_{in} + (\epsilon_r - 1)\ \{a^z_{on}\ A8_{on}\} \\ b^z_{on} = b^z_{in} + (\epsilon_r - 1)\ \{b^z_{on}\ A8_{on}\} \end{cases}$$

These become the following sets of linear equations:

(40)

$$\begin{cases} a^\rho_{on}\ [1 - (\epsilon - 1)\ A1_{on}] - b^\phi_{on}\ [(\epsilon_r - 1)\ A3_{on}] = a^\rho_{in} \\ a^\rho_{on}\ [(\epsilon_r - 1)\ A4_{on}] + b^\phi_{on}\ [1 - (\epsilon_r - 1)\ A6_{on}] = b^\phi_{in} \\ a^\phi_{on}\ [1 - (\epsilon_r - 1)\ A6_{on}] - b^\rho_{on}\ [(\epsilon_r - 1)\ A4_{on}] = a^\phi_{in} \\ a^\phi_{on}\ [(\epsilon_r - 1)\ A3_{on}] + b^\rho_{on}\ [1 - (\epsilon_r - 1)\ A1_{on}] = b^\rho_{in} \end{cases}$$

$$(40)\ \text{cont.} \quad \begin{cases} a^z_{on}\,[1 - (\varepsilon_r - 1)\ A8_{on}] = a^z_{in} \\ b^z_{on}\,[1 - (\varepsilon_r - 1)\ A8_{on}] = b^z_{in} \end{cases}$$

For a linearly polarized plane wave incident along the ring axis, only the $n = 1$ mode in ϕ is needed. This situation represents the utmost simplification of Eq. (17). Calculated and measured backscattering data are compared in Fig. 10 for several polystyrene rings of different radius where ε_r is taken to be 2.54-j 0.00. Each ring considered had a geometrical wall cross section 0.100" x 0.100". The scattering cross section was measured twice for each ring; where only one circle is evident, the experimental data were in nearly exact agreement for both measurements. The agreement between the calculated and measured results is seen to be excellent.

As can be seen from Eq. (16), the formulas defining the coefficients in the system of linear equations are independent of the dielectric constant. The dielectric constant appears only in the solution of the set of simultaneous equations and in the calculation of the far scattered fields; these two operations represent relatively efficient computer operations. (The numerical integrations and solution of the simultaneous linear equations occupy most of the computation-time. These need not be repeated for each new permittivity or loss tangent.) Thus, once the basic integrations have been performed, it is a matter requiring relatively little additional labor to calculate the effect of the dielectric constant and to include the effect of the loss tangent on the scattered fields. This is an interesting characteristic of the integral

equation approach to homogeneous dielectric scattering problems. Fig. 11 shows the calculated backscattering cross section versus

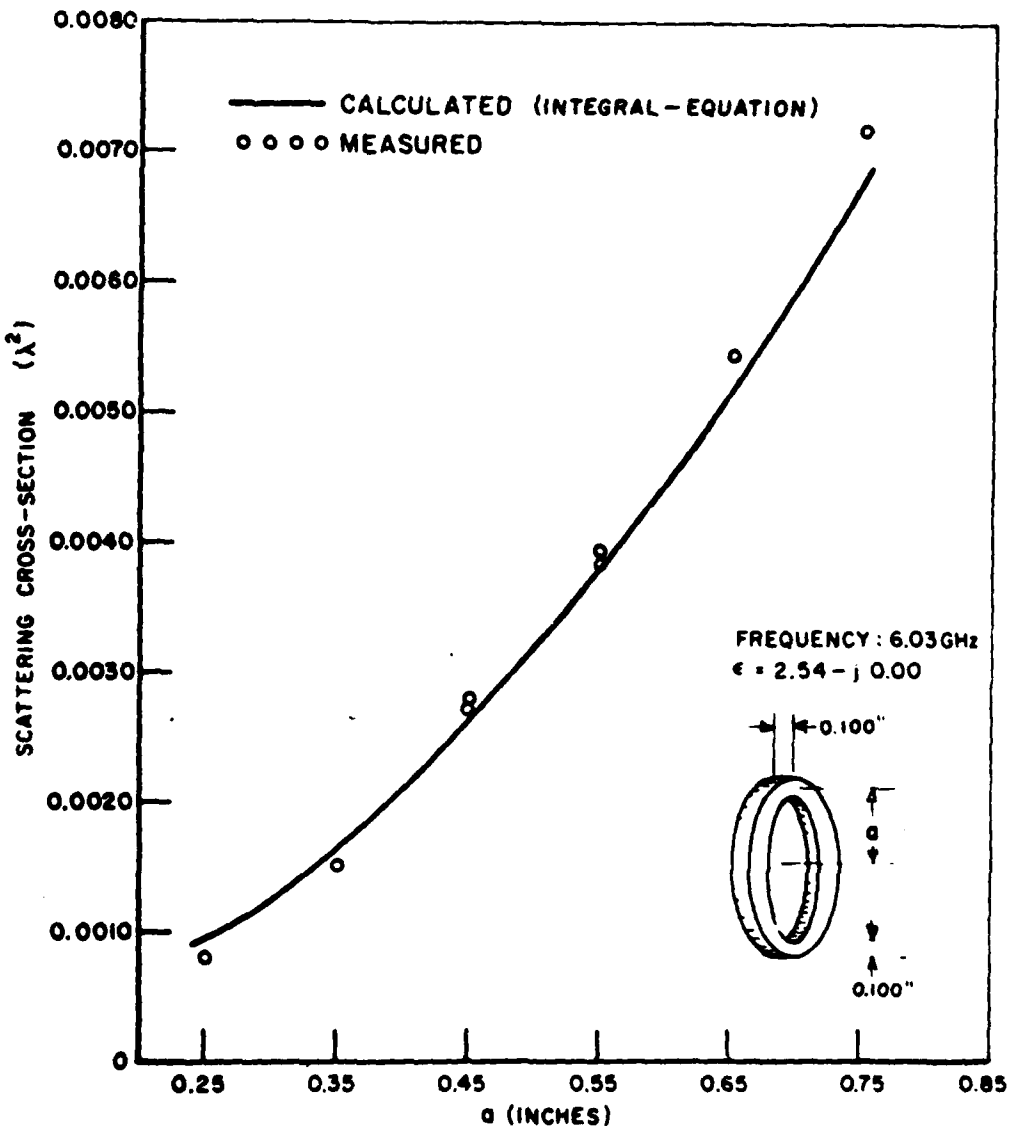

Fig. 10--Backscattering cross section versus mean ring radius for a polystyrene ring with a plane, linearly polarized wave incident on axis.

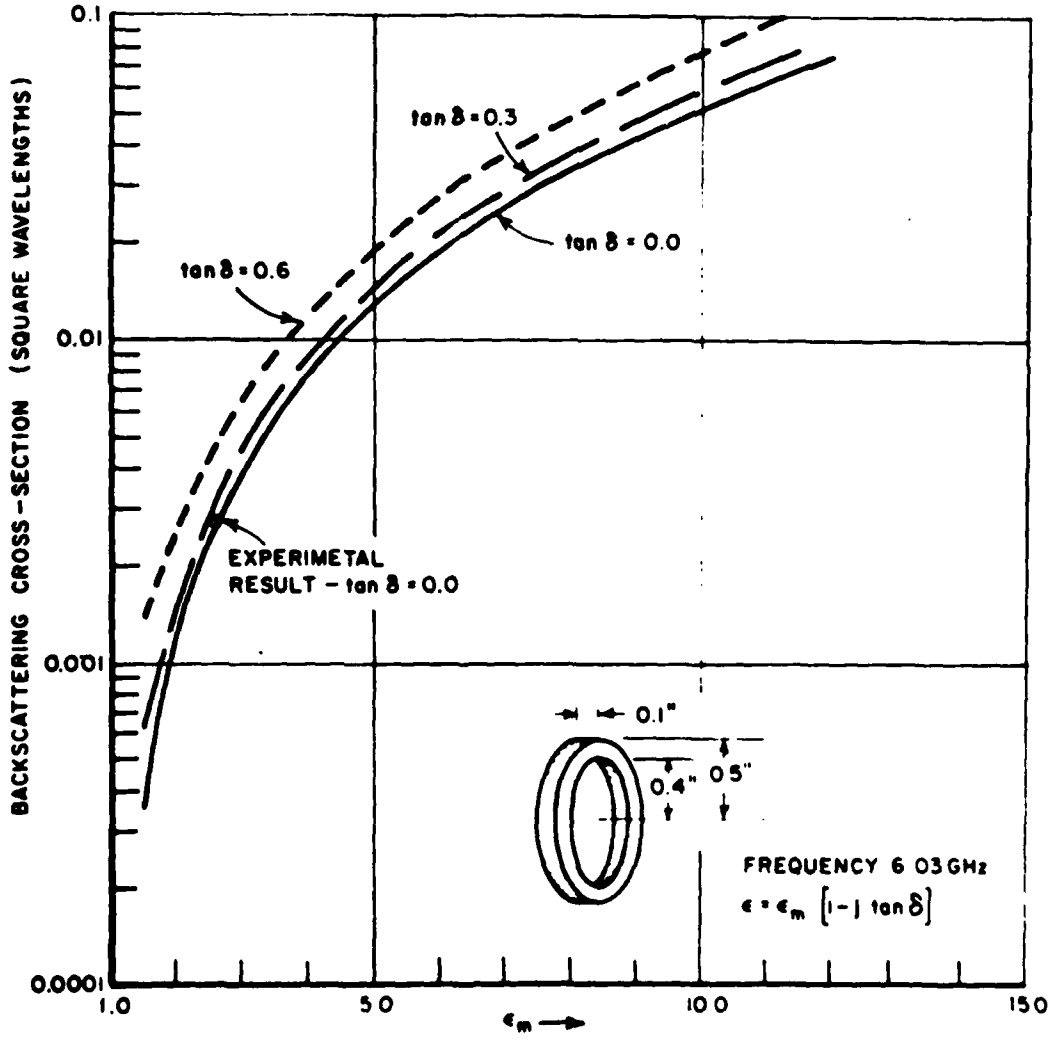

Fig. 11--Calculated backscattering cross section versus dielectric constant for the ring shown with a plane, linearly polarized wave incident on axis.

dielectric constant for a plane wave incident along the axis of a ring with an outer radius of 0.5 inches. The effect of the loss tangent is also included parametrically.

A comparison of the calculated and experimental backscattering cross section for TE or TM plane waves incident at an arbitrary incidence angle is presented next. Four polystyrene rings were considered. Calculations were performed for several incidence angles, out to nearly 90^{o}, for each ring. Both TE and TM backscattering patterns were measured for all four rings. Figures 12 through 19 show the comparison of the measured and calculated data. The agreement is seen to be excellent.

A portion of the small disagreement in the TE cases may arise from scattering from the support strings; the strings were parallel to the incident field in this case. For the TM case, the incident field was normal to the support strings and the string scattering was not so noticeable.

The number of modes in ϕ required for a particular ring scattering problem depend on the ring radius and the propagation angle of the incident field, i.e., the number of incident modes which have significant magnitude. In the case discussed here, both the incident modes and the far-field scattered modes contain factors $J_{n+1}(ua)$ or $J_{n-1}(ua)$; the problem of determining the necessary number of modes reduces to an examination of the Bessel functions of the first kind. In the examples presented here, the incident field modes became negligibly small for $n \geq 10$; therefore only ten ϕ-modes were required. For more complicated incident fields and for larger rings, more modes may be required; the exact number would of course depend on the accuracy desired.

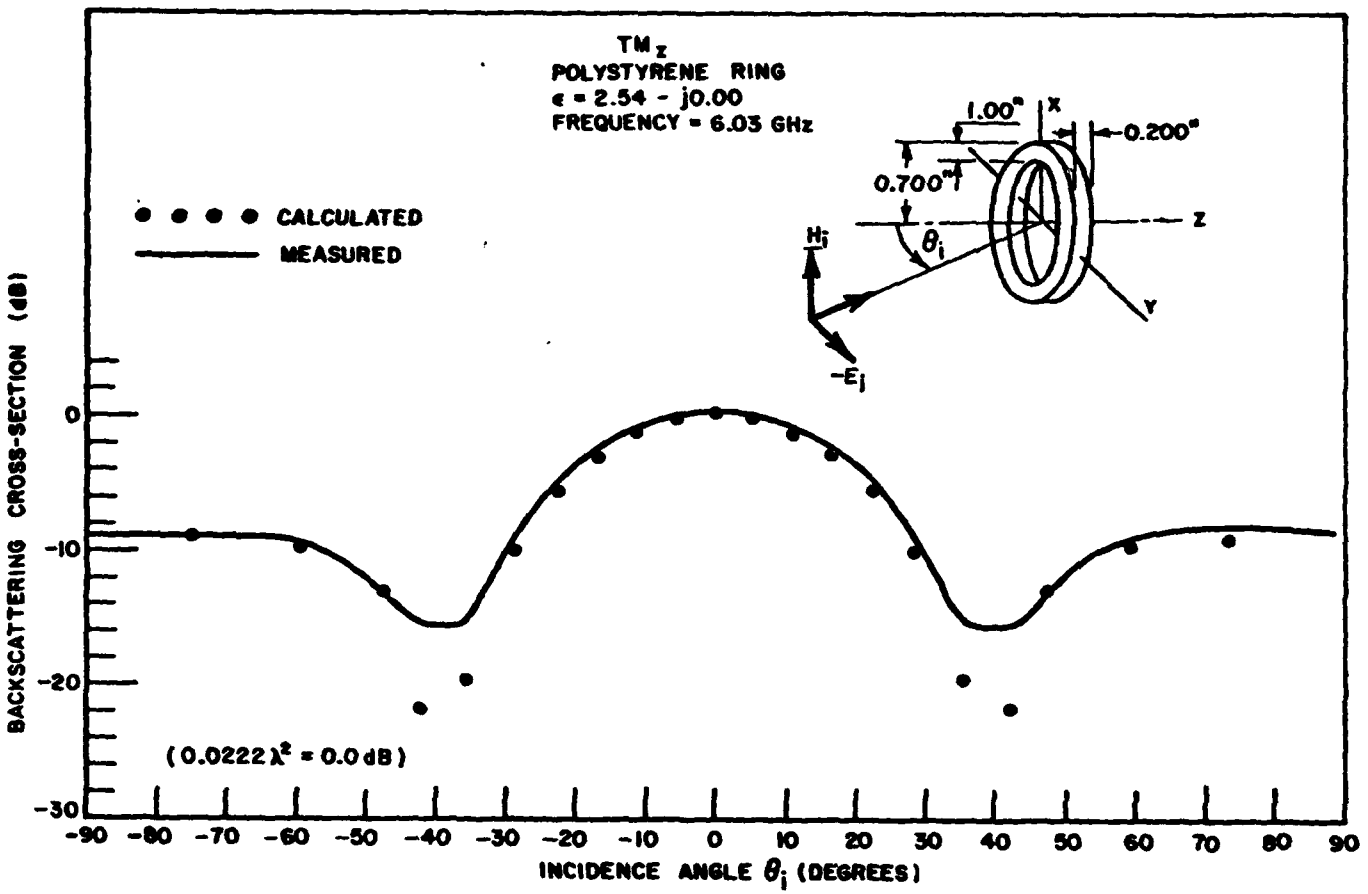

Fig. 12--Plot of backscattering cross section versus incidence angle for a TM_z plane wave incident on a dielectric ring.

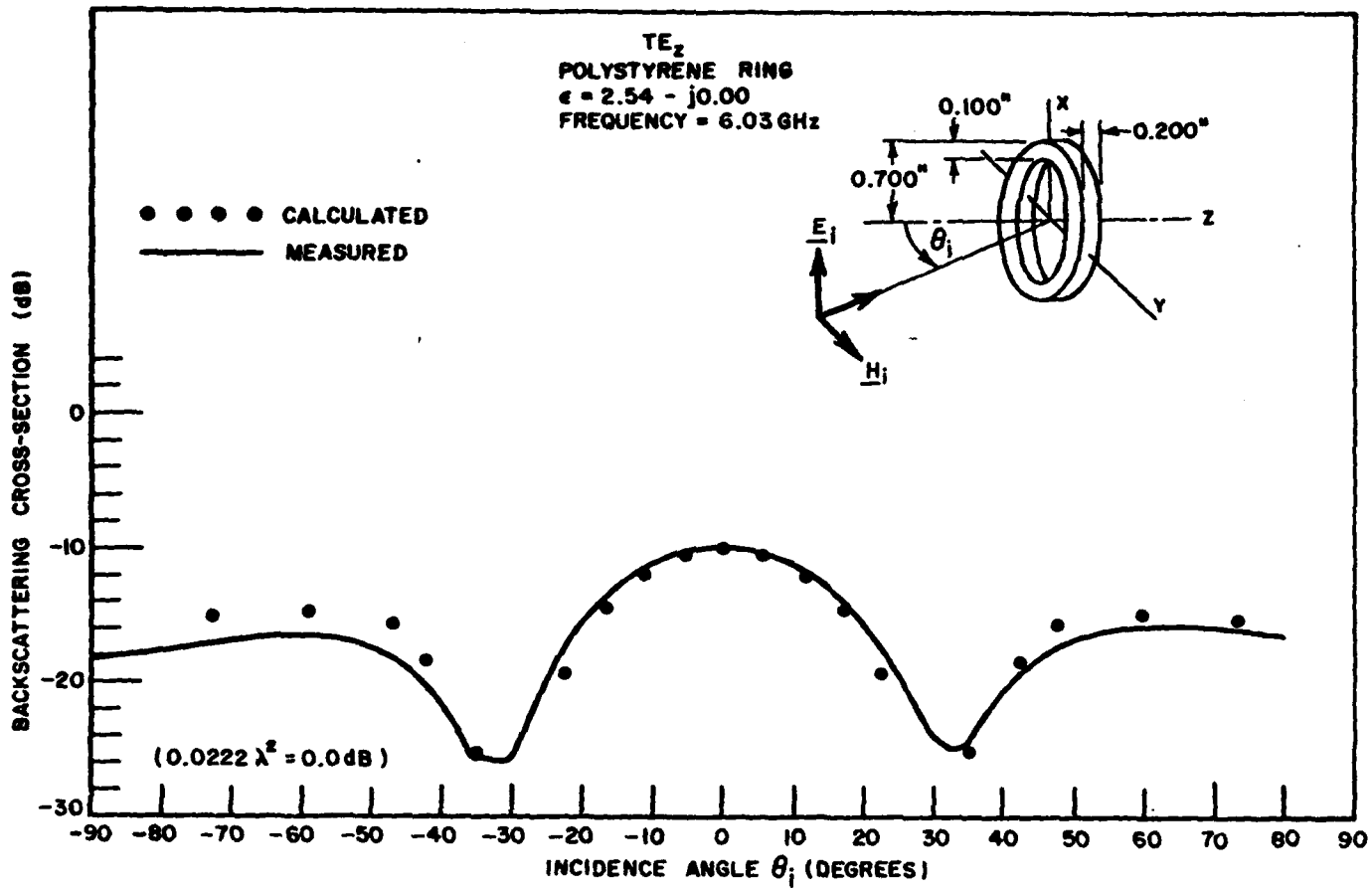

Fig. 13--Plot of backscattering cross section versus incidence angle for a TE_z plane wave incident on a dielectric ring.

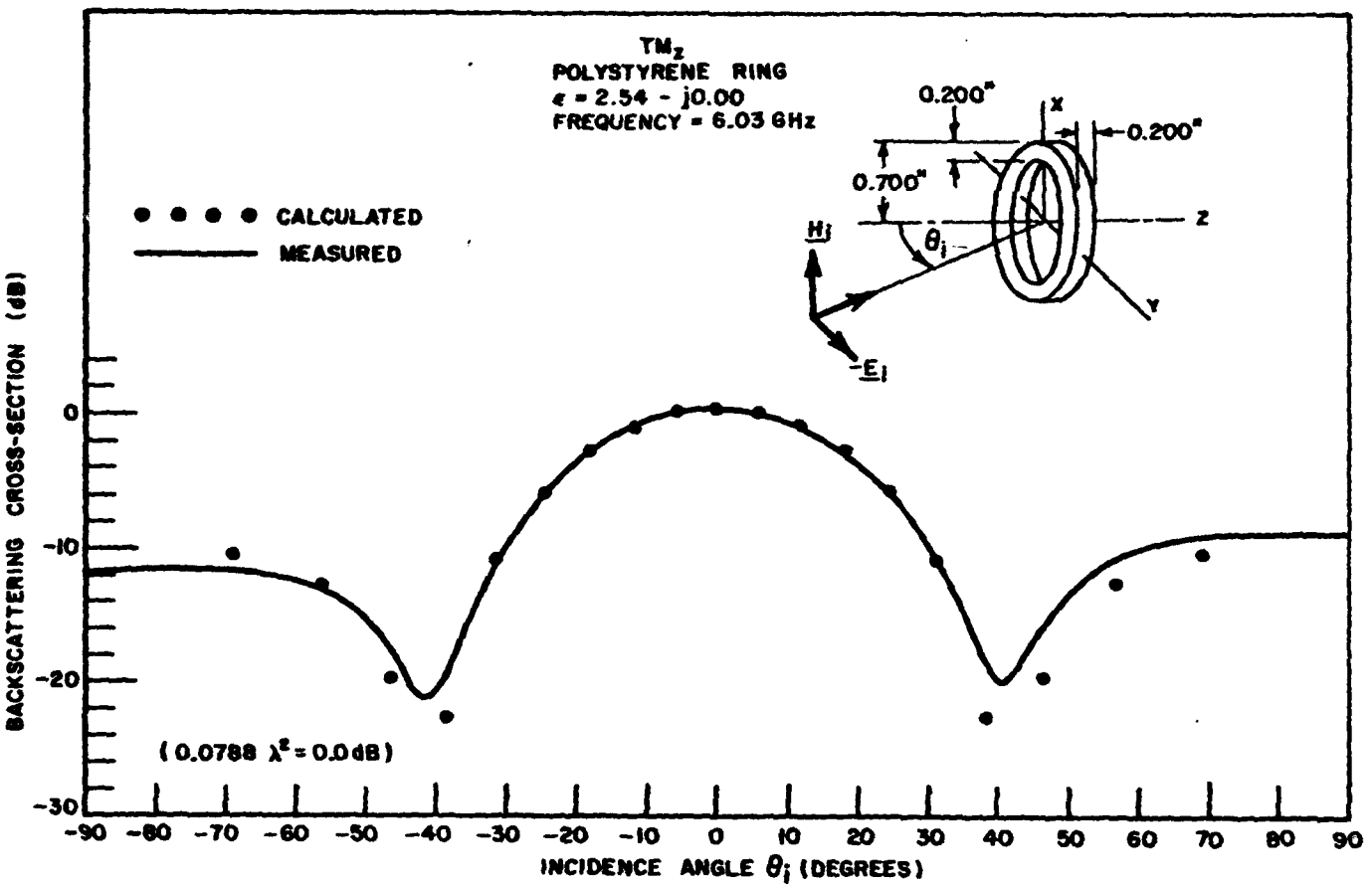

Fig. 14--Plot of backscattering cross section versus incidence angle for a TM_z plane wave incident on a dielectric ring.

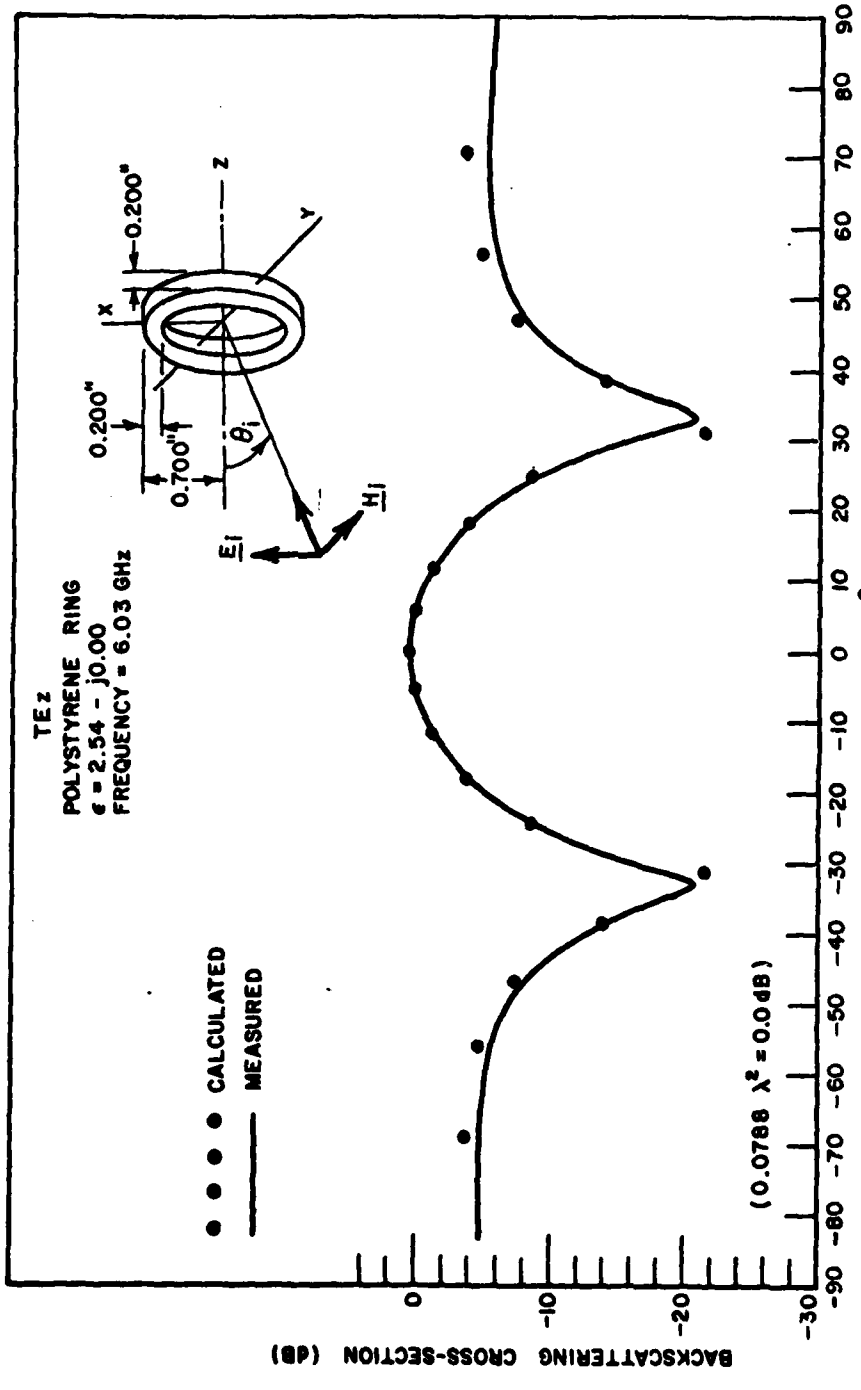

Fig. 15--Plot of backscattering cross section versus incidence angle for a TE_z plane wave incident on a dielectric ring.

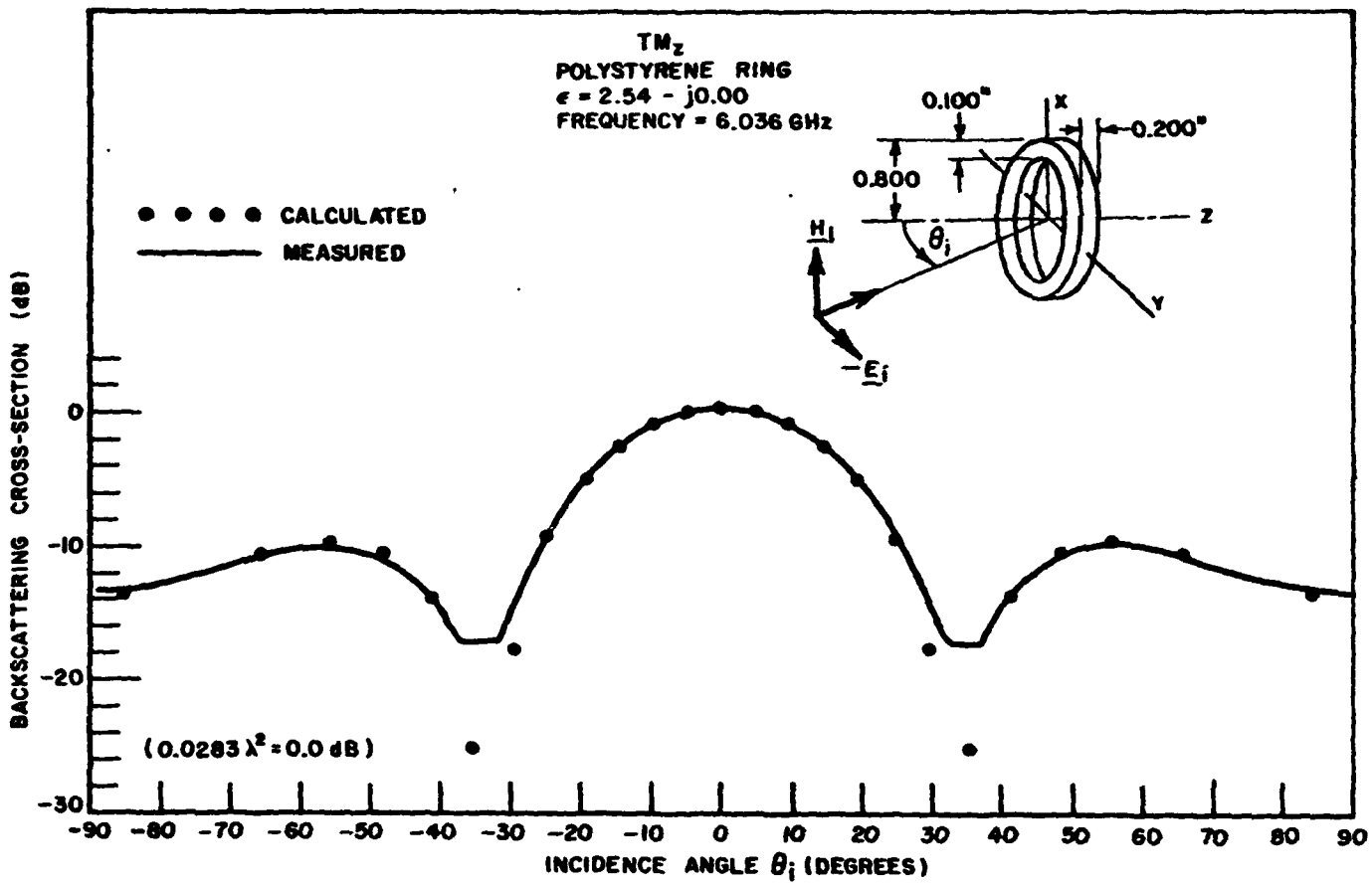

Fig. 16--Plot of backscattering cross section versus incidence angle for a TM_z plane wave incident on a dielectric ring.

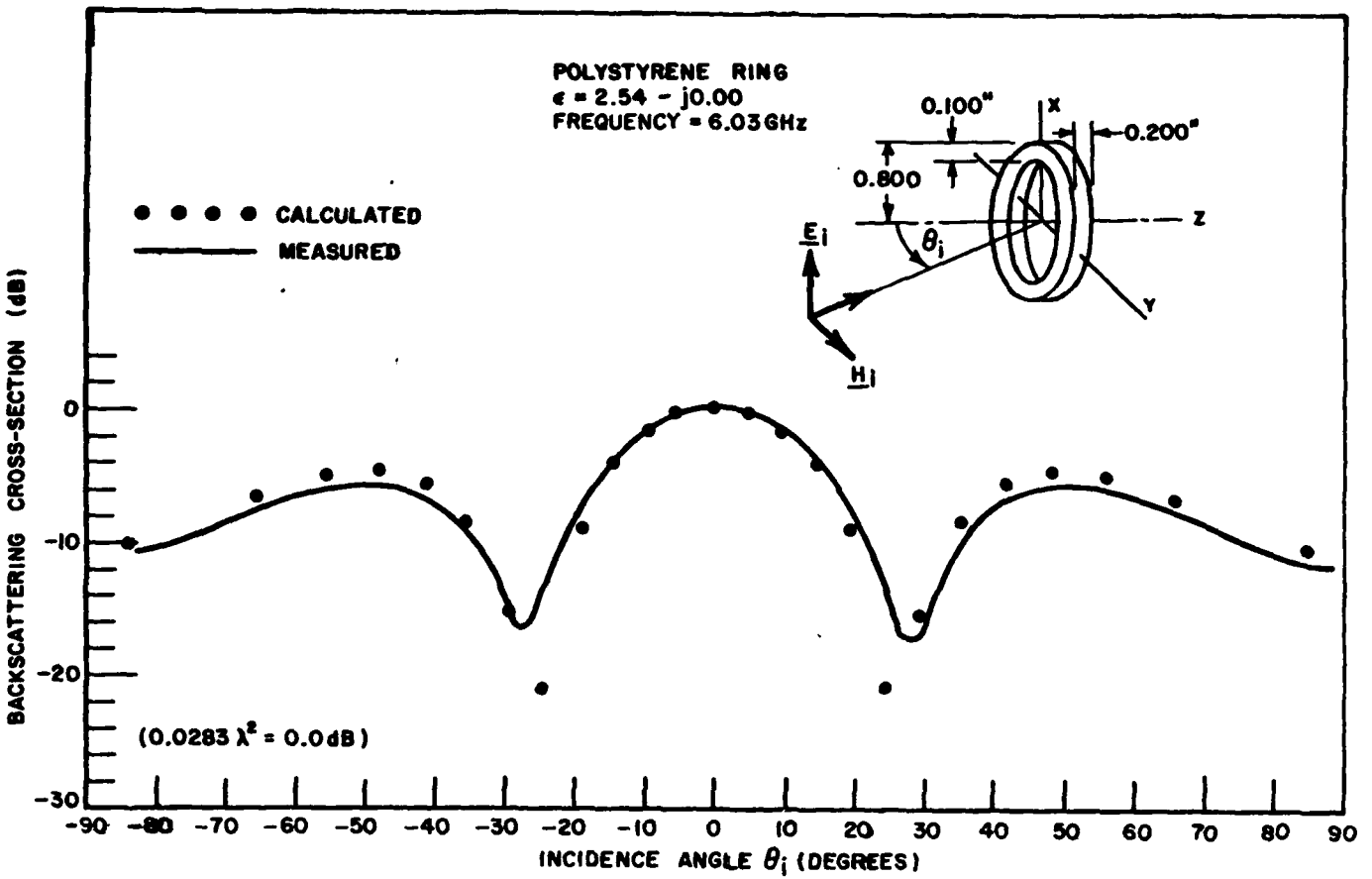

Fig. 17--Plot of backscattering cross section versus incidence angle for a TE_z plane wave incident on a dielectric ring.

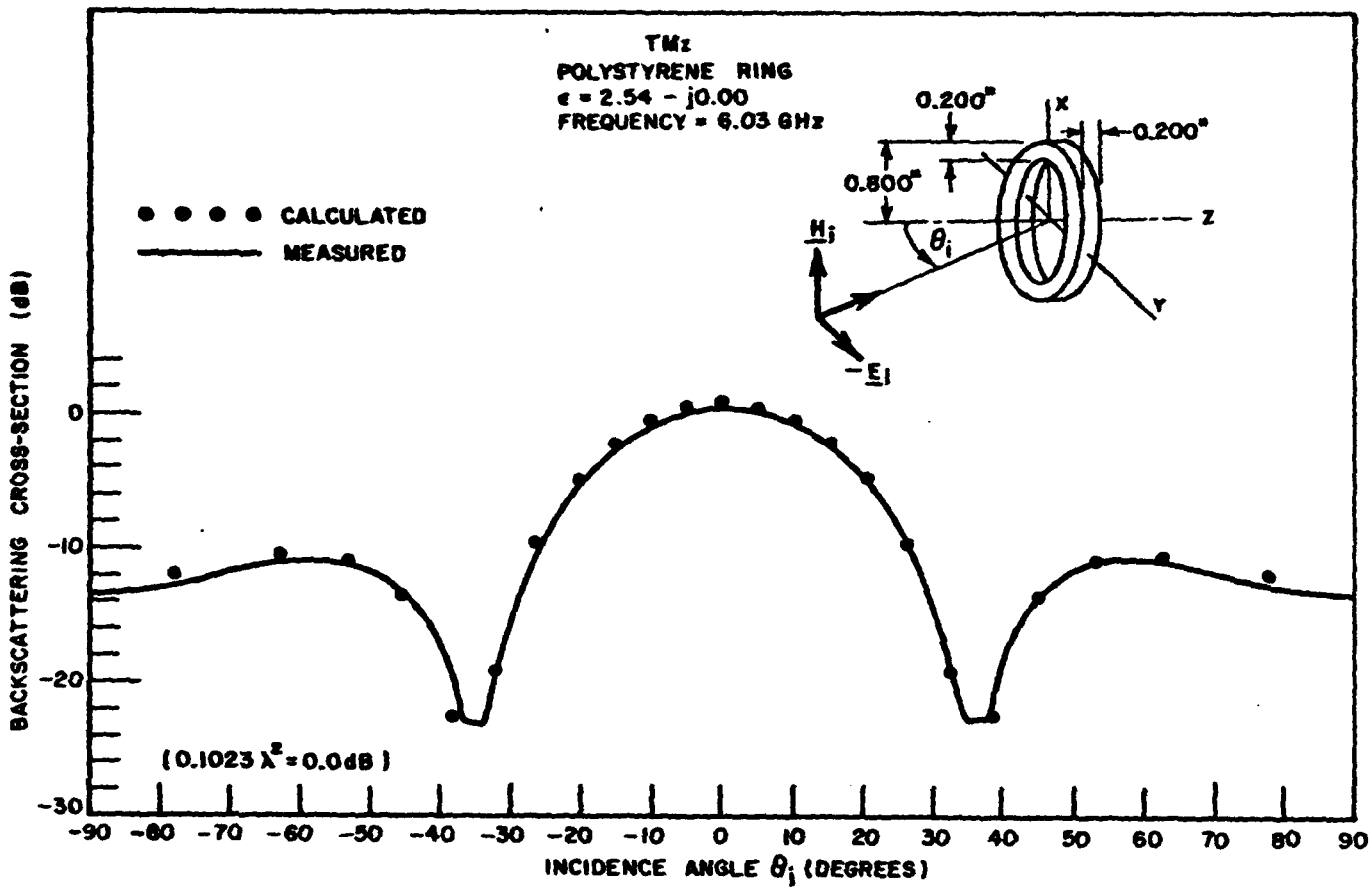

Fig. 18--Plot of backscattering cross section versus incidence angle for a TM_z plane wave incident on a dielectric ring.

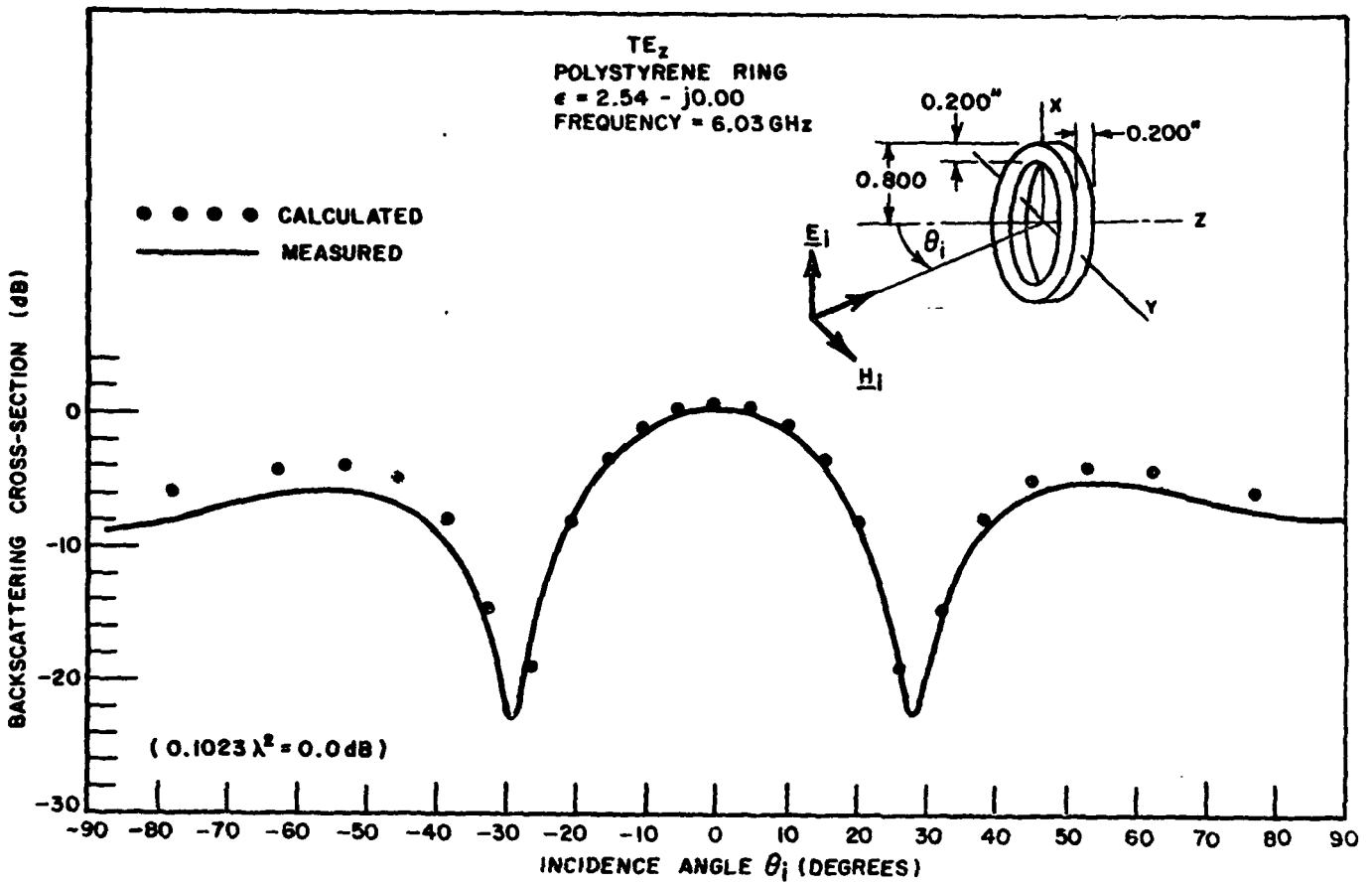

Fig. 19--Plot of backscattering cross section versus incidence angle for a TE_z plane wave incident on a dielectric ring.

It should be noted that the only inherent assumption in the ring scattering calculation is that the thickness and length are sufficiently small compared with a wavelength that field variations with ρ and z can be neglected. Aside from practical problems such as lengthy integration times and summations over many ϕ-modes, there is nothing preventing application of this technique to rings with larger radii if the above restrictions are kept in mind.

B. Dielectric Tube Scattering

The final situation considered is that of a homogeneous thin-wall cylindrical shell with a linearly polarized plane wave incident along the shell axis. Shells up to one wavelength long are considered and several terms of the z-expansion are required for a good solution for the field in the tube. Choice of on-axis incidence requires only the $n = 1$ mode in ϕ and the amount of computer storage required is considerably reduced from the arbitrary incidence calculation. The geometry of the problem is shown in Fig. 20.

In this calculation, all the coefficients given in Eq. (16) were retained in the system of equations. Although rapid access computer storage restrictions limited the maximum z-mode index to two, this was found to be adequate for the cases considered. For tubes much larger than one wavelength, however, more modes would be needed.

The calculations and experiments were performed for polystyrene tubes with an outer radius of 0.500" and a wall thickness of 0.100". The frequency was 6.23 GHz, the dielectric constant used in the calcu-

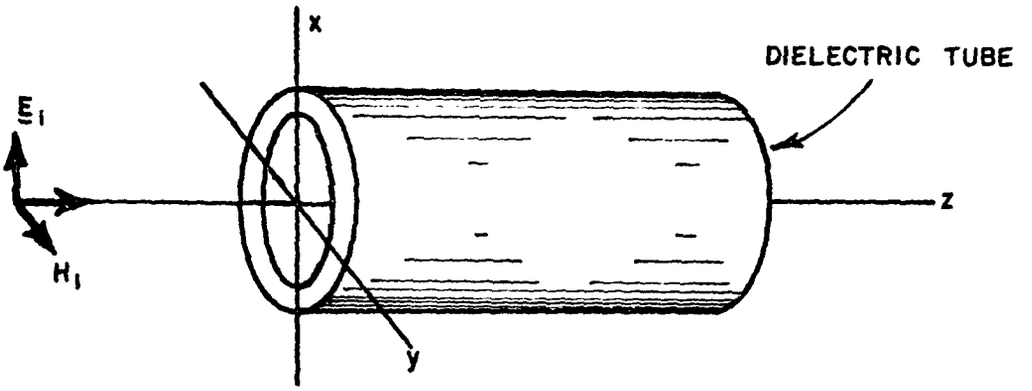

Fig. 20--Plane wave incident along dielectric tube axis.

lations was $\epsilon_r = 2.54 - j0.00$ and the tube lengths ranged from 0.100" to 1.960".

The experimental data, the averaged data and the calculated back-scattering cross section are given in Table I. A comparison of the caculated and measured scattering cross section is shown in Fig. 21.

The agreement between the calculated and measured cross sections again is excellent. The increasing disagreement for the larger tubes undoubtedly arises from the three-mode limitation in the z-expansion.

TABLE I

Length (inches)	Measured Cross Section (λ^2)			Average Experimental Cross Section	Calculated Cross Section
0.100	.00300	.00320	.00335	.00318	.00323
0.253	.0150	.0157		.0153	.0150
0.353	.0221	.0226		.0223	.0217
0.501	.0237	.0231	.0226	.0231	.0227
0.601	.0180	.0150	.0180	.0170	.0169
0.746	.00582	.00595	.00543	.00573	.00532
0.846	.00064	.00065		.00064	.00060
0.982	.00350	.00342	.00375	.00356	.00387
1.082	.0130	.0133		.0131	.0127
1.253	.0284	.0278	.0272	.0278	.0291
1.353	.0320	.0320		.0321	.0325
1.470	.0254	.0259	.0254	.0256	.0274
1.570	.0150	.0150		.0150	.0176
1.748	.00232	.00223	.00254	.00236	.00265
1.848	.00305	.00254	.00300	.00286	.00370
1.960	.0133	.0143	.0130	.0135	.0155

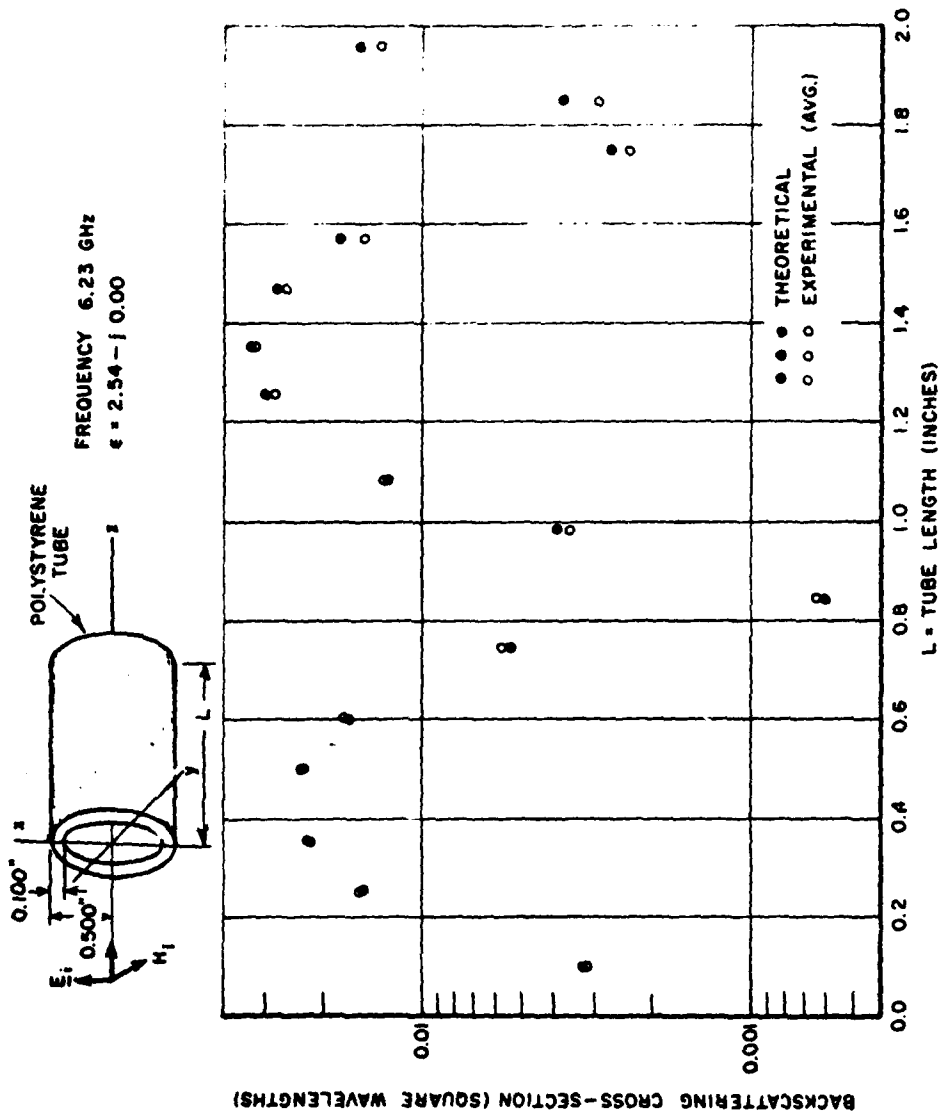

Fig. 21--Plot of backscattering cross section vs. tube length.

CHAPTER VI

CONCLUSIONS

Accurate calculation of radome boresight error is a challenging task. Rigorous series solutions of the boundary-value problem are usually not practical for the general radome shell and the accuracy of present-day approximate methods of radome analysis is generally not known. An essentially rigorous technique for application to radome scattering is the integral equation method. The first step in the development of an integral equation analysis of radome shells is discussed in this report, namely the calculation of the backscattering from thin-wall, finite-length, circular cylindrical shells.

The unknown function in the integral equation is the field within the dielectric shell. The integral equation derivation and the method of solution of the equation by the point matching technique are discussed. The field within the dielectric shell is found in terms of expansion coefficients in a double Fourier series over the shell. The far scattered fields are determined by using the calculated total field and the equivalent current concept.

The technique is applied to calculation of the backscattering of a linearly polarized incident wave by dielectric rings and tubes. A comparison of the calculated and measured backscattering was made for the following three particular cases:

(1) a thin, short, homogeneous, dielectric ring for axial incidence

(2) a thin, short, homogeneous, dielectric ring for arbitrary incidence with TE and TM polarization

(3) a thin-wall cylindrical shell for axial incidence.

The dielectric material for each of the above cases is polystyrene. Agreement between the calculated and measured results is excellent in all three cases.

The general numerical integration procedures, the far field integration formulas, the experimental methods and the computer programs used are all discussed.

In addition, a useful expression is derived for the electric field at the center of a rectangular parallelepiped of current density. This expression is needed when integrating throughout a volume of source current density to calculate the field at a point within the source region.

The numerical technique used seems to be particularly suitable for treatment of arbitrary shaped shells of revolution which could be considered to be made up of a large number of dielectric rings. Longitudinally inhomogeneous bodies are also amenable to analysis by the ring-subdivision method; each ring would be homogeneous, of course, so that this approach would give a piecewise uniform approximation to the inhomogeneity being considered.

In summary, excellent results have been obtained by applying an integral equation technique to calculation of the plane wave scattering from thin-wall dielectric cylindrical shells. This work is significant to the general radome scattering problem for two reasons. First, the excellent theoretical and experimental agreement implies a high degree of accuracy

obtainable with the method. Second, a workable mode of application of the integral equation technique has been established and this approach can be extended to more complex dielectric shell configurations and to more general fields.

APPENDIX A

EXPERIMENTAL METHODS AND EQUIPMENT

Measurement of the backscattering cross section of the rings and tubes was accomplished using a one horn monostatic backscattering cross ection system operating in a large microwave darkroom. A block diagram of the measurement system is shown in Fig. 22.

A measurement is made by following the steps outlined. The three-stub tuner is adjusted to create a load mismatch precisely balancing out the background return from the darkroom when no target is present. A reference cross section level is then established by using a standard sphere with known cross section as the target and recording the back-scattering return. The sphere is then removed, the target is placed in position and the target return is recorded. The absolute value of the target cross section is then found by measuring the relative levels of the target and sphere and calculating the target cross section directly from the known sphere cross section. In all cases the reference sphere is chosen to provide a reference level of the same order of magnitude as the target cross section.

The linearity of the system was checked by comparing the measured levels of two reference spheres. For the range of cross sections considered, the relative sphere levels were within $\pm$0.1 dB of their known relative values. This is considered to be very good. The wide range linearity (30 dB range) was also checked using a precision attenuator;

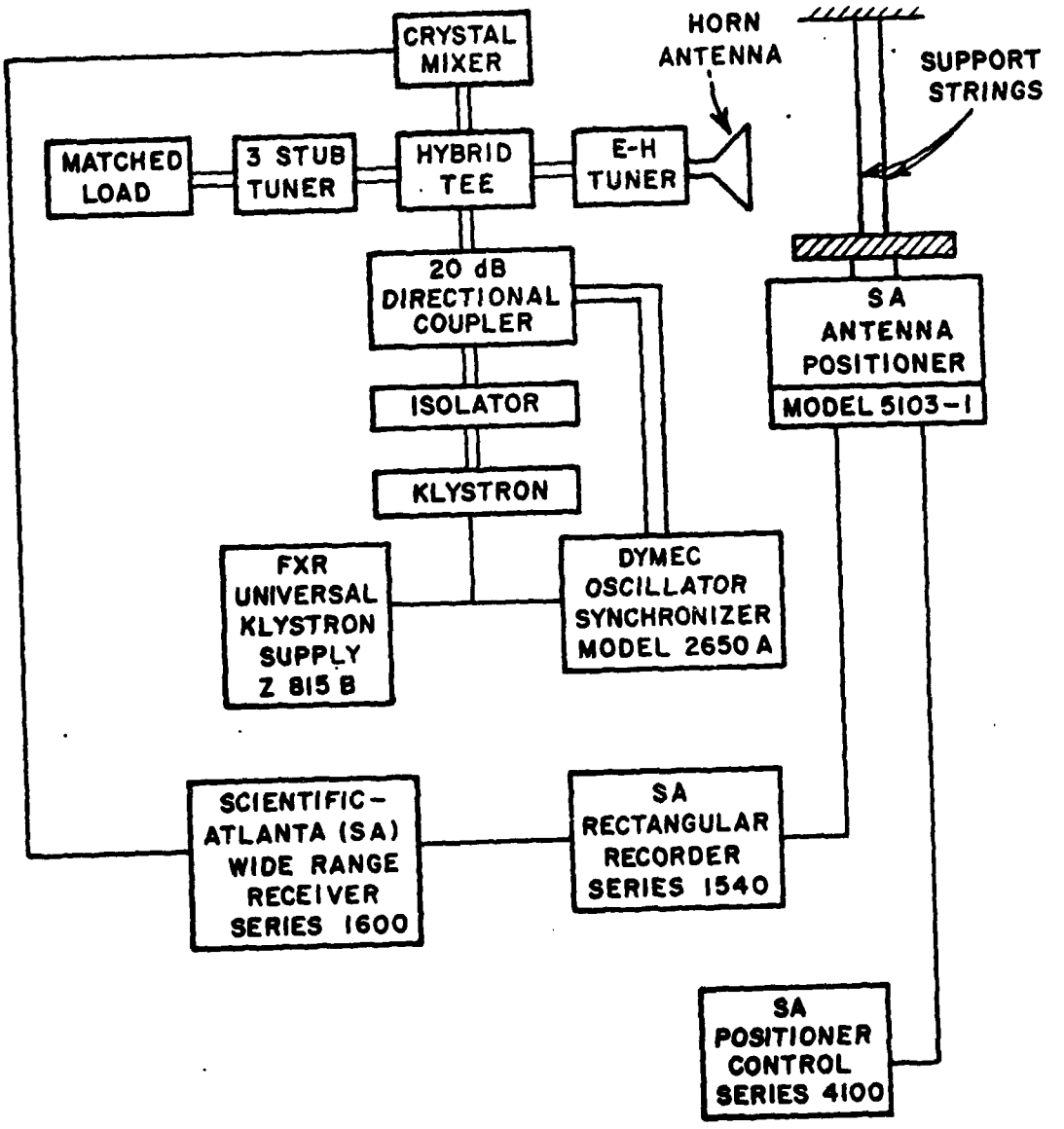

Fig. 22--Block diagram of monostatic cross section measurement apparatus.

this check gave relative levels within 0.1dB of the attenuator values.

For the case of the on-axis scattering of the thinnest, shortest rings (Fig. 10), the cross section levels were somewhat low to obtain good "far zone" scattering results. As pointed out by Kouyoumjian and Peters,[29] however, accurate cross section measurements do not require that the target be in the far zone of the antenna but only that the incident fields have plane wave properties in the vicinity of the target and that the antenna-target interaction be very small.

The thin, short rings were measured by suspending them on strings in the horn mouth with the center of the rings on the horn axis. Kouyoumjian[30] shows that in the neighborhood of maximum points along a horn axis, the field is nearly a uniform plane wave. The axial field variation of the measurement horn was probed using a 0.25" sphere. For the thin rings, the axial incident field variation over the rings was found to be less than 0.5 dB and the horn-mouth location was found to be very close to a maximum point. For small rings and small cross sections, antenna-ring interaction can undoubtedly be neglected. Thus, reasonably good plane wave scattering measurements are expected. No quantitative estimate of the errors has been made, however.

Measurement of the ring patterns and the tube cross sections imposes a larger axial extent of the target than can be tolerated for a horn-mouth measurement. The larger cross section, however, allowed use of the more standard far-zone cross section measurement. Observed repeatability and linearity were again very good.

APPENDIX B
COMPUTER PROGRAMS

A discussion of the computer programs used to calculate the ring and tube fields and backscattering cross section is presented in this appendix. The programs are written in the Fortran IV language for processing on the Ohio State University IBM 7094 computer.

Flow charts outlining the computations are given for all the programs used. Definition of the input and calling parameters and a complete statement listing of the programs are also included.

A. Arbitrary Plane Wave Incidence on a Dielectric Ring

The program flow chart is shown in Fig. 23 and the statement listing of the computer program is given in Fig. 24. The input data card variables and the subroutine calling paramenters are defined below.

(1) Cards needed once for each run:

Card Number 1	Format (I10, 7F 10.5)	
Columns	Quantity	Description
1-10	NCASE	NCASE = the number of different rings to be calculated.

(2) Cards needed once for each different ring:

Card Number 2	Format (I10,7F 10.5)	
Columns	Quantity	Description
1-10 (right-adjusted)	NX	NX = the maximum ϕ-mode index to be used
11-20	AI	AI = the mean ring radius in inches.

Columns	Quantity	Description
21-30	DI	DI = the radial thickness of the ring in inches.
31-40	WI	WI = the width of the ring in the z-direction in inches.
41-50	FREQ	FREQ = the frequency in gigahertz.
51-60	Re(ER)	ER = the complex relative dielectric constant of the ring material.
61-70	Im(ER)	

Card Number 3 Format (I10,7F 10.5)

Columns	Quanity	Description
1-10 (right-adjusted)	NANG	NANG = the number of incidence angles to be calculated for the ring.
11-20	REF	REF = the reference cross section for calculation of the theoretical cross section in dB.

(3) Cards needed once for each different incidence angle for each ring.

Card Number 4 Format (8F 10.6)

Columns	Quantity	Description
1-10 11-20 21-30 etc.	B(I), I=1,10	B(I) = the I-th order Bessel function of the first kind. Used in calculation of the incident field Fourier coefficients for a particular incidence angle.

Card Number 5 Format (8F 10.6)

Columns	Quantity	Description
1-10	TH	TH = the incidence angle for one calculation for one ring.

The calling parameters for the NRCELL subroutine are defined as follows:

M = the number of subcells along each side of the larger cell (a total of M^3 subcells)

RC,PC,ZC are the ρ,ϕ,z coordinates respectively of the larger (near) cell

AL = 0.0

NX1 = the maximum ϕ-mode index to be used plus 1.

XM,YM,ZM = the rectangular coordinates of the matching point for which the NRCELL subroutine was called.

AA,BB,CC = the incremental dimensions of the large (near) cell in the ρ,ϕ and z directions respectively.

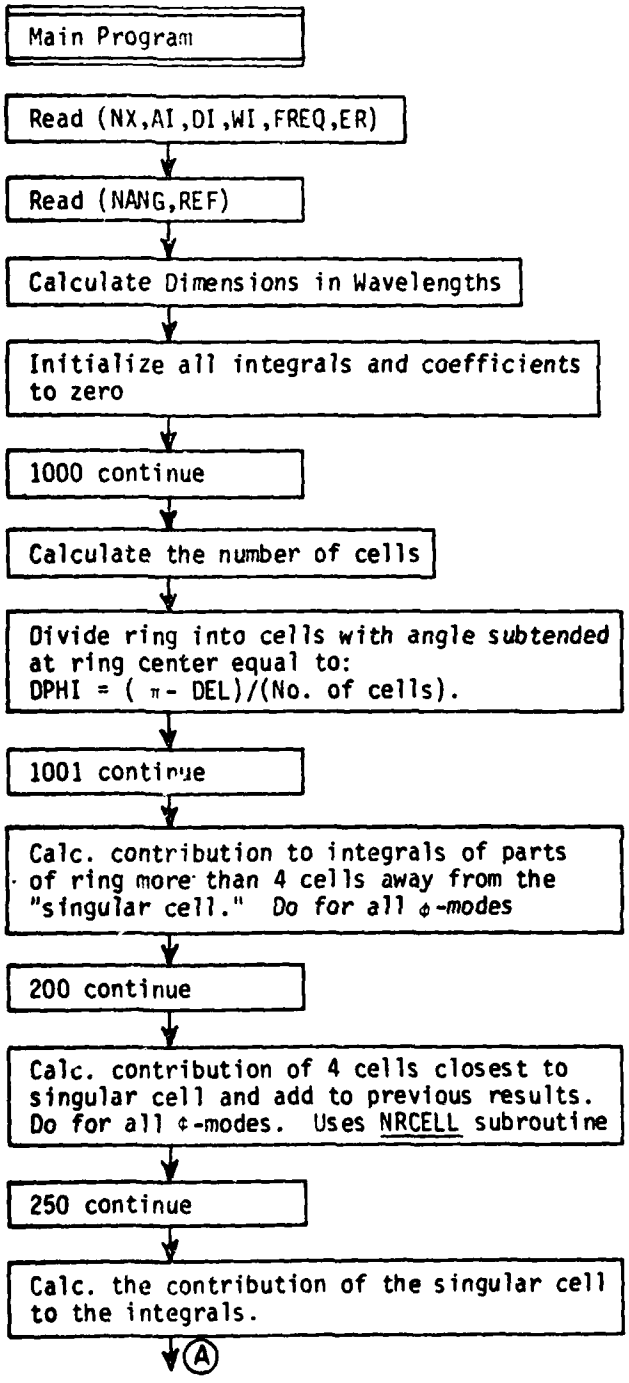

Fig. 23--Flow chart, ring scattering computer program.

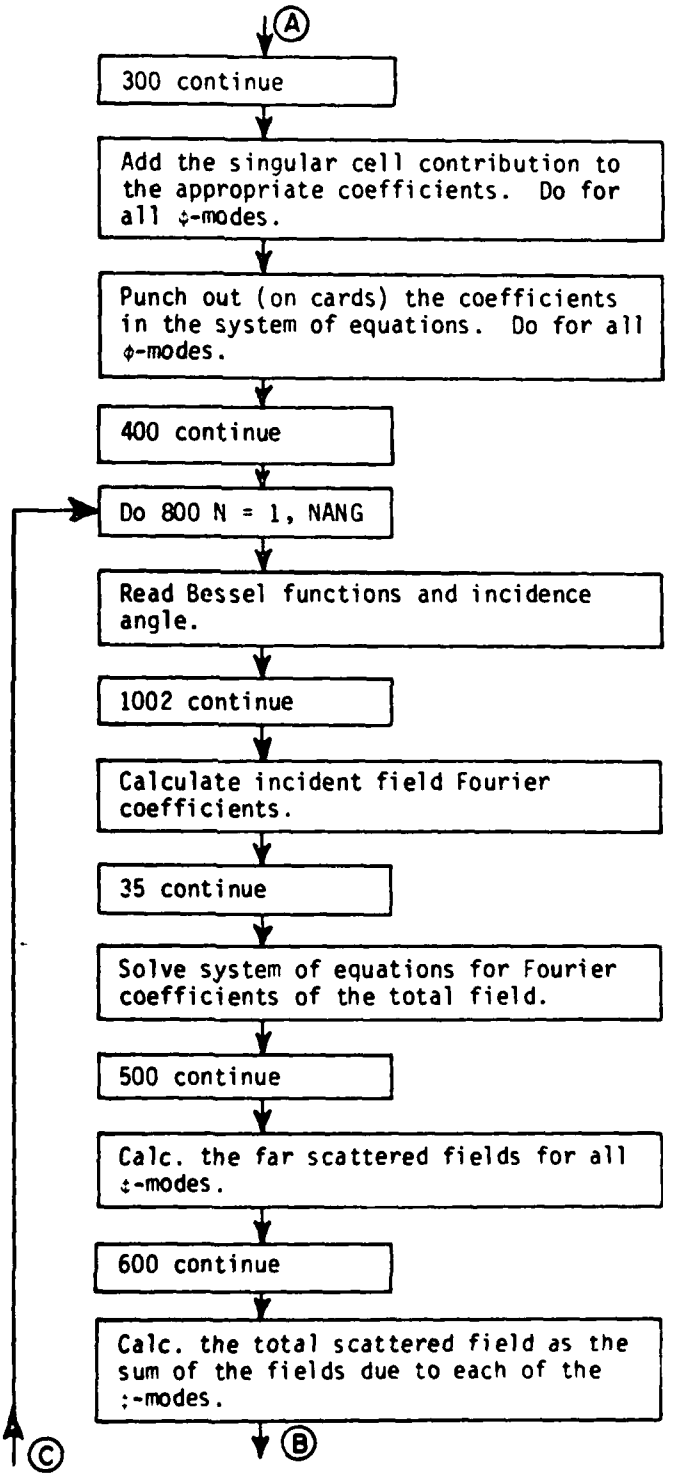

Fig. 23--(continued).

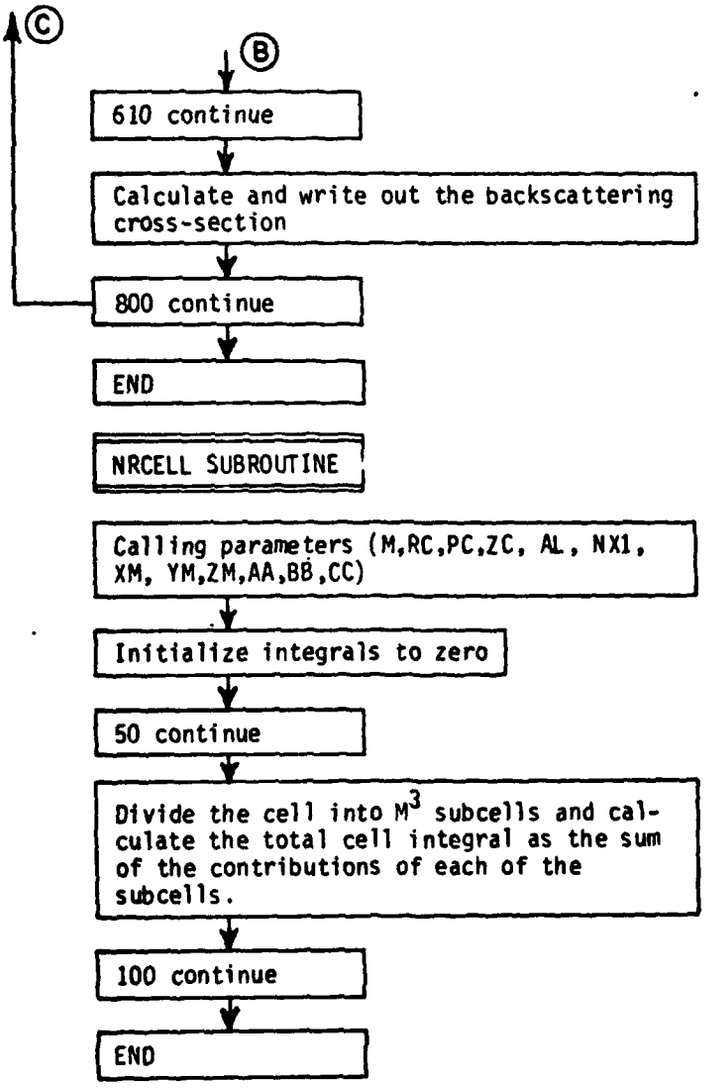

Fig. 23--(continued).

```
 VANDOEREN, R.              JOBN FGJ921      3
$EXECUTE        IBJOB
$IBJOB
$IBFTC MAIN     NODECK
    1 FORMAT (I10,7F10.5)
    2 FORMAT (15X,2I5)
   22 FORMAT (5X,8F14.8)
    3 FORMAT(4X,21H REST OF RING RESULTS/4X,14F8.4)
    4 FORMAT(6X,21H SINGULAR CELL RESULT/10X,4F8.4)
    7 FORMAT (5F15.8)
   15 FORMAT (8F10.6)
      COMPLEX A1(10),A3(10),A4(10),A6(10),A8(10)
      COMPLEX AT(10),BT(10),AP(10),BP(10),AL(10),BL(10)
      COMPLEX AIT(10),BIT(10),AIP(10),BIP(10),AIL(10),BIL(10)
      COMPLEX CJ,CI,ETH(10),EPS(10),ETHT,EPST
      COMPLEX XP,P,Q
      COMPLEX DET,ER
      COMPLEX V1(10),V2(10),V3(10),V4(10),V5(10),V6(10),V8(10)
      COMPLEX V9(10),V11(10),V16(10)
      COMPLEX P1(10),P2(10),P3(10),P4(10),P5(10),P6(10),P7(10),P8(10)
      COMPLEX P9(10),P10(10),P11(10),P12(10),P13(10),P14(10),P15(10)
      COMPLEX P16(10)
      COMMON P1,P2,P3,P4,P5,P6,P7,P8,P9,P10,P11,P12,P13,P14,P15,P16
      COMPLEX AITM(10),BITM(10),AIPM(10),BIPM(10),AILM(10),BILM(10)
      COMPLEX ATM(10),BTM(10),APM(10),BPM(10),ALM(10),BLM(10)
      COMPLEX ETHM(10),EPSM(10),ETHMT,EPSMT
      DIMENSION B(10)
      COMPLEX EE
      COMPLEX XPP,XPQ
      READ (5,1) NCASE
C     NCASE IS THE NUMBER OF RING CASES TO BE RUN.
      DO 801 NCAS=1,NCASE
      READ (5,1) NX,AI,DI,WI,FREQ,ER
C     NX IS THE MAXIMUM PHI-MODE INDEX.
C     AI= MEAN RADIUS OF THE RING IN INCHES.
C     DI= THICKNESS OF RING IN RADIAL DIRECTION (INCEHES).
C      WU=WIDTH OF RING IN Z-DIRECTION (INCHES).
C      ER = RELATIVE DIELECTRIC CONSTANT OF RING.
C      FREQ = FREQUENCY IN GHZ.
      READ (5,1) NANG,REF
C     NANG IS THE NUMBER OF INCIDENCE ANGLES FOR A GIVEN RING.
C     REF IS THE REFERENCE CROSS-SECTION FOR THE PARTICULAR RING.
      AL=0.0
      NX1=NX+1
      Y00= 11.8028/FREQ
      Y11= Y00/SQRT(ER)
      A=AI/Y00
      D=DI/Y00
      W=WI/Y00
      WA0=6.28319/Y00
      WA=6.28319/Y11
C      A IS THE MEAN RADIUS OF THE RING.
C      D IS THE THICKNESS IN THE RADIAL DIRECTION OF THE RING.
C      W IS THE WIDTH OF THE RING IN THE Z-DIRECTION.
C      ALL THE ABOVE ARE IN TERMS OF FREE SPACE WAVELENGTHS
      DO 32 J=1,10
      V1(J)=(0.,0.)
      V2(J)=(0.,0.)
      V3(J)=(0.,0.)
      V4(J)=(0.,0.)
      V5(J)=(0.,0.)
      V6(J)=(0.,0.)
      V8(J)=(0.,0.)
      V9(J)=(0.,0.)
```

Fig. 24--Ring scattering computer program statement listing.

```
      V11(J)=(0.,0.)
      V16(J)=(0.,0.)
      AT(J)=(0.,0.)
      BT(J)=(0.,0.)
      AP(J)=(0.,0.)
      BP(J)=(0.,0.)
      AL(J)=(0.,0.)
      BL(J)=(0.,0.)
      AIT(J)=(0.,0.)
      BIT(J)=(0.,0.)
      AIP(J)=(0.,0.)
      BIP(J)=(0.,0.)
      AIL(J)=(0.,0.)
      BIL(J)=(0.,0.)
      ETH(J)=(0.,0.)
      EPS(J)=(0.,0.)
      ETHM(J)=(0.,0.)
      EPSM(J)=(0.,0.)
   32 CONTINUE
      ETHT=(0.,0.)
      EPST=(0.,0.)
      ETHMT=(0.,0.)
      EPSMT=(0.,0.)
      DO 403 IND=1,NX1
      READ (5,16) J,A1,FREQ
      READ (5,17) A1(J),A3(J),A4(J),A6(J),A8(J)
  403 CONTINUE
      GO TO 401
 1000 CONTINUE
      N=(3.14159*A)/0.01
      DEL=0.01/A
C       THE CELL FROM -DEL TO +DEL IS ACCOUNTED FOR ANALYTICALLY.
      IF (N.LT.30) N=30
      T6=N
      DPHI=(3.14159-DEL)/T6
      DV=W*D*A*DPHI/6.28319
      WTT=((W/2.)**3)*0.666667
 1001 CONTINUE
      DO 200 K=20,N
      T1=K
      PH=DEL+DPHI/2.+T1*DPHI
      C=COS(PH)
      S=SIN(PH)
      X=A*(1.-C)
      Y=-A*S
      Z=0.0
      R=SQRT(X*X+Y*Y+Z*Z)
      AR=6.28319*R
      ARS=AR**2
      R3=R**3
      R5=R**5
      PR=(-1.+ARS)/R3
      PI=-AR/R3
      P=CMPLX(PR,PI)
      QR=(3.-ARS)/R5
      QI=3.*AR/R5
      Q=CMPLX(QR,QI)
      XP=CMPLX(COS(AR),-SIN(AR))
      XPP=XP*P
      XPQ=XP*Q
      DO 60 NN=1,NX1
      T1=NN-1
      SN=SIN(T1*PH)
      CN=COS(T1*PH)
```

Fig. 24--(continued).

```
      CND=CN*DV
      SND=SN*DV
      V1(NN)=V1(NN)+C*CND*XPP
      V2(NN)=V2(NN)+S*SND*XPP
      V3(NN)=V3(NN)+X*X*C*CND*XPQ
      V4(NN)=V4(NN)+X*X*S*SND*XPQ
      V5(NN)=V5(NN)+X*Y*S*CND*XPQ
      V6(NN)=V6(NN)+X*Y*C*SND*XPQ
      V8(NN)=V8(NN)+Y*Y*S*SND*XPQ
      V9(NN)=V9(NN)+Y*Y*C*CND*XPQ
      V11(NN)=V11(NN)+CND*XPP
      V16(NN)=V16(NN)+WTT*CND*XPQ
   60 CONTINUE
  200 CONTINUE
      DO 201 J=1,NX1
      WRITE (6,1) J
      WRITE (6,3) V1(J),V2(J),V3(J),V4(J),V5(J),V6(J),V8(J),V9(J),V11(J)
  201 CONTINUE
      XM=A
      YM=0.0
      ZM=0.0
      AA=D
      BB=5.*DPHI
      CC=W
C     DOWN TO 250 IS THE CALCULATION FOR THE 4 CELLS NEAREST THE  ***
C     *** SINGULAR POINT ( THE OBSERVATION POINT).
      DO 250 J=1,4
      T1=J-1
      DPH=5.*DPHI
      PHI=DEL+DPH/2.+T1*DPH
      C=COS(PHI)
      S=SIN(PHI)
      XC=A*C
      YC=A*S
      ZC=0.0
      IF (J.EQ.1) M=20
      IF (J.EQ.2) M=10
      IF (J.EQ.3) M=8
      IF (J.EQ.4) M=6
      CALL NRCELL (M,A,PHI,ZC,AL,NX1,XM,YM,ZM,AA,BB,CC)
      DO 202 JJ=1,NX1
      WRITE (6,2) J,JJ
      WRITE (6,22) P1(JJ),P2(JJ),P3(JJ),P4(JJ),P5(JJ),P6(JJ),P7(JJ),P8(J
     2J),P9(JJ),P10(JJ),P11(JJ),P12(JJ),P13(JJ),P14(JJ),P15(JJ),P16(JJ)
      V1(JJ)=V1(JJ)+P1(JJ)
      V2(JJ)=V2(JJ)+P2(JJ)
      V3(JJ)=V3(JJ)+P3(JJ)
      V4(JJ)=V4(JJ)+P4(JJ)
      V5(JJ)=V5(JJ)+P5(JJ)
      V6(JJ)=V6(JJ)+P6(JJ)
      V8(JJ)=V8(JJ)+P8(JJ)
      V9(JJ)=V9(JJ)+P9(JJ)
      V11(JJ)=V11(JJ)+P11(JJ)
      V16(JJ)=V16(JJ)+P16(JJ)
      WRITE (6,2) JJ
      WRITE (6,22) V1(JJ),V2(JJ),V3(JJ),V4(JJ),V5(JJ),V6(JJ),V8(JJ),V9(J
     2J),V11(JJ),V16(JJ)
  202 CONTINUE
  250 CONTINUE
C     FROM HERE TO 300 IS CALCULATED THE SINGULAR CELL CONTRIBUTION.
      A1=D/2.
      B1=A*DEL
      C1=W/2.
      SQ=SQRT(A1*A1+B1*B1+C1*C1)
```

Fig. 24--(continued).

```
      T2=2./3.14159
      ST=T2*(ATAN((A1*C1)/(B1*SQ))+ATAN((A1*B1)/(C1*SQ)))-1.
      SP=T2*(ATAN((B1*A1)/(C1*SQ))+ATAN((B1*C1)/(A1*SQ)))-1.
      SL=T2*(ATAN((C1*B1)/(A1*SQ))+ATAN((C1*A1)/(B1*SQ)))-1.
  300 CONTINUE
C     ER IS THE RELATIVE DIELECTRIC CONSTANT OF THE DIELECTRIC RING.
      DO 400 J=1,NX1
      A1(J)=V1(J)+V3(J)+V5(J)+ST
      A3(J)=-V2(J)-V4(J)+V6(J)
      A4(J)=V2(J)+V6(J)+V8(J)
      A6(J)=V1(J)+V9(J)-V5(J)+SP
      A8(J)=V11(J)+V16(J)+SL
      WRITE (6,8) J,A1(J),A3(J),A4(J),A6(J),A8(J)
   16 FORMAT (I10,7F10.6)
   17 FORMAT (8F10.6)
      PUNCH 16, J,A1,FREQ
      PUNCH 17, A1(J),A3(J),A4(J),A6(J),A8(J)
  400 CONTINUE
  401 CONTINUE
      DO 800 N11=1,NANG
      READ (5,15) (B(J),J=1,10)
C     THE B.S ARE BESSEL FUNCTIONS USED IN THE INCIDENT FIELD CALC.
      READ (5,15) TH
 1002 CONTINUE
      ST=SIN(3.14159-TH)
      CT=COS(3.14159-TH)
      THD=TH*57.3
C     DOWN TO 35 IS CALC. OF THE INCIDENT FIELD COEFFICIENTS.
      AIT(1)=(0.,0.)
      BIT(1)=(0.,0.)
      AIP(1)=CMPLX(0.,-B(2))
      BIP(1)=(0.,0.)
      AITM(1)=-CT*AIP(1)
      BITM(1)=(0.,0.)
      AIPM(1)=(0.,0.)
      BIPM(1)=(0.,0.)
      AILM(1)=-ST*CMPLX(B(1),0.)
      BILM(1)=(0.,0.)
      DO 35 J=1,4
      J1=2*J
      J1P1=J1+1
      J1M1=J1-1
      AIT(J1)=CMPLX((B(J1M1)+B(J1P1)),0.)
      BIT(J1)=(0.,0.)
      AIP(J1)=(0.,0.)
      BIP(J1)=CMPLX((-B(J1M1)+B(J1P1)),0.)
      AITM(J1)=(0.,0.)
      BITM(J1)=-CT*BIP(J1)
      AIPM(J1)=CT*AIT(J1)
      BIPM(J1)=(0.,0.)
      AILM(J1)=(0.,0.)
      BILM(J1)=-CMPLX(0.,2.*ST*B(J1))
      J2=2*J+1
      J2P1=J2+1
      J2M1=J2-1
      AIT(J2)=(0.,0.)
      BIT(J2)=CMPLX(0.,(B(J2M1)+B(J2P1)))
      AIP(J2)=CMPLX(0.,(B(J2M1)-B(J2P1)))
      BIP(J2)=(0.,0.)
      AITM(J2)=-CT*AIP(J2)
      BITM(J2)=(0.,0.)
      AIPM(J2)=(0.,0.)
      BIPM(J2)=CT*BIT(J2)
      AILM(J2)=-CMPLX(2.*ST*B(J2),0.)
```

Fig. 24--(continued).

```
      BILM(J2)=(0.,0.)
   35 CONTINUE
C     FOLLOWING IS THE SOLUTINE FOR THE FOURIER COEFF. OF THE FIELDS.
      EE=ER-1.
      DO 500 J=1,NX1
      DET=(1.-EE*A1(J))*(1.-EE*A6(J))+EE*A3(J)*EE*A4(J)
      AT(J)=(A1T(J)*(1.-EE*A6(J))+B1P(J)*EE*A3(J))/DET
      BP(J)=(B1P(J)*(1.-EE*A1(J))-A1T(J)*EE*A4(J))/DET
      AP(J)=(A1P(J)*(1.-EE*A1(J))+B1T(J)*EE*A4(J))/DET
      BT(J)=(B1T(J)*(1.-EE*A6(J))-A1P(J)*EE*A3(J))/DET
      AL(J)=(0.,0.)
      BL(J)=(0.,0.)
      ATM(J)=(A1TM(J)*(1.-EE*A6(J))+B1PM(J)*EE*A3(J))/DET
      BPM(J)=(B1PM(J)*(1.-EE*A1(J))-A1TM(J)*EE*A4(J))/DET
      APM(J)=(A1PM(J)*(1.-EE*A1(J))+B1TM(J)*EE*A4(J))/DET
      BTM(J)=(B1TM(J)*(1.-EE*A6(J))-A1PM(J)*EE*A3(J))/DET
      ALM(J)=A1LM(J)/(1.-EE*A8(J))
      BLM(J)=B1LM(J)/(1.-EE*A8(J))
    8 FORMAT (5X,110,/,5X,6F15.8,/,5X,6F15.8,/)
      WRITE (6,18)
      WRITE (6,8) J,A1T(J),B1T(J),A1P(J),B1P(J),A1L(J),B1L(J)
      WRITE (6,8) J,AT(J),BT(J),AP(J),BP(J),AL(J),BL(J)
      WRITE (6,19)
      WRITE (6,8) J,A1TM(J),B1TM(J),A1PM(J),B1PM(J),A1LM(J),B1LM(J)
      WRITE(6,8) J,ATM(J),BTM(J),APM(J),BPM(J),ALM(J),BLM(J)
  500 CONTINUE
C     THE FOLLOWING IS CALC. OF THE SCATTERED FIELDS.
      CJ=(0.,1.)
      ETH(1)=-2.*B(2)*CT*CJ*AT(1)+2.*B(1)*ST*AL(1)
      EPS(1)=-2.*B(2)*CJ*AP(1)
      ETHM(1)=-2.*B(2)*CT*CJ*ATM(1)+2.*B(1)*ST*ALM(1)
      EPSM(1)=-2.*B(2)*CJ*APM(1)
      DO 600 J=1,3
      J1=2*J
      IF (J1.EQ.2.OR.J1.EQ.6.OR.J1.EQ.10) C1=-CJ
      IF (J1.EQ.4.OR.J1.EQ.8) C1=CJ
      JM=J1-1
      JP=J1+1
      JMM=JM-1
      JPP=JP+1
      S1=(-1.)**J
      ETH(JP)=S1*C1*(((-AT(JP)-BP(JP))*B(JPP)+(AT(JP)-BP(JP))*B(J1))*CT+
     22.*AL(JP)*(-CJ)*B(JP)*ST)
      EPS(JP)=S1*C1*((BT(JP)-AP(JP))*B(JPP)+(BT(JP)+AP(JP))*B(J1))
      WRITE (6,9)
      WRITE (6,8) JP,ETH(JP),EPS(JP)
    9 FORMAT (5X,18HJP,ETH(JP),EPS(JP))
      ETHM(JP)=S1*C1*(((-ATM(JP)-BPM(JP))*B(JPP)+(ATM(JP)-BPM(JP))*B(J1)
     2)*CT+2.*ALM(JP)*(-CJ)*B(JP)*ST)
      EPSM(JP)=S1*C1*((BTM(JP)-APM(JP))*B(JPP)+(BTM(JP)+APM(JP))*B(J1))
      WRITE (6,900)
  900 FORMAT (5X,20HJP,ETHM(JP),EPSM(JP))
      WRITE (6,8) JP,ETHM(JP),EPSM(JP)
      J2=(2*J)-1
      JM=J2-1
      JP=J2+1
      JMM=JM-1
      JPP=JP+1
      IF (J2.EQ.1.OR.J2.EQ.5.OR.J2.EQ.9) C2=-1.0
      IF (J2.EQ.3.OR.J2.EQ.7) C2=1.0
      J2P=(J2+1)/2
      S1=(-1.)**J2P
      ETH(JP)=S1*C2*(((BT(JP)-AP(JP))*B(JPP)+(-BT(JP)-AP(JP))*B(J2))*CT+
     22.*BL(JP)*CJ*B(JP)*ST)
```

Fig. 24--(continued).

```
      EPS(JP)=SI*C2*((AT(JP)+BP(JP))*B(JPP)+(AT(JP)-BP(JP))*B(J2))
      ETHM(JP)=SI*C2*(((BTM(JP)-APM(JP))*B(JPP)+(-BTM(JP)-APM(JP))*B(J2)
     2)*CT+2.*BLM(JP)*CJ*B(JP)*ST)
      EPSM(JP)=SI*C2*((ATM(JP)+BPM(JP))*B(JPP)+(ATM(JP)-BPM(JP))*B(J2))
      WRITE (6,10)
   10 FORMAT (5X,18HJP,ETH(JP),EPS(JP))
      WRITE (6,8) JP,ETH(JP),EPS(JP)
      WRITE (6,900)
      WRITE (6,8) JP,ETHM(JP),EPSM(JP)
  600 CONTINUE
      DO 610 J=1,10
      ETHT=ETHT+ETH(J)
      EPST=EPST+EPS(J)
      ETHMT=ETHMT+ETHM(J)
      EPSMT=EPSMT+EPSM(J)
  610 CONTINUE
   18 FORMAT (5X,33HTHE FOLLOWING IS FOR TE INCIDENCE,/)
      WRITE (6,18)
      WRITE (6,11) ETHT,EPST
   11 FORMAT (10X,10HE-THETA = ,2F12.6,/,10X,8HE-PSI = ,2F12.6)
      F1=4.*(3.14159**5)*((D*W*A)**2)*((CABS(1.-ER))**2)
      SIGTH=F1*((CABS(ETHT))**2)
      SIGPS=F1*((CABS(EPST))**2)
      SIGTHD=10.*ALOG10(SIGTH/REF)
      SIGPSD=10.*ALOG10(SIGPS/REF)
      WRITE (6,12)
   12 FORMAT (/,5X,42HTE SAME POL. BACKSCATTERING CROSS SECTION.)
      WRITE (6,13) SIGPS,SIGPSD
   13 FORMAT (15X,8HSIGMA = ,F14.8,15X,12HSIGMA(DB) = ,F14.8)
      WRITE (6,14)
   14 FORMAT (/,5X,42HTE OPP. POL. BACKSCATTERING CROSS SECTION.)
      WRITE (6,13) SIGTH,SIGTHD
   19 FORMAT (5X,33HTHE FOLLOWING IS FOR TM INCIDENCE,/)
      WRITE (6,19)
      WRITE (6,11) ETHMT,EPSMT
      SIGTH=F1*((CABS(ETHMT))**2)
      SIGPS=F1*((CABS(EPSMT))**2)
      SIGTHD=10.*ALOG10(SIGTH/REF)
      SIGPSD=10.*ALOG10(SIGPS/REF)
   20 FORMAT(/,5X,42HTM SAME POL. BACKSCATTERING CROSS SECTION.)
      WRITE (6,20)
      WRITE (6,13) SIGTH,SIGTHD
   21 FORMAT (/,5X,42HTM OPP. POL. BACKSCATTERING CROSS SECTION.)
      WRITE (6,21)
      WRITE (6,13) SIGPS,SIGPSD
      WRITE (6,15) A,D,W,FREQ,THD,ER,REF
      ETHT=(0.,0.)
      EPST=(0.,0.)
      ETHMT=(0.,0.)
      EPSMT=(0.,0.)
  800 CONTINUE
  801 CONTINUE
      STOP
      END
$IBFTC CC       NODECK
      SUBROUTINE NRCELL(M,RC,PC,ZC,AL,NX1,XM,YM,ZM,AA,BB,CC)
C     NX1 IS THE MAXIMUM PHI-MODE INDEX PLUS 1.
C     RC,PC,ZC DEFINE THE CENTER OF THE NEAR CELL
C     XM,YM,ZM ARE THE MATH POINT COORDINATES.
C     CELL DIMENSIONS ARE R=AA, PHI=BB, L=CC.
C     P1 THROUGH P16 ARE THE VARIOUS INTEGRALS.
C     M IS THE NUMBER OF SUBCELLS ALONG EACH EDGE OF THE MAIN CELL.
C     M*M*M IS THE TOTAL NO. OF SUBCELLS.  M IS EVEN
      COMMON /XXX/ XM(10),ZM(10)
```

Fig. 24--(continued).

```
      COMPLEX XP,P,Q
      COMPLEX P1(10),P2(10),P3(10),P4(10),P5(10),P6(10),P7(10),P8(10)
      COMPLEX P9(10),P10(10),P11(10),P12(10),P13(10),P14(10)
      COMPLEX P15(10),P16(10)
      COMMON P1,P2,P3,P4,P5,P6,P7,P8,P9,P10,P11,P12,P13,P14,P15,P16
      COMPLEX XPP,XPQ
      REAL L,LS
      DO 50 N=1,NX1
      P1(N)=(0.,0.)
      P2(N)=(0.,0.)
      P3(N)=(0.,0.)
      P4(N)=(0.,0.)
      P5(N)=(0.,0.)
      P6(N)=(0.,0.)
      P7(N)=(0.,0.)
      P8(N)=(0.,0.)
      P9(N)=(0.,0.)
      P10(N)=(0.,0.)
      P11(N)=(0.,0.)
      P12(N)=(0.,0.)
      P13(N)=(0.,0.)
      P14(N)=(0.,0.)
      P15(N)=(0.,0.)
      P16(N)=(0.,0.)
   50 CONTINUE
      T1=M
      T2=M/2
      A=AA/T1
      B=BB/T1
      C=CC/T1
      RADS=RC-(T2-0.500)*A
      PHIS=PC-(T2-0.500)*B
      LS=-(T2-0.500)*C
      DO 100 I=1,M
      T1=I-1
      PHI=PHIS+T1*B
      C1=COS(PHI)
      S1=SIN(PHI)
      DO 100 J=1,M
      T1=J-1
      RAD=RADS+T1*A
      DO 100 K=1,M
      T1=K-1
      L=LS+T1*C
      X=XM-(RAD*COS(AL)-L*SIN(AL))*COS(PHI)
      Y=YM-(RAD*COS(AL)-L*SIN(AL))*SIN(PHI)
      Z=ZM-(ZC+L*COS(AL))
      R=SQRT(X*X+Y*Y+Z*Z)
      R3=R**3
      R5=R**5
      AR=6.28319*R
      PR=(-1.+AR*AR)/R3
      PI=-AR/R3
      P=CMPLX(PR,PI)
      QR=(3.-AR*AR)/R5
      QI=3.*AR/R5
      Q=CMPLX(QR,QI)
      AP=RAD**2*COS(AL)
      DV=AP*B*A*C/6.28319
      XP=CMPLX(COS(AR),-SIN(AR))
      XPP=XP*P
      XPQ=XP*Q
      DO 100 N=1,NX1
      T2=N-1
```

Fig. 24--(continued).

```
      CN=COS(T2*PHI)
      SN=SIN(T2*PHI)
      CND=CN*DV
      SND=SN*DV
      P1(N)=P1(N)+C1*CND*XPP
      P2(N)=P2(N)+S1*SND*XPP
      P3(N)=P3(N)+X*X*C1*CND*XPQ
      P4(N)=P4(N)+X*X*S1*SND*XPQ
      P5(N)=P5(N)+X*Y*S1*CND*XPQ
      P6(N)=P6(N)+X*Y*C1*SND*XPQ
      P7(N)=P7(N)+X*Z*CND*XPQ
      P8(N)=P8(N)+Y*Y*S1*SND*XPQ
      P9(N)=P9(N)+Y*Y*C1*CND*XPQ
      P10(N)=P10(N)+Y*Z*SND*XPQ
      P11(N)=P11(N)+CND*XPP
      P12(N)=P12(N)+Z*X*C1*CND*XPQ
      P13(N)=P13(N)+Z*X*S1*SND*XPQ
      P14(N)=P14(N)+Z*Y*S1*CND*XPQ
      P15(N)=P15(N)+Z*Y*C1*SND*XPQ
      P16(N)=P16(N)+Z*Z*CND*XPQ
  100 CONTINUE
      RETURN
      END
$DATA
          1
          9     0.750      0.100      0.200      6.030      2.540      0.000      0.000
```

Fig. 24--(continued).

B. Tube Scattering with an Axially Incident Plane Wave

The flow chart of the basic operations is shown in Fig. 24 and the statement listing is given in Fig. 25. The input and calling parameters are defined below.

The data cards needed for each run are as follows:

Card Number 1 Format (2I5,7F10.5)

Columns	Quantity	Description
1-5 (right adjusted)	NNN	NNN = the maximum ϕ-mode index (NNN = 2 for on-axis incidence)
6-10 (right adjusted)	MMM	MMM = the maximum z-mode index.
11-20	A	A = the mean ring radius in inches.
21-30	T	T = the tube wall thickness in inches.
31-40	TL	TL = the total tube length in inches.
41-50	FR	FR= the frequency in gigahertz.
51-60	Re(ER)	ER = the complex relative dielectric constant of the tube material.
61-70	Im(ER)	

Card Number 2 Format (11I5)

Columns	Quantity	Description
1-5 (right adjusted)	JT	JT = the total number of rings into which the shell is divided.

Columns	Quantity	Description
6-10	JZ(1)	JZ(I) = the index of the I-th matching ring. There will be 2(MMM) + 1 matching rings.
11-15	JZ(2)	
16-20	JZ(3)	
.	.	
.	.	
.	.	

(right adjusted)

The calling parameters for the RING subroutines are defined below:

NX = the maximum ϕ-mode index

MX = the maximum z-mode index

A = the inner radius of the tube in inches

Z1 = the z-coordinate of the center of the particular ring (in waelengths)

AL = 0.0 (always)

T = the ring thickness in wavelengths

TL = the total tube length in wavelengths

DL = the length of the particular ring (in wavelengths)

The calling parameters for the NRCELL subroutine are defined below:

M = the number of subdividions of the large cell along each side. There are M^3 total subcells.

RC,PC,ZC = the ρ,ϕ, z coordinates, respectively, of the center of the large cell.

AL = 0.0 (always)

NX1 = the maximum ϕ-mode index plus 1.

XM,YM,ZM = the rectangular coordinates of the match point for a given calculation.

AA,BB,CC = the large cell dimensions in terms of the polar coordinates, ρ, ϕ, z respectively.

The function FL(Z) gives the distance along the shell (tube) as a function of the z-coordinate of the point on the shell. This generalized

function approach is used in anticipation of the general case when the arc length along the shell will be a more complicated function of z such as a polynomial with several terms.

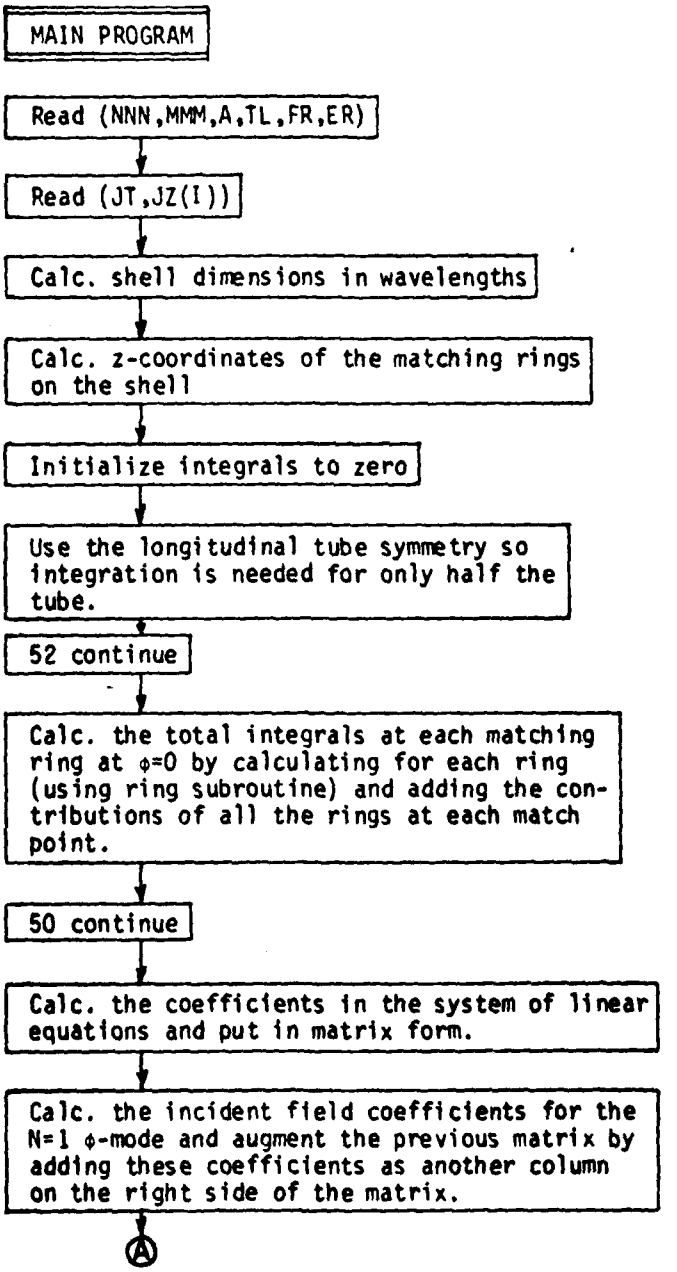

Fig. 25--Flow chart of the tube scattering computer program.

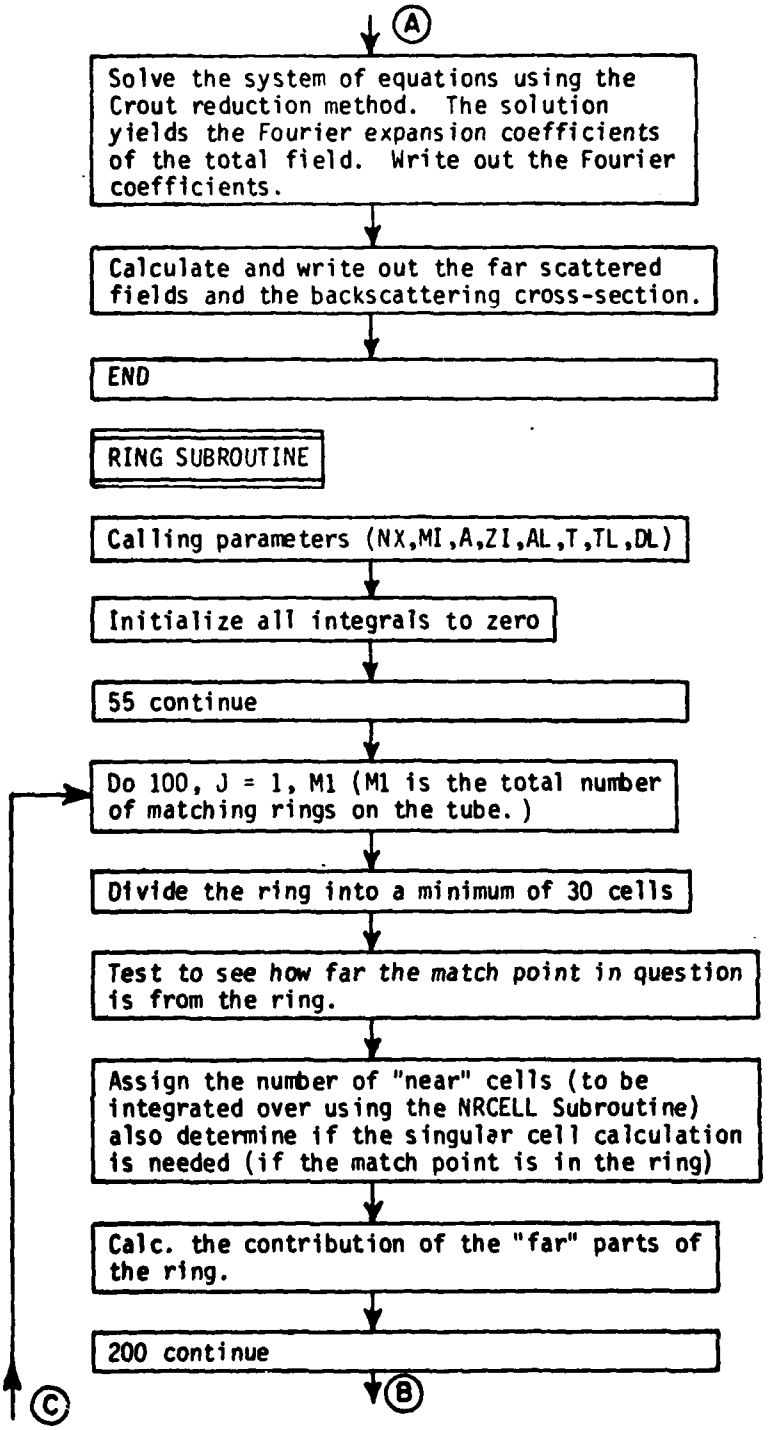

Fig. 25--(continued).

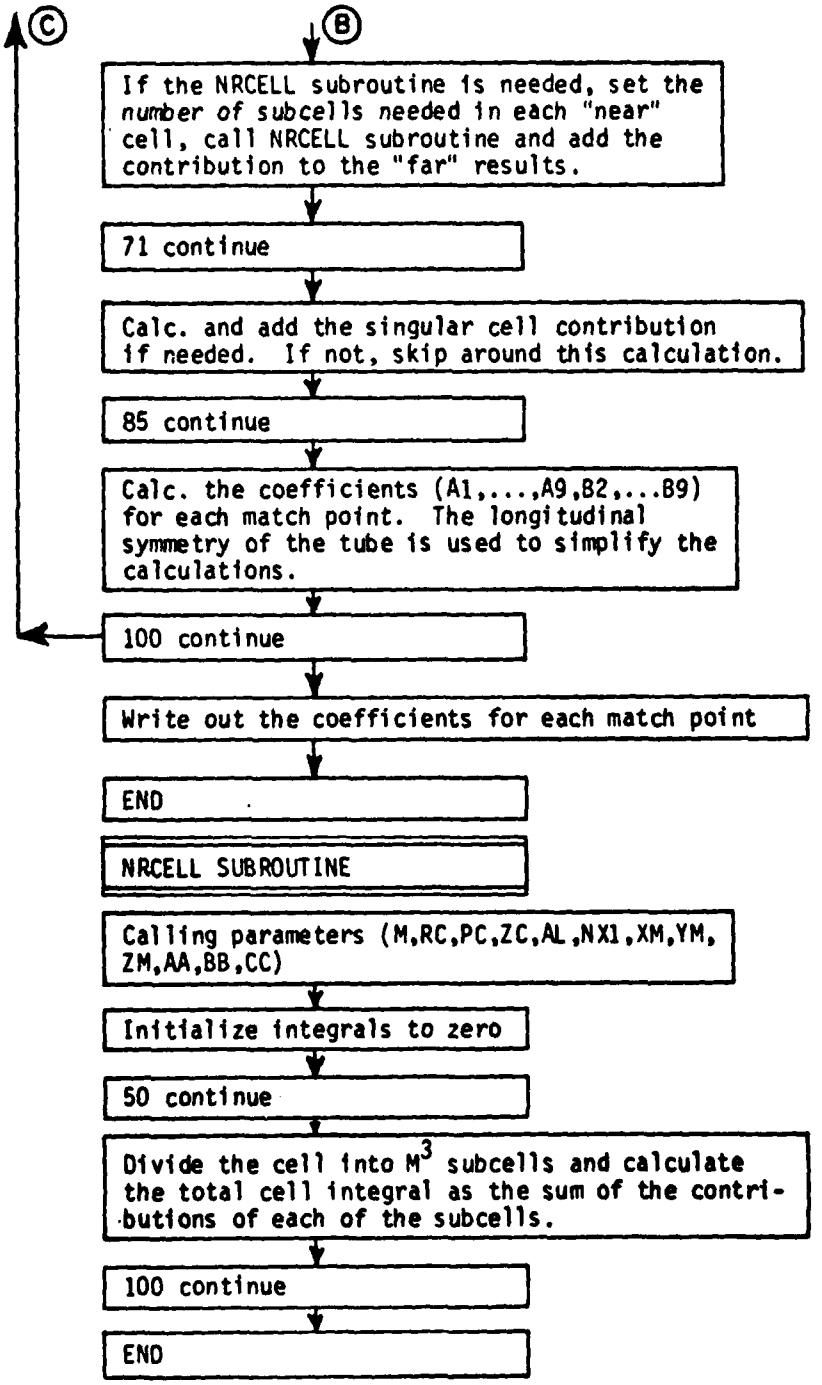

Fig. 25--(continued).

```
 VAN DOEREN, R. E.        JOBN FGB230      8
$EXECUTE        IBJOB
$IBJOB
$IBFTC MAIN     NODECK
     1 FORMAT (2I5,7F10.5)
    22 FORMAT (5X,4HJ = ,I5)
     2 FORMAT (12F10.4,/)
     3 FORMAT (5X,6E16.7,/,5X,6E16.7,/,5X,6E16.7,//)
     4 FORMAT (5X,6HMXX = ,I5)
     5 FORMAT (5X,6E16.7,/,10X,6E16.7,/)
     6 FORMAT(5X,17HER,T,L,A,WAV,FR  ,7F11.6,/,5X,8HSIGMA = ,F16.9)
     7 FORMAT(2X,10HATAU(0,1)=,2F10.5,11H BPHI(0,1)=,2F10.5,11H ATAU(1,1)
    2=,2F10.5,11H BPHI(1,1)=,2F10.5)
     8 FORMAT(5X,2I5)
     9 FORMAT (5X,5HJT = ,I5,/)
    10 FORMAT (1115)
    11 FORMAT (5X,14HTHE A,S FOLLOW)
    12 FORMAT (5X,14HTHE B,S FOLLOW)
    13 FORMAT (5X,28HTHE AUGMENTED MATRIX FOLLOWS)
    14 FORMAT (5X,28HTHE AUXILIARY MATRIX FOLLOWS)
       COMPLEX FTHS,FS
       COMPLEX A1(6,3,2),A2(6,3,2),A3(6,3,2),A4(6,3,2),A5(6,3,2)
       COMPLEX A6(6,3,2),A7(6,3,2),A8(6,3,2),A9(6,3,2)
       COMPLEX B1(6,3,2),B2(6,3,2),B3(6,3,2),B4(6,3,2),B5(6,3,2)
       COMPLEX B6(6,3,2),B7(6,3,2),B8(6,3,2),B9(6,3,2)
       COMPLEX AA1(6,3,2),AA2(6,3,2),AA3(6,3,2),AA4(6,3,2),AA5(6,3,2)
       COMPLEX AA6(6,3,2),AA7(6,3,2),AA8(6,3,2),AA9(6,3,2)
       COMPLEX BB1(6,3,2),BB2(6,3,2),BB3(6,3,2),BB4(6,3,2),BB5(6,3,2)
       COMPLEX BB6(6,3,2),BB7(6,3,2),BB8(6,3,2),BB9(6,3,2)
       COMMON /AAA/ AA1,AA2,AA3,AA4,AA5,AA6,AA7,AA8,AA9,BB1,BB2,BB3,BB4,B
      2B5,BB6,BB7,BB8,BB9
       COMPLEX C(72,72),E,FF,FTH,FPS,ER
       COMPLEX ARG,ARG2,EX
       COMMON /XXX/ XM(10),ZM(10)
       COMMON /JWW/ JWW
       DIMENSION JZ(10)
       INTEGER ODEV
       READ (5,1) NNN,MMM,A,T,TL,FR,ER
C      NNN IS THE MAXIMUM PHI-MODE INDEX.
C      MMM IS THE MAXIMUM L-MODE INDEX.
C      A IS THE MEAN RING RADIUS ( OR TUBE RADIUS).
C      A,T,)L, ARE IN INCHES. FR IS IN GIGAHERTZ.
C      ER IS THE RELATIVE DIELECTRIC CONSTANT (COMPLEX IN GENERAL).
C      DD IS THE APPROX. LENGTH IN WAV. OF EACH ELEMENTAL RING.
       NX=NNN+1
       MX=MMM+1
       MMX=2*MX-1
C      MMX IS THE NUMBER OF MATCHING RINGS OVER THE TUBE.
       MI=MMM
       READ (5,10) JT,(JZ(I),I=1,MMX)
C      JT IS AN ODD INTEGER (THE TOTAL NUMBER OF RINGS FOR INTEGRATION).
       WAV=11.803/FR
       A=A/WAV
       T=T/WAV
       TL=TL/WAV
       T1=JT
       DL=TL/T1
       DO 41 J=1,MMX
       T1=JZ(J)-1
       ZM(J)=T1*DL+DL/2.
       XM(J)=A
    41 CONTINUE
       WRITE (6,1) MMX,JT,(ZM(J),J=1,MMX)
       WRITE (6,1) MMX,JT,(XM(J),J=1,MMX)
```

Fig. 26--Tube scattering computer program statement listing.

```
      AL=0.0
      N=NX
      DO 52 J=1,MMX
      DO 52 M=1,MX
      A1(J,M,N)=(0.,0.)
      A2(J,M,N)=(0.,0.)
      A3(J,M,N)=(0.,0.)
      A4(J,M,N)=(0.,0.)
      A5(J,M,N)=(0.,0.)
      A6(J,M,N)=(0.,0.)
      A7(J,M,N)=(0.,0.)
      A8(J,M,N)=(0.,0.)
      A9(J,M,N)=(0.,0.)
      B1(J,M,N)=(0.,0.)
      B2(J,M,N)=(0.,0.)
      B3(J,M,N)=(0.,0.)
      B4(J,M,N)=(0.,0.)
      B5(J,M,N)=(0.,0.)
      B6(J,M,N)=(0.,0.)
      B7(J,M,N)=(0.,0.)
      B8(J,M,N)=(0.,0.)
      B9(J,M,N)=(0.,0.)
   52 CONTINUE
C     THE SYMMETRY OF THE TUBE IS USED SO INTEGRATION IS NEEDED OVER****
C     **** ONLY ONE HALF OF THE TUBE
      JT2=(JT+1)/2
      AI=A-T/2.
      DO 50 J1=1,JT2
      JWW=J1
      T1=J1
      Z1=(T1*DL)-DL/2.
      N=NX-1
      CALL RING (N,M1,AI,Z1,AL,T,TL,DL)
      N=NX
      DO 55 J=1,MMX
      DO 55 M=1,MX
      A1(J,M,N)=A1(J,M,N)+AA1(J,M,N)
      A2(J,M,N)=A2(J,M,N)+AA2(J,M,N)
      A3(J,M,N)=A3(J,M,N)+AA3(J,M,N)
      A4(J,M,N)=A4(J,M,N)+AA4(J,M,N)
      A5(J,M,N)=A5(J,M,N)+AA5(J,M,N)
      A6(J,M,N)=A6(J,M,N)+AA6(J,M,N)
      A7(J,M,N)=A7(J,M,N)+AA7(J,M,N)
      A8(J,M,N)=A8(J,M,N)+AA8(J,M,N)
      A9(J,M,N)=A9(J,M,N)+AA9(J,M,N)
      B1(J,M,N)=B1(J,M,N)+BB1(J,M,N)
      B2(J,M,N)=B2(J,M,N)+BB2(J,M,N)
      B3(J,M,N)=B3(J,M,N)+BB3(J,M,N)
      B4(J,M,N)=B4(J,M,N)+BB4(J,M,N)
      B5(J,M,N)=B5(J,M,N)+BB5(J,M,N)
      B6(J,M,N)=B6(J,M,N)+BB6(J,M,N)
      B7(J,M,N)=B7(J,M,N)+BB7(J,M,N)
      B8(J,M,N)=B8(J,M,N)+BB8(J,M,N)
      B9(J,M,N)=B9(J,M,N)+BB9(J,M,N)
   55 CONTINUE
   50 CONTINUE
      DO 60 J=1,MMX
      DO 60 M=1,MX
      WRITE (6,8) J,M
      WRITE (6,11)
      WRITE (6,5)     A1(J,M,N),A2(J,M,N),A3(J,M,N),A4(J,M,N),A5(J,M,N),A
     26(J,M,N),A7(J,M,N),A8(J,M,N),A9(J,M,N)
      WRITE (6,12)
      WRITE (6,5) B1(J,M,N),B2(J,M,N),B3(J,M,N),B4(J,M,N),B5(J,M,N),B6(J
```

Fig. 26--(continued).

```
     2,M,N),B7(J,M,N),B8(J,M,N),B9(J,M,N)
  60 CONTINUE
     E=ER-1.
C    NEXT STEP IS CALCULATION OF THE COEFFICIENT MATRIX.
     DO 70 J1=1,MMX
     DO 70 M1=1,MX
C    THE FOLLOWING SETS UP THE COEFFICIENT MATRIX.
C    THE MATRIX IS FILLED IN FROM LEFT TO RIGHT.
C    THE SMALLEST VALUE OF M IS TO THE LEFT.M INCREASES TO THE RIGHT.
     M=M1-1
     T1=M
     J=J1-1
     CM=COS(6.28319*T1*ZM(J1))
     SM=SIN(6.28319*T1*ZM(J1))
     IS=6*J
     IF (M1.EQ.1) KS=0
     IF (M1.GE.2) KS=12*M-6
     I1=IS+1
     I2=IS+2
     I3=IS+3
     I4=IS+4
     I5=IS+5
     I6=IS+6
     K1=KS+1
     K2=KS+2
     K3=KS+3
     K4=KS+4
     K5=KS+5
     K6=KS+6
     K7=KS+7
     K8=KS+8
     K9=KS+9
     K10=KS+10
     K11=KS+11
     K12=KS+12
     C(I1,K1)=CM-E*A1(J1,M1,N)
     C(I1,K2)=(0.,0.)
     C(I1,K3)=-E*A3(J1,M1,N)
     C(I1,K4)=(0.,0.)
     C(I1,K5)=-E*A2(J1,M1,N)
     C(I1,K6)=(0.,0.)
     IF (M1.EQ.1) GO TO 500
     C(I1,K7)=SM-E*B1(J1,M1,N)
     C(I1,K8)=(0.,0.)
     C(I1,K9)=-E*B3(J1,M1,N)
     C(I1,K10)=(0.,0.)
     C(I1,K11)=-E*B2(J1,M1,N)
     C(I1,K12)=(0.,0.)
 500 CONTINUE
     C(I2,K1)=(0.,0.)
     C(I2,K2)=C(I1,K1)
     C(I2,K3)=(0.,0.)
     C(I2,K4)=-C(I1,K3)
     C(I2,K5)=(0.,0.)
     C(I2,K6)=C(I1,K5)
     IF (M1.EQ.1) GO TO 501
     C(I2,K7)=(0.,0.)
     C(I2,K8)=C(I1,K7)
     C(I2,K9)=(0.,0.)
     C(I2,K10)=-C(I1,K9)
     C(I2,K11)=(0.,0.)
     C(I2,K12)=C(I1,K11)
 501 CONTINUE
     C(I3,K1)=E*A4(J1,M1,N)
```

Fig. 26--(continued).

```
      C(I3,I2)=(0.,0.)
      C(I3,K3)=CM-E*A6(J1,M1,N)
      C(I3,K4)=(0.,0.)
      C(I3,K5)=E*A5(J1,M1,N)
      C(I3,K6)=(0.,0.)
      IF  (M1.EQ.1) GO TO 502
      C(I3,K7)=E*B4(J1,M1,N)
      C(I3,K8)=(0.,0.)
      C(I3,K9)=SM-E*B6(J1,M1,N)
      C(I3,K10)=(0.,0.)
      C(I3,K11)=E*B5(J1,M1,N)
      C(I3,K12)=(0.,0.)
  502 CONTINUE
      C(I4,K1)=(0.,0.)
      C(I4,K2)=-C(I3,K1)
      C(I4,K3)=(0.,0.)
      C(I4,K4)=C(I3,K3)
      C(I4,K5)=(0.,0.)
      C(I4,K6)=-C(I3,K5)
      IF (M1.EQ.1) GO TO 503
      C(I4,K7)=(0.,0.)
      C(I4,K8)=-C(I3,K7)
      C(I4,K9)=(0.,0.)
      C(I4,K10)=C(I3,K9)
      C(I4,K11)=(0.,0.)
      C(I4,K12)=-C(I3,K11)
  503 CONTINUE
      C(I5,K1)=-E*A7(J1,M1,N)
      C(I5,K2)=(0.,0.)
      C(I5,K3)=-E*A9(J1,M1,N)
      C(I5,K4)=(0.,0.)
      C(I5,K5)=CM-E*A8(J1,M1,N)
      C(I5,K6)=(0.,0.)
      IF (M1.EQ.1) GO TO 504
      C(I5,K7)=-E*B7(J1,M1,N)
      C(I5,K8)=(0.,0.)
      C(I5,K9)=-E*B9(J1,M1,N)
      C(I5,K10)=(0.,0.)
      C(I5,K11)=SM-E*B8(J1,M1,N)
      C(I5,K12)=(0.,0.)
  504 CONTINUE
      C(I6,K1)=(0.,0.)
      C(I6,K2)=C(I5,K1)
      C(I6,K3)=(0.,0.)
      C(I6,K4)=-C(I5,K3)
      C(I6,K5)=(0.,0.)
      C(I6,K6)=C(I5,K5)
      IF( M1.EQ.1) GO TO 505
      C(I6,K7)=(0.,0.)
      C(I6,K8)=C(I5,K7)
      C(I6,K9)=(0.,0.)
      C(I6,K10)=-C(I5,K9)
      C(I6,K11)=(0.,0.)
      C(I6,K12)=C(I5,K11)
  505 CONTINUE
   70 CONTINUE
      MX1=(6*MMX)+1
C     DOWN TO 80 IS CALC. THE LAST COLUMN OF THE AUGMENTED MATRIX.
      DO 80 J1=1,MMX
      J=J1-1
      IS=6*J
      ARG3=6.28319*ZM(J1)
      ARG=CMPLX(0.,ARG3)
      I1=IS+1
```

Fig. 26--(continued).

```
      I2=IS+2
      I3=IS+3
      I4=IS+4
      I5=IS+5
      I6=IS+6
      C(I1,MX1)=CEXP(-ARG)
      C(I2,MX1)=(0.,0.)
      C(I3,MX1)=-CEXP(-ARG)
      C(I4,MX1)=(0.,0.)
      C(I5,MX1)=(0.,0.)
      C(I6,MX1)=(0.,0.)
      IF (J.EQ.1) WRITE (6,1) J,J,ARG,C(1,MX1),C(3,MX1)
   80 CONTINUE
      JJJ=6*MMX
      JJJ1=JJJ+1
      WRITE (6,13)
      DO 82 J=1,JJJ
      WRITE (6,8) J
      WRITE (6,5) (C(J,M),M=1,JJJ1)
   82 CONTINUE !
C     THE COEFFIECENT MATRIC IS 6*MMX BY 6*MMX.
C     THE AUGMENTED MATRIX IS 6*MMX BY (6*MMX+1)
C     THE FOLLOWING IS THE CROUT REDUCTION OF THE COEFFICIENT MATRIX.
      MXX=6*MMX
      NN=MXX+1
      DO 118 L=1,MXX
      LLL=L-1
      DO 118 IC=L,MXX
      II=IC+1
      IF (LLL.EQ.0) GO TO 1171
      DO 117 K=1,LLL
      C(IC,L)=C(IC,L)-C(IC,K)*C(K,L)
  117 C(L,II)=C(L,II)-C(L,K)*C(K,II)
 1171 CONTINUE
  118 C(L,II)=C(L,II)/C(L,L)
      WRITE (6,14)
      WRITE (6,4) MXX
      DO 120 J=1,MXX
      WRITE (6,22) J
      WRITE (6,2) (C(J,I),I=1,MXX)
  120 CONTINUE
      IF (MXX.EQ.1) GO TO 124
      DO 123 L=2,MXX
      IC=NN-L
      II=IC+1
      DO 122 K=II,MXX
  122 C(IC,NN)=C(IC,NN)-C(IC,K)*C(K,NN)
  123 CONTINUE
  124 DO 126 J=1,MXX
      WRITE (6,3) C(J,NN)
  126 CONTINUE
C     THE  FOLLOWING COMMENTS APPLY FOLLOWING THE CROUT REDUCTION.
C     C(1,NN)=A(0,1) SUPER(TAU)
C     C(2,NN)=B(0,1) SUPER (TAU)
C     C(3,NN)=B(0,1)SUPER(PHI)
C     C(4,NN)=A(0,1)SUPER(PHI)
C     C(5,NN)=A(0,1) SUPER (L)
C     C(6,NN)=B(0,1) SUPER (L)
C     C(M,NN)=AS(0,1) SUPER (TAU)
C     C(8,NN)=BS(0,1) SUPER (TAU)
C     AND SO ON .........
C     NN IS THE INDEX OF THE LAST COLUMN OF THE REDUCED MATRIX.
      WRITE (6,7) C(1,NN),C(3,NN),C(7,NN),C(9,NN)
C     THE REST IS CALC. OF THE SCATTERING CROSS-SECTION.
```

Fig. 26--(continued).

```
      FTH=(0.,0.)
      FPS=(0.,0.)
      FTHS =(0.,0.)
      JTTTT=2*JT
      DL=DL/2.
      DO 201 M=1,MX
      FF=(0.,0.)
      FS=(0.,0.)
      MM=M-1
      T2=M-1
      IF (M.EQ.1) MS=0
      IF (M.GE.2) MS=12*MM-6
      MS1=MS+1
      MS2=MS+2
      MS3=MS+3
      MS4=MS+4
      MS7=MS+7
      MS9=MS+9
      DO 200 J=1,JTTTT
      T1=J
      Z=(T1*DL)-DL/2.
      ARG1=6.28319*Z
      ARG2=CMPLX(0.,-ARG1)
      EX=CEXP(ARG2)
      CM=COS(2.*T2*3.14159*Z)
      SM=SIN(2.*T2*3.14159*Z)
      FF=FF+CM*EX
      FS=FS+SM*EX
  200 CONTINUE
      FTH=FTH+(C(MS1,NN)-C(MS3,NN))*FF
      IF (M.EQ.1) GO TO 2011
      FTHS=FTHS +(C(MS7,NN)-C(MS9,NN))*FS
 2011 CONTINUE
      WRITE (6,2) FF,FS,FTH,FTHS
  201 CONTINUE
C     NN IS THE INDEX OF THE LAST COLUMN OF THE REDUCED MATRIX.
      CO1=4.*(3.14159**5)*((T*DL*A)**2)
      CO2=(CABS(1.-ER))**2
      SIG=CO1*CO2*((CABS(FTH+FTHS))**2)
      WRITE (6,6) ER,T,TL,A,WAV,FR,SIG
  202 CONTINUE
      STOP
      END
$IBFTC DECK1  NODECK
      SUBROUTINE RING (NX,MI,A,Z1,AL,T,TL,DL)
C     ALL DIMENSION ARE IN WAVELENGTHS.
C     NX IS THE MAXIMUM PHI MODE INDEX.
C     MI IS THE MAXIMUM L-MODE INDEX.
C     Z1 IS THE Z-COORDINATE OF THE CENTER OF THE INNER SURFACE .
C     AL=0.0 IN ALL CASES.
C     AL IS THE VALUE OF ALPHA AT THE RING BEING INTEGRATED OVER HERE.
C     A IS THE INNER SURFACE RADIUS OF THE RING BEING INTEGRATED OVER.
C     T IS THE RING THICKNESS NORMAL TO THE SHELL SURFACE.
C     DL IS THE INCREMENTAL ARC LENGTH ALONG THE SHELL.
      REAL L,LJ
      COMMON /XXX/ X0(10),Z0(10)
C     X0,Z0 ARE THE MATCHING POINT COORDINATES.
      COMMON /JWW/ JWW
      MX=MI+1
      MI=2*MX-1
C     MI IS THE NUMBER OF MATCHING RINGS OVER THE TUBE.
      NX1=NX+1
      DIMENSION ST(5),SP(5),SL(5)
      COMPLEX XP,P,Q,P1(3),P2(3),P3(3),P4(3),P5(3),P6(3),P7(3),P8(3)
```

Fig. 26--(continued).

```
      COMPLEX P9(3),P10(3),P11(3),P12(3),P13(3),P14(3),P15(3),P16(3)
      COMMON P1,P2,P3,P4,P5,P6,P7,P8,P9,P10,P11,P12,P13,P14,P15,P16
      COMPLEX V1(5,2),V2(5,2),V3(5,2),V4(5,2),V5(5,2),V6(5,2),V7(5,2)
      COMPLEX V8(5,2),V9(5,2),V10(5,2),V11(5,2),V12(5,2),V13(5,2)
      COMPLEX V14(5,2),V15(5,2),V16(5,2)
      COMPLEX XPP,XPO
      COMPLEX A1(6,3,2),A2(6,3,2),A3(6,3,2),A4(6,3,2),A5(6,3,2)
      COMPLEX A6(6,3,2),A7(6,3,2),A8(6,3,2),A9(6,3,2)
      COMPLEX B1(6,3,2),B2(6,3,2),B3(6,3,2),B4(6,3,2),B5(6,3,2)
      COMPLEX B6(6,3,2),B7(6,3,2),B8(6,3,2),B9(6,3,2)
      COMMON /AAA/ A1,A2,A3,A4,A5,A6,A7,A8,A9,B1,B2,B3,B4,B5,B6,B7,B8,B9
C     FIRST SUBSCRPT IN A1 ETC. IDENTIFIES THE MATCHING RING.
C     SECOND SUBSCRPT IS THE L-MODE INDEX PLUS 1
C     THE THIRD SUBSCRIPT IS THE PHI-MODE INDEX PLUS 1.
      DO 50 N=1,NX1
      DO 50 I=1,M1
      V1(I,N) =(0.,0.)
      V2(I,N) =(0.,0.)
      V3(I,N) =(0.,0.)
      V4(I,N) =(0.,0.)
      V5(I,N) =(0.,0.)
      V6(I,N) =(0.,0.)
      V7(I,N) =(0.,0.)
      V8(I,N) =(0.,0.)
      V9(I,N) =(0.,0.)
      V10(I,N)=(0.,0.)
      V11(I,N)=(0.,0.)
      V12(I,N)=(0.,0.)
      V13(I,N)=(0.,0.)
      V14(I,N)=(0.,0.)
      V15(I,N)=(0.,0.)
      V16(I,N)=(0.,0.)
   50 CONTINUE
      DO 55 J=1,M1
      DO 55 M=1,MX
      DO 55 N=1,NX1
      A1(J,M,N)=(0.,0.)
      A2(J,M,N)=(0.,0.)
      A3(J,M,N)=(0.,0.)
      A4(J,M,N)=(0.,0.)
      A5(J,M,N)=(0.,0.)
      A6(J,M,N)=(0.,0.)
      A7(J,M,N)=(0.,0.)
      A8(J,M,N)=(0.,0.)
      A9(J,M,N)=(0.,0.)
      B1(J,M,N)=(0.,0.)
      B2(J,M,N)=(0.,0.)
      B3(J,M,N)=(0.,0.)
      B4(J,M,N)=(0.,0.)
      B5(J,M,N)=(0.,0.)
      B6(J,M,N)=(0.,0.)
      B7(J,M,N)=(0.,0.)
      B8(J,M,N)=(0.,0.)
      B9(J,M,N)=(0.,0.)
   55 CONTINUE
      DO 100 J=1,M1
C     J HERE RUNS OVER THE NUMBER OF MATCHING RINGS ON THE BODY (SHELL).
C     ALPHA MEASURED FROM TANGENT TO Z-AXIS. CCW IS POSITIVE, CW IS NEG.
      RC=(A/COS(AL))+T/2.
      AC=RC*COS(AL)
      ZC=ZI+(T/2.)*SIN(AL)
      XC=AC
      NO=3.14159*AC/0.01
      IF (NO.LT.30) NO=30
```

Fig. 26--(continued)

```
      TT1=N0
      DPHI=3.14159/TT1
      DV=T*DL*AC*DPHI/6.28319
      RTEST=SQRT((XC-X0(J))**2+(ZC-Z0(J))**2)
      DD1=1.1*DL
      DD2=2.1*DL
      IF (RTEST.LT.DD2) K0=11
      IF (RTEST.LT.DD1) K0=16
      IF (RTEST.LT.0.001) K0=22
      IF (RTEST.GT.DD2) K0=1
C     DOWN TO 200 IS CALCULATED THE CONTRIB. OF THE FAR PARTS OF RING.
      N01=N0+1
      DO 200 K=K0,N01
      TT1=K-1
      PH=(DPHI/2.)+TT1*DPHI
      C=COS(PH)
      S=SIN(PH)
      X=X0(J)-AC*C
      Y=-AC*S
      Z=Z0(J)-ZC
      IF (Z.LT.0.01) WTT=0.666667*((DL/2.)**3)
      IF (Z.GT.0.01) WTT=Z*Z
      R=SQRT(X**2+Y**2+Z**2)
      AR=6.28319*R
      ARS=AR**2
      R3=R**3
      R5=R**5
      PR=(-1.+ARS)/R3
      PI=-AR/R3
      P=CMPLX(PR,PI)
      QR=(3.-ARS)/R5
      QI=3.*AR/R5
      Q=CMPLX(QR,QI)
      XP=CMPLX(COS(AR),-SIN(AR))
      XPP=XP*P
      XPQ=XP*Q
      DO 200 N=1,NX1
      TT2=N-1
      CN=COS(TT2*PH)
      SN=SIN(TT2*PH)
      V1(J,N)=V1(J,N)+CN*C*DV*XPP
      V2(J,N)=V2(J,N)+SN*S*DV*XPP
      V3(J,N)=V3(J,N)+X*X*CN*C*DV*XPQ
      V4(J,N)=V4(J,N)+X*X*SN*S*DV*XPQ
      V5(J,N)=V5(J,N)+X*Y*CN*S*DV*XPQ
      V6(J,N)=V6(J,N)+X*Y*SN*C*DV*XPQ
      V7(J,N)=V7(J,N)+X*Z*CN*DV*XPQ
      V8(J,N)=V8(J,N)+Y*Y*SN*S*DV*XPQ
      V9(J,N)=V9(J,N)+Y*Y*CN*C*DV*XPQ
      V10(J,N)=V10(J,N)+Y*Z*SN*DV*XPQ
      V11(J,N)=V11(J,N)+CN*DV*XPP
      V12(J,N)=V12(J,N)+Z*X*CN*C*DV*XPQ
      V13(J,N)=V13(J,N)+Z*X*SN*S*DV*XPQ
      V14(J,N)=V14(J,N)+Z*Y*CN*S*DV*XPQ
      V15(J,N)=V15(J,N)+Z*Y*SN*C*DV*XPQ
      V16(J,N)=V16(J,N)+WTT*CN*DV*XPQ
  200 CONTINUE
      DO 201 N=1,NX1
    1 FORMAT (//,5X,4I5)
    2 FORMAT (5X,8F11.6,/,5X,8F11.6,/,5X,8F11.6,/,5X,8F11.6,//)
      WRITE (6,1) J,N
      WRITE (6,2) V1(J,N),V2(J,N),V3(J,N),V4(J,N),V5(J,N),V6(J,N),V7(J,N
     2),V8(J,N),V9(J,N),V10(J,N),V11(J,N),V12(J,N),V13(J,N),V14(J,N),V15
     2(J,N),V16(J,N)
```

Fig. 26--(continued).

```
  201 CONTINUE
      IF (K0.EQ.1) GO TO 71
      IF (K0.EQ.11) N1=2
      IF (K0.EQ.16) N1=3
      IF (K0.EQ.22) N1=4
C     NOTE THAT K0=1 OR N1=2,3,4.
C     IF K0=1, THE MATCH POINT IS FAR. NRCELL SUBROUTINE IS NOT NEEDED.
      DIMENSION MZ(4)
      IF (N1.NE.2) GO TO 61
      MZ(1)=4
      MZ(2)=4
      GO TO 63
   61 IF (N1.NE.3) GO TO 62
      MZ(1)=10
      MZ(2)=4
      MZ(3)=4
      GO TO 63
   62 MZ(1)=20
      MZ(2)=10
      MZ(3)=4
      MZ(4)=4
   63 CONTINUE
      DO 70 I=1,N1
      TT3=I-1
      DPH=5.*DPHI
      IF (N1.NE.4) GO TO 65
      PHI=DPHI+DPH/2.+TT3*DPH
      GO TO 66
   65 PHI=DPH/2.+TT3*DPH
   66 CONTINUE
      XC=AC*COS(PHI)
      YC=AC*SIN(PHI)
      ZC=ZC
      XM=X0(J)
      YM=0.0
      ZM=Z0(J)
      AA=T
      BB=DPH
      CC=DL
      MM=MZ(I)
      CALL NRCELL(MM,AC,PHI,ZC,AL,NX1,XM,YM,ZM,AA,BB,CC)
      DO 70 N=1,NX1
      V1(J,N)=V1(J,N)+P1(N)
      V2(J,N)=V2(J,N)+P2(N)
      V3(J,N)=V3(J,N)+P3(N)
      V4(J,N)=V4(J,N)+P4(N)
      V5(J,N)=V5(J,N)+P5(N)
      V6(J,N)=V6(J,N)+P6(N)
      V7(J,N)=V7(J,N)+P7(N)

      V8(J,N)=V8(J,N)+P8(N)
      V9(J,N)=V9(J,N)+P9(N)
      V10(J,N)=V10(J,N)+P10(N)
      V11(J,N)=V11(J,N)+P11(N)
      V12(J,N)=V12(J,N)+P12(N)
      V13(J,N)=V13(J,N)+P13(N)
      V14(J,N)=V14(J,N)+P14(N)
      V15(J,N)=V15(J,N)+P15(N)
      V16(J,N)=V16(J,N)+P16(N)
      WRITE (6,1) I,J,N
      WRITE (6,2) P1(N),P2(N),P3(N),P4(N),P5(N),P6(N),P7(N),P8(N),P9(N),
     2P10(N),P11(N),P12(N),P13(N),P14(N),P15(N),P16(N)
      WRITE (6,2) V1(J,N),V2(J,N),V3(J,N),V4(J,N),V5(J,N),V6(J,N),V7(J,N
     2),V8(J,N),V9(J,N),V10(J,N),V11(J,N),V12(J,N),V13(J,N),V14(J,N),V15
```

Fig. 25 -- (continued)

Fig. 26--(continued).

```
     2(J,N),V16(J,N)
   70 CONTINUE
   71 CONTINUE
      IF (K0.LT.22) GO TO 80
C     IF K0=22, THE MATCHING POINT IS IN THIS RING ITSELF.
C     DOWN TO 80 IS THE SINGULAR CELL CONTRIBUTION.
      A1=T/2.
      B1=AC*DPHI
      C1=DL/2.
      SQ=SQRT(A1**2+B1**2+C1**2)
      TT2=2./3.14159
      ST(J)=-1.+TT2*(ATAN((A1*C1)/(B1*SQ))+ATAN((A1*B1)/(C1*SQ)))
      SP(J)=-1.+TT2*(ATAN((B1*A1)/(C1*SQ))+ATAN((C1*B1)/(A1*SQ)))
      SL(J)=-1.+TT2*(ATAN((C1*B1)/(A1*SQ))+ATAN((C1*A1)/(B1*SQ)))
    3 FORMAT (5X,8F11.6)
      WRITE (6,1) J
      WRITE (6,3) ST(J),SP(J),SL(J)
      GO TO 85
   80 CONTINUE
      ST(J)=0.0
      SP(J)=0.0
      SL(J)=0.0
   85 CONTINUE
      N=2
    5 FORMAT (3I10)
    6 FORMAT (8F10.6)
      PUNCH 5,JWW,J,N
      PUNCH 6,ST(J),SP(J),SL(J),V1(J,N),V2(J,N),V3(J,N),V4(J,N),V5(J,N),
     2V6(J,N),V7(J,N),V8(J,N),V9(J,N),V10(J,N),V11(J,N),V12(J,N),V13(J,N
     2),V14(J,N),V15(J,N),V16(J,N)
C     JWW IS THE RING INDEX,J THE M.P. INDEX,N THE PHI-MODE INDEX...
      C=COS(ALP(J))
      S=SIN(ALP(J))
      CA=COS(AL)
      SA=SIN(AL)
  300 CONTINUE
      L=FL(Z1)
C     FL(Z) IS A FUNCTION GIVING L AS A FUNCTION OF Z .
      DO 90 N=1,NX1
      DO 90 M=1,MX
      TT5=M-1
      G=TT5*3.14159
      CM=COS(2.*G*L)
      SM=SIN(2.*G*L)
      COMPLEX T1,T2,T3,T4,T5,T6,T7,T8,T9,T10,T11,T12,T13,T14,T15,T16
      T1=V1(J,N)
      T2=V2(J,N)
      T3=V3(J,N)
      T4=V4(J,N)
      T5=V5(J,N)
      T6=V6(J,N)
      T7=V7(J,N)
      T8=V8(J,N)
      T9=V9(J,N)
      T10=V10(J,N)
      T11=V11(J,N)
      T12=V12(J,N)
      T13=V13(J,N)
      T14=V14(J,N)
      T15=V15(J,N)
      T16=V16(J,N)
      A1(J,M,N)=CM*(T1+T3+T5+ST(J))+A1(J,M,N)
      A2(J,M,N)=CM*T7+A2(J,M,N)
      A3(J,M,N)=CM*(-T2-T4+T6)+A3(J,M,N)
```

Fig. 26--(continued).

AD-A128 678 APPLICATION OF AN INTEGRAL EQUATION METHOD TO SCATTERING BY DIELECTRIC CY..(U) OHIO STATE UNIV COLUMBUS ELECTROSCIENCE LAB R E VAN DOEREN 24 FEB 69

2/2

UNCLASSIFIED ESL-TR-2604-1 N00019-68-C-0267 F/G 12/1 NL

END
DATE FILMED
6-83
DTIC

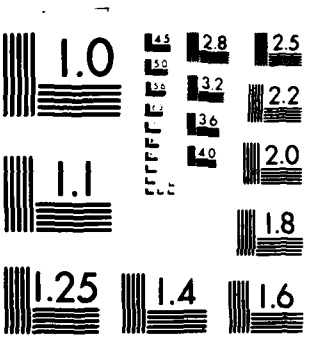

```
      A4(J,M,N)=CM*(T2+T6+T8)+A4(J,M,N)
      A5(J,M,N)=CM*T10+A5(J,M,N)
      A6(J,M,N)=CM*(T1-T5+T9+SP(J))+A6(J,M,N)
      A7(J,M,N)=CM*(T12+T14)+A7(J,M,N)
      A8(J,M,N)=CM*(T11+T16+SL(J))+A8(J,M,N)
      A9(J,M,N)=CM*(-T13+T15)+A9(J,M,N)
      B1(J,M,N)=SM*(T1+T3+T5+ST(J))+B1(J,M,N)
      B2(J,M,N)=SM*T7+B2(J,M,N)
      B3(J,M,N)=SM*(-T2-T4+T6)+B3(J,M,N)
      B4(J,M,N)=SM*(T2+T6+T8)+B4(J,M,N)
      B5(J,M,N)=SM*T10+B5(J,M,N)
      B6(J,M,N)=SM*(T1-T5+T9+SP(J))+B6(J,M,N)
      B7(J,M,N)=SM*(T12+T14)+B7(J,M,N)
      B8(J,M,N)=SM*(T11+T16+SL(J))+B8(J,M,N)
      B9(J,M,N)=SM*(-T13+T15)+B9(J,M,N)
C     THE FOLLOWING USES THE MIRROR IMAGE SYMMETRY TO CALC. ALL THE A,S.
      IF ((ABS(Z1-(TL/2.)))-LT-0.001) GO TO 90
      JJ=M1-J+1
      LJ=TL-L
      CMJ=COS(2.*TT5*3.14159*LJ)
      SMJ=SIN(2.*TT5*3.14159*LJ)
      A1(JJ,M,N)=CMJ*(T1+T3+T5+ST(J))+A1(JJ,M,N)
      A2(JJ,M,N)=CMJ*(-T7)+A2(JJ,M,N)
      A3(JJ,M,N)=CMJ*(-T2-T4+T6)+A3(JJ,M,N)
      A4(JJ,M,N)=CMJ*(T2+T6+T8)+A4(JJ,M,N)
      A5(JJ,M,N)=CMJ*(-T10)+A5(JJ,M,N)
      A6(JJ,M,N)=CMJ*(T1-T5+T9+SP(J))+A6(JJ,M,N)
      A7(JJ,M,N)=CMJ*(-T12-T14)+A7(JJ,M,N)
      A8(JJ,M,N)=CMJ*(T11+T16+SL(J))+A8(JJ,M,N)
      A9(JJ,M,N)=CMJ*(T13-T15)+A9(JJ,M,N)
      B1(JJ,M,N)=SMJ*(T1+T3+T5+ST(J))+B1(JJ,M,N)
      B2(JJ,M,N)=SMJ*(-T7)+B2(JJ,M,N)
      B3(JJ,M,N)=SMJ*(-T2-T4+T6)+B3(JJ,M,N)
      B4(JJ,M,N)=SMJ*(T2+T6+T8)+B4(JJ,M,N)
      B5(JJ,M,N)=SMJ*(-T10)+B5(JJ,M,N)
      B6(JJ,M,N)=SMJ*(T1-T5+T9+SP(J))+B6(JJ,M,N)
      B7(JJ,M,N)=SMJ*(-T12-T14)+B7(JJ,M,N)
      B8(JJ,M,N)=SMJ*(T11+T16+SL(J))+B8(JJ,M,N)
      B9(JJ,M,N)=SMJ*(T13-T15)+B9(JJ,M,N)
   90 CONTINUE
  100 CONTINUE
    8 FORMAT (5X,37HTHE A,S (FROM RING SUBROUTINE) FOLLOW)
    9 FORMAT (5X,37HTHE B,S (FROM RING SUBROUTINE) FOLLOW)
   10 FORMAT(5X,3I3,6E16.7,/,5X,6E16.7,/,5X,6E16.7,/)
      DO 101 I=1,M1
      DO 101 J=1,MX
      DO 101 K=1,NX1
      WRITE (6,8)
      WRITE (6,10) I,J,K,A1(I,J,K),A2(I,J,K),A3(I,J,K),A4(I,J,K),A5(I,J,
     2K),A6(I,J,K),A7(I,J,K),A8(I,J,K),A9(I,J,K)
      WRITE (6,9)
      WRITE (6,10) I,J,K,B1(I,J,K),B2(I,J,K),B3(I,J,K),B4(I,J,K),B5(I,J,
     2K),B6(I,J,K),B7(I,J,K),B8(I,J,K),B9(I,J,K)
  101 CONTINUE
      RETURN
      END
$IBFTC DECK2   NODECK
      SUBROUTINE NRCELL(M,RC,PC,ZC,AL,NX1,XM,YM,ZM,AA,BB,CC)
C     NX1 IS THE MAXIMUM PHI-MODE INDEX PLUS 1.
C     RC,PC,ZC DEFINE THE CENTER OF THE NEAR CELL
C     XM,YM,ZM ARE THE MATH POINT COORDINATES.
C     CELL DIMENSIONS ARE R=AA, PHI=BB, L=CC.
C     P1 THROUGH P16 ARE THE VARIOUS INTEGRALS.
C     M IS THE NUMBER OF SUBCELLS ALONG EACH EDGE OF THE MAIN CELL.
```

Fig. 26--(continued).

```
C     M*M*M IS THE TOTAL NO. OF SUBCELLS.  M IS EVEN
      COMPLEX XP,P,Q
      COMPLEX P1(3),P2(3),P3(3),P4(3),P5(3),P6(3),P7(3),P8(3),P9(3)
      COMPLEX P10(3),P11(3),P12(3),P13(3),P14(3),P15(3),P16(3)
      COMMON P1,P2,P3,P4,P5,P6,P7,P8,P9,P10,P11,P12,P13,P14,P15,P16
      COMPLEX XPP,XPQ
      REAL L,LS
      DO 50 N=1,NX1
      P1(N)=(0.,0.)
      P2(N)=(0.,0.)
      P3(N)=(0.,0.)
      P4(N)=(0.,0.)
      P5(N)=(0.,0.)
      P6(N)=(0.,0.)
      P7(N)=(0.,0.)
      P8(N)=(0.,0.)
      P9(N)=(0.,0.)
      P10(N)=(0.,0.)
      P11(N)=(0.,0.)
      P12(N)=(0.,0.)
      P13(N)=(0.,0.)
      P14(N)=(0.,0.)
      P15(N)=(0.,0.)
      P16(N)=(0.,0.)
   50 CONTINUE
      T1=M
      T2=M/2
      A=AA/T1
      B=BB/T1
      C=CC/T1
      RADS=RC-(T2-0.500)*A
      PHIS=PC-(T2-0.500)*B
      LS=-(T2-0.500)*C
      DO 100 I=1,M
      T1=I-1
      PHI=PHIS+T1*B
      C1=COS(PHI)
      S1=SIN(PHI)
      DO 100 J=1,M
      T1=J-1
      RAD=RADS+T1*A
      DO 100 K=1,M
      T1=K-1
      L=LS+T1*C
      X=XM-(RAD*COS(AL)-L*SIN(AL))*COS(PHI)
      Y=YM-(RAD*COS(AL)-L*SIN(AL))*SIN(PHI)
      Z=ZM-(ZC+L*COS(AL))
      R=SQRT(X*X+Y*Y+Z*Z)
      R3=R**3
      R5=R**5
      AR=6.28319*R
      PR=(-1.+AR*AR)/R3
      PI=-AR/R3
      P=CMPLX(PR,PI)
      QR=(3.-AR*AR)/R5
      QI=3.*AR/R5
      Q=CMPLX(QR,QI)
      AP=RAD*COS(AL)
      DV=AP*B*A*C/6.28319
      XP=CMPLX(COS(AR),-SIN(AR))
      XPP=XP*P
      XPQ=XP*Q
      DO 100 N=1,NX1
      T2=N-1
```

Fig. 26--(continued).

```
      CN=COS(T2*PHI)
      SN=SIN(T2*PHI)
      CND=CN*DV
      SND=SN*DV
      P1(N)=P1(N)+C1*CND*XPP
      P2(N)=P2(N)+S1*SND*XPP
      P3(N)=P3(N)+X*X*C1*CND*XPQ
      P4(N)=P4(N)+X*X*S1*SND*XPQ
      P5(N)=P5(N)+X*Y*S1*CND*XPQ
      P6(N)=P6(N)+X*Y*C1*SND*XPQ
      P7(N)=P7(N)+X*Z*CND*XPQ
      P8(N)=P8(N)+Y*Y*S1*SND*XPQ
      P9(N)=P9(N)+Y*Y*C1*CND*XPQ
      P10(N)=P10(N)+Y*Z*SND*XPQ
      P11(N)=P11(N)+CND*XPP
      P12(N)=P12(N)+Z*X*C1*CND*XPQ
      P13(N)=P13(N)+Z*X*S1*SND*XPQ
      P14(N)=P14(N)+Z*Y*S1*CND*XPQ
      P15(N)=P15(N)+Z*Y*C1*SND*XPQ
      P16(N)=P16(N)+Z*Z*SND*XPQ
  100 CONTINUE
      RETURN
      END
$IBFTC DECK3    NODECK
      FUNCTION FL(Z)
      FL=Z
      RETURN
      END
$DATA
    1    2     0.450     0.100     1.570     6.230     2.540     0.000
   11    2    4    6    8   10
```

Fig. 26--(continued).

BIBLIOGRAPHY

1. Stratton, J.A., Electromagnetic Theory, McGraw Hill Book Co., New York, 1941, p. 572.
2. Mie, G., "Beitrage zur Optik truber Medien, speziell kolloidlaer Metallosungen," Ann. Physik, Vol. 25, 1908, p. 377.
3. Rayleigh, Lord, "On the Electromagnetic Theory of Light," Phil. Mag., 12, 1881, p. 81.
4. Wait, J.R., "Scattering of a Plane Wave from a Circular Dielectric Cylinder at Oblique Incidence," Can. Journ. Phys., Vol. 33, 1955, p. 189.
5. Yeh, C., "Scattering of Obliquely Incident Light Waves by Elliptical Fibers,: J. Optc. Soc. Am., Vol 54, 1964, p. 1227.
6. Yeh, C., "Diffraction of Waves by a Dielectric Parabolic Cylinder," Journal of the Optical Society of America, Vol. 57 February 1967, pp. 195-201.
7. Stratton, op. cit., pp. 511-514.
8. Tice, T.E. and Adney, J.E., "Transmission through a Dielectric Spherical Shell," Report 531-3, Ohio State University, Antenna Laboratory, 1 August 1953 (AD 16 877).
9. Andreasen, M.G., "Radiation from a Radial Dipole through a Thin Dielectric Spherical Shell," IRE Trans. of Antennas and Propagation, Vol. AP-5, October 1957, pp 337-342.
10. Morse, P.M. and Feshbach, N., Methods of Theoretical Physics,

McGraw Hill Book Co., New York, 1953, Part II, pp. 1762-1767.

11. Ibid., Part I, pp. 655-664.

12. Cohen, M.H., "Application of the Reaction Concept to Scattering Probelms," IRE Trans. on Antennas and Propagation, Vol. AP-3, October 1955, pp. 193-199.

13. Montroll, E., and Hart, R., "On the Scattering of Plane Waves by Soft Obstacles: II Scattering by Cylinders, Spheroids and Disks," J. Appl. Phys., Vol. 22, 1951, p. 1278.

14. Lind, A., "Resonance Electromagnetic Scattering by Finite Circular Cylinders," Ph.D. Thesis, Department of Physics, Rensselaer Polytechnic Institute, Troy, New York, July 1966.

15. Oguchi, T., "Attenuation of Electromagnetic Wave due to Rain with Distorted Raindrops," J. Radio Res., Labs. (Japan), Vol. 7, September 1960, pp. 467-485.

16. Phillipson, L.L., "An Analytical Study of Scattering by Thin Dielectric Rings," IEEE Trans. on Antennas and Propagation, Vol. AP-6, January 1958, pp. 3-8.

17. Peters, L. and Thomas, D.J., "A Geometrical Optics Approach for the Radar Cross Section of Thin Shells," Journal of Geophysical Research, Vol. 67, May 1962, pp 2073-2075.

18. Kouyoumjian, R.G., et.al., "A Modified Geometrical Optics Method for Scattering by Dielectric Bodies," IEEE Trans. on Antennas and Propagation, Vol AP-11, November 1963, pp 690-693.

19. Peters, L., et.al., "Approximations for Dielectric or Plasma Scatterers," Proc. of the IEEE, Vol. 53, August 1965, pp. 882-892.

20. Rhodes, D.R., "On the Theory of Scattering by Dielectric Bodies," Report 475-1, Ohio State University, ElectroScience Laboratory, 1 July 1953.

21. Harrington, R.F., Field Computation by Moment Methods, The MacMillan Co., New York, 1968.

22. Richmond, J.H., "The Calculation of Radome Diffraction Patterns," Report 118-13, The Ohio State University, ElectroScience Laboratory, 15 September 1963.

23. Richmond, J.H., "Diffraction by a Coaxial Array of Metal or Dielectric Toroids," Report 1751-5, Ohio State University, ElectroScience Laboratory, 9 July 1964, (AD 447 526).

24. Richmond, J.H., "Digital Computer Solutions of the Rigorous Equations for Scattering Problems," Proceedings of the IEEE, Vol. 53, August 1965, pp 796-804.

25. Richmond, J.H., "Scattering by a Dielectric Cylinder of Arbitrary Cross Section Shape," IEEE Trans. on Antennas and Propagation, Vol. AP-13, May 1965, pp. 334-341.

26. Richmond, J.H., "TE-Wave Scattering by a Dielectric Cylinder of Arbitrary Cross Section Shape," IEEE Trans. on Antennas and Propagation, Vol. AP-14, July 1966, pp. 460-464.

27. Waterman, P.C., "Scattering by Dielectric Obstacles," The Mitre Corporation, Report MTP-84, July 1968.

28. Richmond, J.H., The Basic Theory of Harmonic Fields, Antennas and Scattering, Academic Press (to be published at a later date).

29. Kouyoumjian, R.G. and Peters, L., "Range Requirements in Radar Cross Section Measurements," Proc. of the IEEE, Vol. 53, August 1965, pp. 920-928.

30. Kouyoumjian, R.G., "The Calculation of the Echo Areas of Perfectly Conducting Objects by the Variational Method," Report 444-13, Ohio State University, ElectroScience Laboratory, 15 November 1953, (AD 48 214).

UNCLASSIFIED
Security Classification

DOCUMENT CONTROL DATA - R&D

(Security classification of title, body of abstract and indexing annotation must be entered when the overall report is classified)

1. ORIGINATING ACTIVITY (Corporate author) ElectroScience Laboratory, Department of Electrical Engineering, The Ohio State University, Columbus, Ohio 43212	2a. REPORT SECURITY CLASSIFICATION Unclassified 2b. GROUP

3. REPORT TITLE

APPLICATION OF AN INTEGRAL EQUATION METHOD TO SCATTERING BY DIELECTRIC CYLINDRICAL SHELLS HAVING FINITE LENGTH

4. DESCRIPTIVE NOTES (Type of report and inclusive dates)

Technical Report

5. AUTHOR(S) (Last name, first name, initial)

R.E. Van Doeren

6. REPORT DATE	7a. TOTAL NO. OF PAGES	7b. NO. OF REFS
24 February 1969	97	30

8a. CONTRACT OR GRANT NO. N00019-68-C-0267 b. PROJECT NO. c. TASK R 008-01-01 d.	9a. ORIGINATOR'S REPORT NUMBER(S) ElectroScience Laboratory 2604-1 9b. OTHER REPORT NO(S) (Any other numbers that may be assigned this report)

10. AVAILABILITY/LIMITATION NOTICES

APPROVED FOR PUBLIC RELEASE
DISTRIBUTION UNLIMITED

11. SUPPLEMENTARY NOTES	12. SPONSORING MILITARY ACTIVITY
	Department of the Navy Naval Air Systems Command Washington, D.C. 20360

13. ABSTRACT An integral equation for the electromagnetic field within a dielectric body is given. The equation is set up for numerical solution for the case of thin-wall cylindrical dielectric shells having finite length.

The solution of the integral equation utilizes a truncated double Fourier expansion of the field in the shell. The integral equation is then enforced at enough points within the shell wall to obtain a sufficient system of linear equations in the unknown expansion coefficients of the field. Numerical integration over the shell volume is used to obtain the coefficients in the system of linear equations. The system of equations is solved numerically for the expansion coefficients of the field in the shell. Calculation of the backscattered fields and the backscattering cross section are then performed.

A comparison of the calculated and measured backscattering cross section is made for rings with arbitrary plane wave incidence and for tubes with axial plane wave incidence. The agreement is excellent in all cases considered.

The numerical methods, experimental arrangement, computer programs and suitable extension of this work are discussed.

DD FORM 1 JAN 64 1473

UNCLASSIFIED
Security Classification

14. KEY WORDS	LINK A		LINK B		LINK C	
	ROLE	WT	ROLE	WT	ROLE	WT
Scattering Dielectric Scattering Dielectric Shell Scattering Radome Scattering Boresight Error Radome Analysis						

INSTRUCTIONS

1. ORIGINATING ACTIVITY: Enter the name and address of the contractor, subcontractor, grantee, Department of Defense activity or other organization *(corporate author)* issuing the report.

2a. REPORT SECURITY CLASSIFICATION: Enter the overall security classification of the report. Indicate whether "*Restricted Data*" is included. Marking is to be in accordance with appropriate security regulations.

2b. GROUP: Automatic downgrading is specified in DoD Directive 5200.10 and Armed Forces Industrial Manual. Enter the group number. Also, when applicable, show that optional markings have been used for Group 3 and Group 4 as authorized.

3. REPORT TITLE: Enter the complete report title in all capital letters. Titles in all cases should be unclassified. If a meaningful title cannot be selected without classification, show title classification in all capitals in parenthesis immediately following the title.

4. DESCRIPTIVE NOTES: If appropriate, enter the type of report, e.g., interim, progress, summary, annual, or final. Give the inclusive dates when a specific reporting period is covered.

5. AUTHOR(S): Enter the name(s) of author(s) as shown on or in the report. Enter last name, first name, middle initial. If military, show rank and branch of service. The name of the principal author is an absolute minimum requirement.

6. REPORT DATE: Enter the date of the report as day, month, year, or month, year. If more than one date appears on the report, use date of publication.

7a. TOTAL NUMBER OF PAGES: The total page count should follow normal pagination procedures, i.e., enter the number of pages containing information.

7b. NUMBER OF REFERENCES: Enter the total number of references cited in the report.

8a. CONTRACT OR GRANT NUMBER: If appropriate, enter the applicable number of the contract or grant under which the report was written.

8b, 8c, & 8d. PROJECT NUMBER: Enter the appropriate military department identification, such as project number, subproject number, system numbers, task number, etc.

9a. ORIGINATOR'S REPORT NUMBER(S): Enter the official report number by which the document will be identified and controlled by the originating activity. This number must be unique to this report.

9b. OTHER REPORT NUMBER(S): If the report has been assigned any other report numbers *(either by the originator or by the sponsor)*, also enter this number(s).

10. AVAILABILITY/LIMITATION NOTICES: Enter any limitations on further dissemination of the report, other than those imposed by security classification, using standard statements such as:

(1) "Qualified requesters may obtain copies of this report from DDC."

(2) "Foreign announcement and dissemination of this report by DDC is not authorized."

(3) "U. S. Government agencies may obtain copies of this report directly from DDC. Other qualified DDC users shall request through _____."

(4) "U. S. military agencies may obtain copies of this report directly from DDC. Other qualified users shall request through _____."

(5) "All distribution of this report is controlled. Qualified DDC users shall request through _____."

If the report has been furnished to the Office of Technical Services, Department of Commerce, for sale to the public, indicate this fact and enter the price, if known.

11. SUPPLEMENTARY NOTES: Use for additional explanatory notes.

12. SPONSORING MILITARY ACTIVITY: Enter the name of the departmental project office or laboratory sponsoring *(paying for)* the research and development. Include address.

13. ABSTRACT: Enter an abstract giving a brief and factual summary of the document indicative of the report, even though it may also appear elsewhere in the body of the technical report. If additional space is required, a continuation sheet shall be attached.

It is highly desirable that the abstract of classified reports be unclassified. Each paragraph of the abstract shall end with an indication of the military security classification of the information in the paragraph, represented as *(TS), (S), (C), or (U).*

There is no limitation on the length of the abstract. However, the suggested length is from 150 to 225 words.

14. KEY WORDS: Key words are technically meaningful terms or short phrases that characterize a report and may be used as index entries for cataloging the report. Key words must be selected so that no security classification is required. Identifiers, such as equipment model designation, trade name, military project code name, geographic location, may be used as key words but will be followed by an indication of technical context. The assignment of links, rules, and weights is optional.

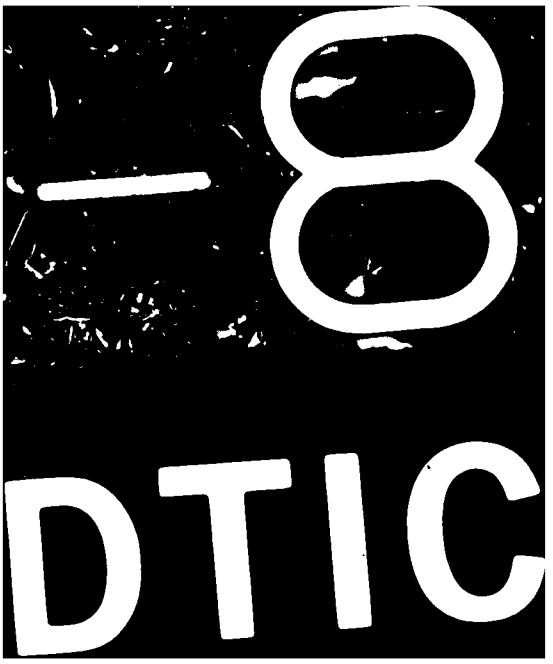
8
DTIC